TECHNICAL REPORT STANDARD PAGE

1. Title and Subtitle
A New Generation of Porous Asphalt Pavement–OGFC Support Study

2. Author(s)
Mostafa A. Elseifi, Ph.D., P.E. (VA); Hossam Abohamer, Ph.D., P.E. (TX); Md. Tanvir A. Sarkar, Ph.D.; Md. Afif Rahman Chowdhury; Sk Raihan Akbar

3. Performing Organization Name and Address
Department of Civil and Environmental Engineering
Louisiana State University, Baton Rouge, LA 70803

4. Sponsoring Agency Name and Address
Louisiana Department of Transportation and Development
P.O. Box 94245, Baton Rouge, LA 70804-9245

5. Report No.
FHWA/LA.25/687

6. Report Date
June 2025

7. Performing Organization Code
LTRC Project Number: 21-6B
SIO Number: DOTLT1000386

8. Type of Report and Period Covered
Final Report
05/2020 – 8/2023

9. No. of Pages
134

10. Supplementary Notes
Conducted in Cooperation with the U.S. Department of Transportation, Federal Highway Administration.

11. Distribution Statement
Unrestricted. This document is available through the National Technical Information Service, Springfield, VA 21161.

12. Key Words
Open-graded friction course; crumb rubber; warm-mix asphalt, seepage analysis

13. Abstract
The objective of this study was to develop and evaluate a new generation of open-graded friction courses (OGFC) that would provide superior durability performance while preserving the functional benefits of the mix. Additionally, a Finite Element (FE) model was developed and used to propose new air voids (AV) guidelines for OGFC applications in Louisiana. Nine OGFC mixes that encompass three Warm-Mix Asphalt (WMA) additives, two pozzolanic fillers (cement and fly ash), and a mix with a reduced nominal maximum aggregate size (NMAS) of 9.5 mm, were evaluated. The most cost-effective OGFC mixes were the mix with reduced NMAS, the mixes prepared with the pozzolanic fillers, and two of the WMA additives. Based on the findings of this project, revision of the Louisiana specifications is recommended to address durability issues with OGFC mixes. It is recommended that the new AV requirements for OGFC mix be 16-20% instead of the current 18-24%. Additionally, the specifications should be modified to incorporate the use of OGFC mixes with 9.5 mm NMAS. The use of WMA additives and pozzolanic fillers is also recommended for enhanced performance and durability.

Project Review Committee

Each research project will have an advisory committee appointed by the LTRC Director. The Project Review Committee is responsible for assisting the LTRC Administrator or Manager in the development of acceptable research problem statements, requests for proposals, review of research proposals, oversight of approved research projects, and implementation of findings.

LTRC appreciates the dedication of the following Project Review Committee Members in guiding this research study to fruition.

LTRC Administrator/Manager

Moses Akentuna, Ph.D., P.E.
Asphalt Research Manager

Members

Samuel Cooper, III
Christophe Fillastre
Ken Free
Philip Graves
Barry Moore
Don Weathers

Directorate Implementation Sponsor

Chad Winchester, P.E.
DOTD Chief Engineer

A New Generation of Porous Asphalt Pavement—OGFC Support Study

By
Mostafa A. Elseifi, Ph.D., P.E. (VA)
Hossam Abohamer, Ph.D., P.E. (TX)
Md. Tanvir A. Sarkar, Ph.D.
Md. Afif Rahman Chowdhury
Sk Raihan Akbar

Department of Civil and Environmental Engineering
Louisiana State University
Baton Rouge, LA 70803

LTRC Project No. 21-6B
SIO No. DOTLT1000386

conducted for
Louisiana Department of Transportation and Development
Louisiana Transportation Research Center

June 2025

Abstract

Open-graded friction course (OGFC) has been used as a surface course mix in Europe and the U.S. for decades as it provides unique safety and environmental benefits. OGFC typically contains a high percentage of air voids, between 18-24%, compared to 2.5-4.5% for conventional hot-mix asphalt (HMA). Due to its large air void content, water will not only drain over the OGFC surface but also through its pores; therefore, the possibility of hydroplaning decreases, and the skid resistance improves during wet weather conditions. For this reason, many researchers and practitioners have championed OGFC to address splash, spray, visibility, and noise issues. With all of these benefits, the use of OGFC as a wearing surface course has faced several challenges mostly due to its inferior durability compared to dense-graded HMA (DGHMA). Raveling is the most serious challenge with OGFC as once this distress is manifested, OGFC deteriorates rapidly, and its replacement is inevitable after only a few years.

The objectives of this study were twofold. First, this study aimed at designing and evaluating a new generation of OGFCs that would provide superior durability and performance while preserving the functional benefits of the mix. Second, a Finite Element (FE) model was developed and used to evaluate the effects of traffic wear and a reduction in permeability on the long-term hydraulic performance of a pavement structure constructed with an OGFC surface layer.

To fulfill the laboratory objective of the study, different additives were evaluated by modifying an approved and practically used OGFC mix (Control Mix–CM). These modifications included three WMA additives (Che1, Che2, and Org), one recycled product (Crumb Rubber), and two different pozzolanic fillers (Portland cement [F_1] and fly ash [F_2]). Additionally, a mix with a reduced NMAS of 9.5 mm was evaluated. In total, nine OGFC mixes were designed, prepared, and evaluated in the laboratory to determine the effects of these modifications on the performance of these mixes at three different stages: production, construction, and field performance.

To fulfill the second objective, an FE model was developed to investigate the effects of the permeability of OGFC (K_{OGFC}), thickness of OGFC (T_{OGFC}), permeability of the existing pavement (K_{HMA}), and traffic wear on the seepage characteristics of a pavement structure constructed with an OGFC layer under different climatic conditions. These results were then analyzed statistically to determine the most significant factors that affect the drainage performance of the pavement structure. Afterward, the most significant factors were used to develop an artificial neural network (ANN) model and an XGBOOST model for the prediction of the time to reach overflow conditions without the need for FE modeling.

Finally, the XGBOOST model was used to propose new AV guidelines for OGFC applications in Louisiana.

Results of the laboratory program indicated that WMA additives, 9.5 mm NMAS, and crumb rubber (CR) reduced the total air void content of the OGFC mix, which in turn reduced the coefficient of permeability. Nevertheless, all the mixes satisfied the requirements of both air void content and coefficient of permeability set forth by NCHRP 1-51. Based on performance testing, Che1, Che2, CR, F_1, F_2, and 9.5 mm NMAS enhanced the raveling resistance of OGFC compared to the control mix (CM) based on the Cantabro abrasion loss test that was conducted on unaged samples. In terms of permanent deformation, all of the mixes satisfied the maximum allowable requirement at 5,000 passes, including the control mix. At 20,000 passes, the mixes that contained organic WMA, CR (without Che1), F_2, F_2, and 9.5 mm NMAS satisfied the permanent deformation requirement set forth by NCHRP 1-51. Based on the results of the Cantabro test and rut depth at 5,000 passes, the most cost-effective OGFC mixes were 9.5 mm NMAS, F_2-OGFC, Che2-OGFC, and Org-OGFC, in this order. On the other hand, considering the results of the Cantabro test and rutting performance at 20,000 passes, the most cost-effective OGFC mixes were F_2-OGFC, 9.5 mm NMAS, Org-OGFC, and F_1-OGFC, in this order.

Results of the FE model indicated that, as the thickness of OGFC increased, the permeability coefficient of OGFC and the permeability coefficient of the underlying layer increased, and the time at which the pavement structure reached overflow condition (T_C) also increased. Results of a parametric study indicated that for a 30 min. rainstorm of 0.04 in./hr., an OGFC layer with an AV content of 14% would drain all rain water without reaching overflow conditions, even after significant traffic wear. For a 60 min. rainstorm of 0.04 in./hr., an OGFC layer with an AV content of 16% would drain all rain water without reaching overflow conditions, even after considerable traffic wear.

Based on the findings of this project, revision of the Louisiana specifications is recommended to address durability issues with OGFC mixes. Results of the study demonstrated that high AV content has a negative effect on OGFC durability. In Louisiana, OGFC mixes are required to have an AV content between 18-24%, which is higher than the AV content recommended by other states. Based on the results of this study, it is recommended that the lower limit of AV requirements for OGFC mixes should be decreased from 18% to 16%. The high limit of AV requirements should also be decreased from 24% to 20% to enhance the durability of the mix. Additionally, the specifications should be modified to incorporate and permit the use of OGFC mixes with 9.5 mm NMAS. The use of WMA additives in OGFC mixes is also recommended for enhanced durability. The replacement of the fillers with Portland cement and fly ash in OGFC mixes was also found to enhance performance and durability.

Acknowledgments

The study was financially supported by the Louisiana Transportation Research Center (LTRC). The authors would like to acknowledge the staff at LTRC for their assistance including Samuel Cooper, Corey Mayeux, and Jeremy Icenogle. The assistance of Paragon Technical Services in this research project is greatly appreciated. Additionally, the assistance of Don Weathers is greatly appreciated.

Implementation Statement

Based on the findings of this project, revision of the Louisiana specifications is recommended to address durability issues with OGFC mixes. Results of the study demonstrated that high AV content has a negative effect on OGFC durability. In Louisiana, OGFC mixes are required to have an AV content between 18-24%, which is higher than the AV content recommended by other states. Based on the results of this study, it is recommended that the lower limit of AV requirements for OGFC mixes be decreased from 18 to 16%. The high limit of AV requirements should also be decreased from 24 to 20% to enhance the durability of the mix. Additionally, the specifications should be modified to incorporate and permit the use of OGFC mixes with 9.5 mm NMAS. The use of WMA additives in OGFC mixes is also recommended for enhanced durability. The replacement of the fillers with Portland cement and fly ash in OGFC mixes is also recommended for enhanced performance and durability.

Table of Contents

List of Tables

List of Figures

Introduction

Open graded friction course (OGFC) has been used as a surface course mix in Europe and the U.S. for decades. OGFC is also known as porous european mix (PEM), porous asphalt (PA), porous friction course (PFC), open graded asphalt (OGA), and porous asphalt concrete (PAC) [1] [2]. OGFC is typically employed as a surface course layer to achieve a number of safety, economic, and environmental benefits [3]. OGFC is a gap-graded asphaltic mixture in which the percentage of fine aggregate (FA) is decreased and the percentage of coarse aggregate (CA) is increased compared to conventional HMA [2]. Consequently, OGFC typically contains a high percentage of air voids, between 15-22% [4], compared to 2.5-4.5% for conventional HMA. Due to its large air void content, water will not only drain over the OGFC surface but also through its pores; therefore, the possibility of hydroplaning decreases and the skid resistance improves during wet weather conditions [5]. For this reason, many researchers and practitioners have advocated for the use of OGFC to address splash, spray, visibility, and noise issues.

Even with all of these benefits, the use of OGFC as a wearing surface course has faced several challenges, primarily due to its inferior durability compared to dense-graded asphalt mixtures. In 1998, a survey conducted by the National Center for Asphalt Technology (NCAT) showed that 22 states had stopped using OGFC [6]. In 2004, a survey conducted by NCAT as part of NCHRP Project 1-55 indicated that only 20 out of the 41 responding agencies were using OGFC [1], which has been attributed to durability issues associated with OGFC. According to a 2014 NCAT survey, the durability issues of OGFC are numerous, including premature raveling, cracking, and stripping. Among these distresses, raveling is the most serious challenge with OGFC, as once this distress is manifested, OGFC deteriorates rapidly, and its replacement is inevitable after only a few years.

During the last two decades, many studies were conducted to enhance OGFC durability and performance. Among these studies, researchers focused on the impacts of aggregate gradation on OGFC performance [7] [8], while others investigated the contribution of stone-on-stone contact [1] [9] and binder additives [10] [11]. In terms of aggregate gradation, it has been found that fine OGFC mixes performed better compared to coarse OGFC mixes; however, it also results in a significant reduction in air void contents [7] [8]. In terms of binder properties, polymers, crumb rubber (CR), and warm mix asphalt (WMA) additives have also been evaluated to improve the mix’s durability in terms of raveling and cracking resistance [12].

Literature Review

This section provides a comprehensive literature review of OGFC mix design and analysis. Additionally, it provides an overview of previous research studies that were conducted to evaluate the functional benefits of OGFC. It also synthesizes previous studies that investigated different methods and technologies that may be used to enhance the durability of OGFC. Further, this section documents other researchers' efforts in investigating the different factors that affect the drainage performance of OGFC using FE modeling. Based on this review, shortcomings and knowledge gaps in the literature were identified.

OGFC Mixture Design

In the U.S., OGFC is commonly designed to achieve a high porosity level of at least 18% [1] [13]; however, other countries such as Japan, China, and New Zealand require a minimum level of porosity of 20% for OGFC [14]. This level of porosity can be achieved by reducing the percentage of fines in the mixture; therefore, a higher percentage of coarse aggregate is used in OGFC compared to regular dense-graded hot-mix asphalt (DGHMA). Additionally, stone-on-stone contact is more important in OGFC than in other types of mixes. The large AV content in OGFC may cause the binder to be more vulnerable to oxidation and water infiltration, which may lead to accelerated aging and moisture damage. To this end, special requirements are specified for the properties and characteristics of the mix components that are used in OGFC.

Two primary OGFC mix design procedures are available in the standards: ASTM D 7064, "Standard Practice for Open-Graded Friction Course (OGFC) Mix Design" [15]; and AASHTO PP 77, "Standard Practice for Materials Selection and Mixture Design of Permeable Friction Courses (PFCs)" [16]. Yet, according to a survey conducted in NCHRP 1-55, most highway agencies are using their own design procedure for OGFC mixes. Similar to DGHMA, the OGFC design procedure consists of four primary steps:

- Materials selection;
- Aggregate blend selection;
- Optimum binder content (OBC) determination; and
- Mixture evaluation.

Materials Selection

As a special mix, OGFC requires carefully selected materials with special characteristics to ensure the quality of the final product and adequate performance. A high-quality aggregate and a polymer-modified binder are desirable to achieve adequate performance against permanent deformation, raveling, and moisture damage in both the short and long term [17]. This section discusses the special requirements that should be considered in the selection of aggregate, binder, and additives for use in OGFC production and construction.

Aggregate Properties

Coarse aggregate is a key component in OGFC in order to provide stone-on-stone contact, while fine aggregate is used to achieve the mixture's stability and cohesiveness [18]. The aggregate in OGFC consists primarily of coarse aggregate, with only 20% of the aggregate passing sieve No. 8 to achieve the target air void content [19]. As previously noted, stone-on-stone contact is more critical in OGFC compared to DGHMA mixes [14]. Therefore, higher internal stresses develop in OGFC compared to conventional dense-graded mixes [20]. Mixture compaction during construction may result in aggregate breakage, which would affect aggregate gradation and OGFC mixture properties more than those of DGHMA [21] [9]. Further, coarse aggregate is a key element in OGFC, as it creates the mixture skeleton that resists permanent deformation.

Generally, OGFC mixes require coarse aggregate with 25% more strength than the aggregate used in conventional dense-graded mixes [17]. However, universal specifications for aggregate mineralogy that can be used in OGFC do not exist due to the limitations and variability of local aggregate sources. In NCHRP 9-41, a nationwide survey was conducted to rank the importance of different aggregate properties used in OGFC [17]. Abrasion resistance, polished aggregate, angularity, shape, cleanliness, and absorption were the aggregate properties that were included in the survey. Results indicated that polished resistance and durability were the most important properties for OGFC mixes. The second level of importance included angularity, abrasion resistance, particle shape, and cleanliness. Finally, aggregate absorption was reported at the third level of importance when it came to the design of OGFC mixes. In Europe, similar properties were reported, as polished resistance (as expressed by the polished stone value) was the most important aggregate property in the design of OGFC [2]. Table 1 presents the aggregate consensus properties, which are commonly considered by the different state agencies in the U.S. for the design of OGFC mixes.

Table 1. Consensus properties of aggregate used in OGFC [17]

Property	Test	Parameter	Typical Value	State/Reference
Abrasion	ASTM C 131	% Maximum Abrasion Loss	30%	Tennessee, Oregon, Oklahoma
			40%	Virginia, Arizona, and Wyoming
			50%	New Jersey and South Carolina
Coarse Aggregate Angularity	ASTM D 5821	% Minimum with one or more fractured faces	75%	New Mexico
			90%	California, Louisiana, Mississippi, Nevada, and Oregon
			92%	Arizona
			95%	Nebraska, North Carolina, and Wyoming
			100%	Oklahoma, Tennessee, and Virginia
		% Minimum with at least two fractured faces	75%	California and Oregon
			85%	Arizona
			90%	Nebraska, North Carolina, Tennessee, and Virginia
			95%	Oklahoma
Fine Aggregate Angularity	ASTM C 1252	% Minimum compacted air voids	45%	Louisiana
Particle Shape	ASTM D 4791	% Maximum with length /thickness >5	10%	Nebraska, Texas, Oregon, Virginia, and North Carolina

Property	Test	Parameter	Typical Value	State/Reference
		% Maximum with length /thickness >3	20%	Mississippi, and Tennessee
			25%	Louisiana and Arizona
Soundness	AASHTO T 104	% Maximum Soundness Loss	9%	Tennessee
			12%	Nevada and Oregon
			15%	North Carolina, South Carolina, and Virginia
			20%	Texas and Wyoming
Cleanliness	ASTM D 2419	% Minimum Sand Equivalent by Weight	45%	Louisiana, North Carolina, Wyoming, and Oregon
			55%	Arizona
Absorption	ASTM C 127	% Maximum Water Absorption	2%	New Jersey and Virginia
			2.5%	Arizona
			4%	Nevada

Binder Properties

The selection of binder type in OGFC is based on a number of factors. Similar to dense-graded mixes, both the anticipated climatic conditions at the project location and traffic volume are considered the primary controlling factors in the selection of OGFC's binder [22] [23]. However, compared to DGHMA mixes, a stiffer asphalt binder with two higher grades is recommended for use in OGFC for a particular climatic condition [22].

The trade-off in asphalt binder stiffness is key to achieving desirable OGFC durability. Soft binders in OGFC tend to drain through aggregate particles due to the large AV and high production temperature, resulting in a fluctuating asphalt binder content throughout the mix [19]. Thus, bleeding spots may be noticed after the construction of an OGFC layer constructed with a soft asphalt binder. More importantly, spots with low binder content may exhibit short-term raveling. However, the use of asphalt binder that is too stiff in OGFC mixes may also lead to detrimental consequences. Stiff binders tend to reach a critical

hardening level early, which may result in long-term raveling, reducing the expected service life of OGFC mixes.

For OGFC, asphalt binders are usually modified with polymers and crumb rubber to produce polymer-modified binder (PMB) and asphalt rubber (AR) binders. Styrene butadiene styrene (SBS), ethylene vinyl acetate (EVA), and styrene butadiene rubber (SBR) are the most widely used polymers in the U.S. and Europe. The rubber used to produce AR binder is usually obtained from the recycling of old vehicle and truck tires [18]. The use of PMB and AR binder was reported to enhance the durability of OGFC due to their high stiffness and ductility. The inclusion of polymers and crumb rubber in OGFC promotes an increased film thickness, which can be achieved by the increase in binder content while decreasing the potential for draindown.

Fibers

Typically, OGFCs consist of a large percentage of coarse aggregate and a low percentage of fillers and fine aggregate. Consequently, the surface area of the aggregate blend in OGFC is less than that of DGHMA [24]. Additionally, compared to dense-graded mixes, OGFC is usually fabricated with a high binder content (6-7%). Due to the combination of low aggregate surface area and high binder content, the binder film thickness in OGFC mixes is thicker than that of DGHMA. It was reported that the binder film thickness is approximately 30 microns in OGFC compared to 8 microns in conventional HMA mixes [5]. Thick binder films tend to draindown under high temperatures during production, transportation, and construction procedures due to the large AV content [25].

Fibers are the most common additives that may be used to address the issue of draindown. According to NCHRP 9-41, 85% of the states that responded to the agency survey reported the use of fibers to control and prevent draindown in OGFC. A wide variety of fibers are available on the market for the use of OGFC. Among these fibers, cellulose and mineral fibers are the most common in the U.S., Australia, and Europe [24] [2]. Besides draindown control, the use of fibers in OGFC enhances the durability of the final product. Hassan et al. concluded that fibers provided OGFC with long-term resistance to raveling similar to that provided by polymers [26]. Similarly, it was reported that the use of different types of fibers in OGFC mixtures increased its resistance to raveling and permanent deformation [27].

Selection of the Optimum Aggregate Gradation

OGFC is a gap-graded mix in which intermediate sizes are absent, between 3/8 in. and the No. 4 sieves [28]. Additionally, fine materials passing No. 200 sieve, ranges from 0-8%, and typical values of uniformity and curvature coefficient are 4 and 1, respectively [28]. Similar

to DGHMA, the selection of aggregate gradation requires blending aggregate from accepted stockpiles to produce three trial blends [1] [29]. Besides the specifications that are required to design DGHMA mixes, adequate stone-on-stone contact and adequate AV content should be simultaneously achieved. Stone-on-stone contact conditions are needed in order to minimize rutting and disintegration, and high AV is needed in OGFC in order to promote water removal and noise reduction [14].

Air Voids

The calculation of AV content requires the measurement of the theoretical maximum specific gravity and the bulk specific gravity of the mixture. The theoretical maximum specific gravity (G_{mm}) is typically measured according to ASTM D 2041 and AASTO T 209, "Standard Test Method for Theoretical Maximum Specific Gravity and Density of Asphalt Mixtures" [30]. Three loose samples are typically prepared for each mixture, and the G_{mm} is calculated for each mix using Equation 1:

$$G_{mm} = \frac{A}{A-(C-B)} \quad (1)$$

where,
A = mass of dry sample in air (g);
B = mass of the pycnometer under water (); and
C = mass of sample and pycnometer under water (g).

The bulk specific gravity (G_{mb}) is calculated using the procedure described in ASTM D 6752, "Standard Test Method for Bulk Specific Gravity and Density of Compacted Asphalt Mixtures Using Automatic Vacuum Sealing Method." In this test method, three Superpave Gyratory Compacted (SGC) replicates with 6 in. (150 mm) and 4.5 in (115 mm) in diameter and height, respectively, are compacted at a typical effort of 50 gyrations. Equation 2 is then used to calculate G_{mb}.

$$G_{mb} = \frac{A}{[C+(B-A)]-E-\frac{B-A}{F_T}} \quad (2)$$

where,
A = mass of dry sample in air (g);
B = mass dry-sealed sample (g);
C = final mass of specimen after removal from sealed bag (g);
E = mass of sealed sample under water (g); and
F_T = apparent specific gravity of the plastic bag, as recommended by the manufacturer at 77° F (25° C).

Once G_{mm} and G_{mb} are obtained, AV can be calculated using Equation 3. The calculated AV content is then compared to the acceptable range for OGFC in Louisiana (18-24 %).

$$\text{AV}\ (\%) = \frac{G_{mm} - G_{mb}}{G_{mm}} * 100 \quad (3)$$

Stone-on-Stone Contact

The stone-on-stone condition is defined as the point at which the dry-rodded voids in coarse aggregate (VCA_{DRC}) is greater than the voids in coarse aggregate in the compacted mix (VCA_{MIX}). This definition implies the need to calculate VCA_{DRC} and VCA_{MIX}. VCA_{DRC} is calculated for loose coarse aggregate using Equation 4:

$$\text{VCA}_{\text{DRC}} = \frac{G_{sb}\gamma_w - \gamma_s}{G_{sb}\gamma_w} \quad (4)$$

where,
G_{sb} = aggregate bulk specific gravity (AASHTO T 85);
γ_w = unit weight of water; and
γ_s = unit weight of loose aggregate (AASHTO T 19).

Compacted samples are used to calculate VCA_{MIX}. Mixes consisting of a pre-specified AC content and three selected blends are compacted using the Superpave Gyratory Compactor (SGC), typically at 50 gyrations [31] to calculate the mix bulk specific gravity (G_{mb}). However, the traditional procedure, AASHTO T 166, cannot be used for G_{mb} determination because of the high permeability of OGFC mixes. High permeability allows water to flow freely and subsequently the saturated surface dry (SSD) weight cannot be accurately measured. Therefore, the CoreLok vacuum-sealing method is recommended for G_{mb} measurements. After G_{mb} measurement, Equation 5 can be used to calculate VCA_{MIX}.

$$\text{VCA}_{\text{MIX}} = 100 - \left[\frac{G_{mb}}{G_{sb}} * P_{4.75}\right] \quad (5)$$

where,
G_{mb} = mix bulk specific gravity;
G_{sb} = aggregate bulk specific gravity (AASHTO T 85); and
$P_{4.75}$ = % aggregate retained on a 4.75-mm sieve.

Selection of the Optimum Binder Content

Similar to DGHMA, the selection of the optimum binder content (OBC) requires the identification of the acceptable range of binder content (BC) from which the OBC is selected. For OGFC mixes, three properties are typically used to determine the OBC: binder draindown, durability, and AV. Figure 1 shows the strategy recommended for OBC selection

in OGFC mixes. As shown in the figure, draindown potential is used to determine the upper limit of BC in OGFC, because excessive binder content in OGFC may result in binder draindown and subsequently a high risk for bleeding and short-term raveling. Additionally, the figure shows that the Cantabro abrasion test is typically used as a durability performance indicator. The Cantabro test is used to determine the lower limit of binder content below which the binder content in OGFC is insufficient to achieve long-term durability. After determining the lower and upper limits of binder content, the selected BC should be selected in order to satisfy the minimum AV, which is typically 18% in the U.S.

Figure 1. OBC selection philosophy for OGFC mixes [9]

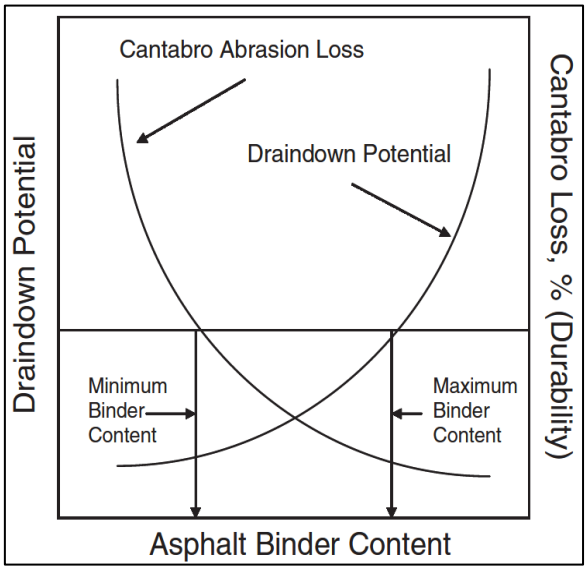

Draindown Test

Draindown characteristics are evaluated according to the test procedure detailed in AASHTO T 305-97, "Draindown Characteristics in Uncompacted Asphalt Mixtures." In this procedure, a sample of a loose mix (approximately 1200 g) is placed in a wire basket. Afterward, the basket is placed on a pan with a known weight in an oven at 15ºC higher than the production temperature for an hour. Draindown is evaluated by dividing the mass of the binder that has drained off by the total mass of the mix, as described by Equation 6. It is recommended that the upper limit of binder draindown be 0.3% [21].

$$\text{Draindown (\%)} = \frac{m_f - m_i}{mt} * 100 \quad (6)$$

where,

m_f = the final weight of the pan (g);

m_i = the initial weight of the pan (g); and

m_t = weight of the test sample (g).

Cantabro Abrasion Test

Abrasion resistance, measured by the Cantabro abrasion test, has been an essential part of OGFC mix design in many European countries [2]. The Cantabro abrasion test is typically conducted according to AASHTO TP 108-14, "Standard Method of Test for Determining the Abrasion Loss of Asphalt Mixture Specimens." In this test, SGC-compacted specimens are weighted to the nearest 0.1 g. Next, the Los Angeles abrasion test is run on the specimen without the steel balls. Operating at a temperature of 25°C, the apparatus is run at a speed of 30-33 revolutions per min. for a duration of 10 min. Afterward, the test specimen is removed and the final mass of the specimen is measured to the nearest 0.1 g. The Cantabro loss value is then calculated based on Equation 7:

$$\text{Cantabro loss } (\%) = 100 * \left[\frac{W_{ini} - W_{final}}{W_{ini}}\right] \quad (7)$$

where,
W_{ini} = initial weight of the sample (g); and
W_{final} = final weight of the sample (g).

Typically, nine SGC samples are prepared for each mix with a diameter of 6 in. (150 mm) and a height of 4.5±0.2 in. (115±5 mm). These nine mixes are divided into three groups with equal average AV. The first group is tested without any conditioning. On the other hand, the second and third groups are conditioned to evaluate the impact of binder aging and moisture on the abrasion resistance of OGFC mixes. For the second group, three samples are aged in an oven for seven days at 60ºC. Additionally, the samples in the third group are submerged in a water bath for 24 hr. at 60ºC. Afterward, the samples in the second group are left to cool to room temperature before testing. For the third group, samples are dried using the core dry machine before conducting the test.

The average Cantabro loss values are compared to the specification limits to evaluate the raveling and durability resistances of the mixes. According to NCHRP 1-55, a maximum of 20% is recommended for the Cantabro loss in the case of unaged samples [1]. While there is no specification for aged and moisture-conditioned specimens, NCHRP 9-41 recommends a maximum Cantabro loss of 30% for OGFC mixes [1].

Performance Evaluation

The objective of the performance evaluation step in OGFC mix design is to ensure that OGFC mix will achieve the desired field performance. OGFC performance tests include permeability, Hamburg Wheel-Tracking, Texas Overlay, Modified Lottman, and boiling tests. A brief description of each test method is presented in the following sections.

Permeability (*k*)

OGFC permeability is typically measured according to FM 5-565, "Florida Method of Test for Measurement of Water Permeability of Compacted Asphalt Paving Mixtures," using the falling head permeability test [32]. In this test, the water is allowed to flow through a saturated sample; the flow rate at which the water flows through the sample pores is used to calculate the sample permeability. To achieve saturated conditions, a two-step procedure should be followed. First, the sample should be submerged in water for at least an hour before testing. Second, after the sample is placed inside the device, the water should be allowed to flow through the sample for 5-10 min. before conducting the test. Equation 8 presents the formula used for calculating the coefficient of permeability, *k*.

$$k = \frac{a * l}{A * t} \ln\frac{h_1}{h_2} * t_c \quad (8)$$

where,
k= coefficient of permeability (cm/sec.);
a = inside cross-sectional area of the buret (cm^2);
l = average thickness of the test sample (cm);
A = average cross-sectional area of the test sample (cm^2);
t = thickness of the test sample (cm);
h_1 = initial head across the test sample (cm);
h_2 = final head across the test sample (cm); and
t_c = temperature correction for water viscosity.

Hamburg Wheel-Tracking Test (HWT)

The Hamburg Wheel-Tracking test (HWT) is a widely used test for assessing HMA resistance to permanent deformation. The HWT test is usually conducted according to AASHTO T 324, "Hamburg Wheel-Track Testing of Compacted Hot Mix Asphalt (HMA)" [33]. Two 6-in. (150 mm) diameter test specimens with a thickness of 2.36 in. (60 mm) are typically prepared for this test. In Louisiana, the criterion for OGFC mixes prepared with PG 76-22 is a maximum of 0.5 in. (12.5 mm) after 5,000 passes [20]. However, according to NCHRP 1-55, the maximum rut depth after 20,000 passes should not exceed 0.5 in. (12.5 mm). Therefore, in the current study, the rut depth of all mixes was evaluated at both 5,000 and 20,000 passes.

Texas Overlay Test

The Texas Overlay Test (TOT) is a recognized test procedure to evaluate OGFC mixes' resistance to reflective and fatigue cracking as described in Tex-248-F [34]. Three test specimens are usually fabricated with 6 in. (150 mm) in diameter by 4.53± 0.2 in (115± 5

mm) in height at a compaction effort of 50 gyrations. Next, these samples are trimmed to 6 in. (150 mm) long by 3±0.02 in. (76.2±0.5 mm) wide by 1.5±0.02 in. (38±0.5 mm) thick. Then, the trimmed samples are glued to the base plate using epoxy 4.2 mm apart. Afterward, the glued samples are left to cure for 24 hr. after applying a weight of 10 lb. (4.5 kg) to the specimen-base plate assembly. Finally, the test is conducted using the Global Asphalt Mixture Performance Tester (AMPT) at 25±0.5ºC.

TOT data are usually analyzed based on two parameters: critical fracture energy (GC) and crack progression rate (CPR), as detailed elsewhere [35]. The critical fracture energy (GC) represents the energy required to initiate a crack at the bottom of the test specimen after the first loading cycle of the TOT test. This parameter is used to evaluate the crack initiation stage. On the other hand, the crack propagation rate (CPR) is typically used to evaluate asphalt mixes' flexibility and fatigue properties during the crack propagation stage. It represents the reduction in load that is required to propagate the crack through the test specimen under cyclic loading.

Modified Lottman Test

The Modified Lottman test is widely used to evaluate the moisture damage resistance of OGFC mixes. The test was conducted according to AASHTO T 283 [36] , with some modifications as detailed in ASTM D 7064, "Standard Practice for Open-Graded Friction Course" [37]. In this procedure, the ratio of the dry indirect tensile strength (ITS) of three test specimens to the ITS of three-conditioned test specimens is calculated and is used to evaluate the moisture-damage resistance of OGFC mixes; this is known as the tensile strength ratio (TSR). The conditioned mixes are conditioned with a single freeze-and-thaw cycle. Before testing, all samples are placed in a water bath at 25ºC for 2 hrs. It is worth noting that the ITS of the dry samples can also be used to evaluate the resistance of the different mixes to fatigue cracking [38] [10].

Boiling Test

The boiling test is used in Louisiana specifications to evaluate the moisture damage resistance of OGFC mixes. The boiling test is conducted according to DOTD TR 317 [39]. This test consists of placing 250 g of loose mixture in a beaker of boiling water for 10 min. Afterward, the water is drained ,and the sample is removed from the beaker and placed on heavy-duty aluminum foil. A visual inspection is then conducted to evaluate if any mix stripping has occurred.

Functional Advantages of OGFC

Since the 1970s, OGFC has been used as a thin surface course layer on top of a regular DGHMA. The wide popularity of OGFC in Europe and Japan is mainly due to its functional and environmental benefits. According to NCHRP 9-41, OGFC's benefits can be categorized into three primary groups [18]*:*

- Safety benefits;
- Driver comfort benefits; and
- Environmental benefits.

Safety Benefits

Due to their large AV content, OGFC mixes' safety-related benefits include reducing hydroplaning potential, increasing pavement surface friction, and reducing back-splash and spray during wet weather conditions.

Hydroplaning. In the U.S., between 6,000 and 445,000 people are killed and injured in weather-related crashes every year [18]. Approximately 73% of these crashes take place in wet-weather conditions [40]. Further, crash data from 1995 to 2005 showed that approximately 24% of total crashes were weather-related, in which approximately 7,400 people were killed and over 673,000 people were injured [41]. It was also reported that about 60% of fatal weather-related crashes in commercial vehicles occur during rainy weather.

One reason for the increase in highway crashes in wet weather is hydroplaning. Hydroplaning is a wet weather-related hazard that occurs when a layer of water accumulates at the vehicle tire and pavement surface interface, as illustrated in Figure 2 [42]. This phenomenon is usually associated with high speed roads (e.g., interstates) and wet pavements [43]. The presence of a water layer reduces, or more seriously, breaks the contact between the tires and the pavement surface. As a result, the vehicle may not stop when the driver applies the brakes, resulting in severe crashes and highway fatalities.

Figure 2. Hydroplaning mechanism (Source: Google images)

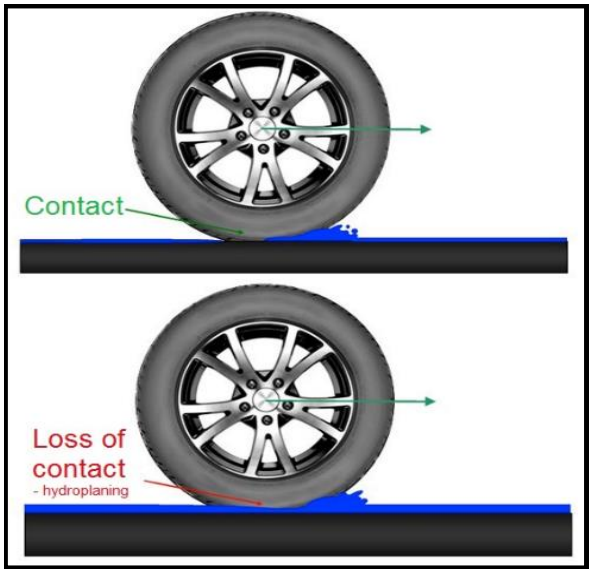

An OGFC can reduce the probability of hydroplaning using three approaches. First, OGFC has high interconnected air voids, which promote permeability and drainage. Consequently, surface water can drain through the OGFC layer, preventing the accumulation of water on the pavement surface. Figure 3 shows the ability of OGFC to drain surface water compared to regular DGHMA. Second, OGFC has a high macro-texture, which provides small channels for water to drain even when the interconnected air voids are clogged [44]. Third, OGFC increases skid resistance (i.e., friction) during wet weather conditions.

Figure 3. OGFC drainage capability [18]

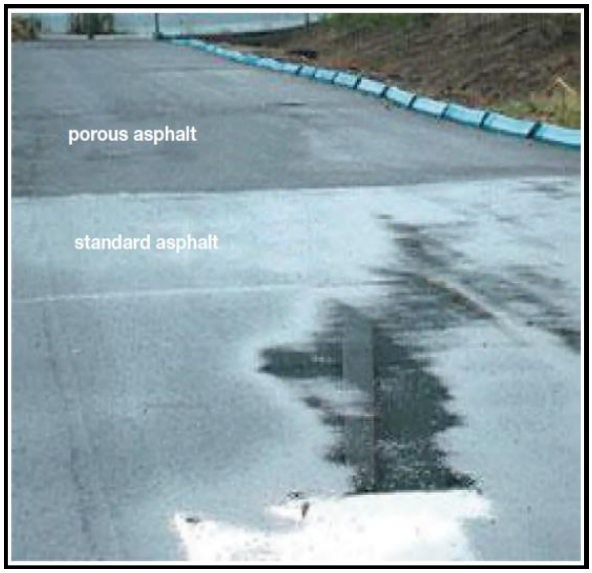

Chen et al. evaluated the skid resistance in terms of Friction Number (FN) for two OGFC test sections and their non-OGFC counterparts. The results indicated good skid resistance for both OGFC and non-OGFC sections, with FN greater than 35. However, the FN of OGFC sections was higher than that of non-OGFC sections, with a minimum value of 50 during the testing period. Additionally, the results showed a significant reduction in the rate of accidents in rainy weather in the OGFC sections [45]. OGFC reduced the accident rate from 1.79 accidents per million vehicles per kilometer (ACC/MVK) to 0.28 ACC/MVK. In Japan, OGFC was applied on pavement sections with high accident rates in rainy conditions, and OGFC sections showed superior performance in different weather conditions. In sunny weather, the number of accidents was low; however, OGFC helped reduce the number of fatalities, as shown in Figure 4. In wet conditions, the number of fatalities was also reduced significantly, as shown in Figure 4. These results may be attributed to the high skid resistance that can be achieved using OGFC even in wet conditions.

Figure 4. Impacts of OGFC on fatality numbers in Japan [46]

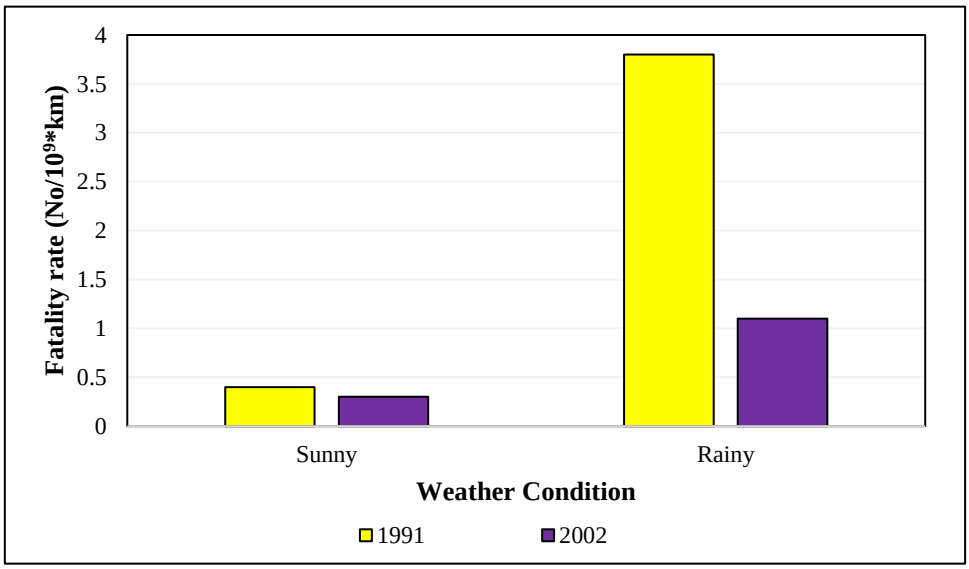

Results also showed that OGFC test sections exhibited better skid resistance than that of DGHMA sections after 1.5 years of service [4]. Similarly, friction test results indicated better skid resistance in the OGFC test sections, with a minimum FN of 36.4 compared to 31.5 for non-OGFC sections in Louisiana [3]. Subsequently, a significant reduction in the accident rate was reported in these sections, especially under wet weather conditions.

Splash and Spray. Splash and spray are hazard phenomena that may reduce road users' safety during wet weather conditions. During or after a rainstorm, DGHMA wearing courses are not able to drain all surface water; therefore, some of the rainwater may remain on the pavement surface. The moving traffic may splash the water into the air in the form of mist (i.e., spray), reducing the visibility of road users. Consequently, the probability of wet

weather-related accidents increases [47]. OGFC has high permeability due to the high interconnected AVs, which prevent the accumulation of water on the pavement surface during or after a rain event.

Flintsch et al. evaluated the relative functional performance of five asphalt and Portland cement concrete (PCC) surfaces under rain and snow conditions [48]. These pavement sections were constructed at the Virginia Smart Road and were evaluated in terms of splash and spray. Among the studied HMA mixes, OGFC provided the best performance in terms of splash and spray based on a qualitative evaluation.

In Louisiana, four OGFC projects were constructed on US-71, I-20, US-61, and US-171 in 2003, 2005, 2007, and 2009, respectively. The splash and spray performance of these projects was qualitatively compared to adjacent Superpave pavement sections [19]. Results indicated that splash and spray can be reduced if OGFC is applied as a wearing surface. Figure 5 compares the splash and spray of two adjacent I-20 projects with OGFC and DGHMA mixtures. As the figure demonstrates, OGFC had almost no splash and spray, which promoted a clear vision for road users during rainy events.

Figure 5. Splash and spray performance for (a) dense-graded mix and (b) OGFC mix [19]

(a)

(b)

Driver Comfort Benefits

Using OGFC as a wearing surface promotes drivers' comfort in terms of two distinctive aspects:

- Degree of vision; and
- Driver speed.

Degree of Vision. During a rainstorm, especially at night, the presence of water film on the pavement surface reflects vehicles' headlights, preventing the driver from following pavement markings. However, since OGFC can rapidly drain rainwater, the water film is reduced at the surface, which promotes adequate visibility for drivers [49], as illustrated in Figure 6.

Driver Speed. Maintaining driver speed during wet weather conditions is considered a driver comfort-related benefit due to the use of OGFC as a wearing surface course [2]. During a rainy event, drivers tend to reduce their speed to avoid hydroplaning and splash and spray when they drive on DGHMA wearing courses. However, with the presence of OGFC, the probability of hydroplaning and splash and spray is significantly decreased, given the rapid drainage of surface water. Therefore, due to the combination of dry surface, reduced splash and spray, and adequate vision, drivers feel more confident and less stressed. Consequently, drivers can use the roadway as they would in normal driving conditions [50].

Figure 6. Pavement marking visibility for (a) dense-graded mix and (b) OGFC mix [18]

(a)

(b)

Environmental Benefits

Noise Reduction. The majority of traffic noise that originates from vehicles occurs due to pavement-tire interaction [51]. This noise reaches its highest level in metropolitan areas where the roads are close to homes and business districts. Traffic noise may have adverse impacts on the quality of life in neighboring homes. Economically, the noise produced may also affect the price of properties in close proximity to highways [18]. One of the most

effective ways to reduce traffic noise is to use OGFC as a wearing surface. This is attributed to the high AV content that enables OGFC to behave as a resonant cavity structure that perfectly absorbs the noise at the pavement-tire interface [40]. Many studies concluded that OGFC can reduce traffic noise by 3-6 dB, which corresponds to a reduction in traffic volume by half [52] [53].

Gu et al. evaluated the benefits of OGFC in terms of noise reduction using the On-Board Sound Intensity Test [4]. Data were collected from two field projects constructed in Elko and Las Vegas by the Nevada Department of Transportation (NDOT) and used in the study. In each project, OGFC and DGHMA pavement sections were constructed to allow a direct comparison. Immediately after construction, OGFC sections in both project locations reduced traffic noise. For example, OGFC exhibited an average sound intensity of 93 dB compared to approximately 96.5 dB for DGHMA in the Elko project. In Las Vegas, OGFC reduced the average sound intensity from 99 dB to 97 dB. These results were attributed to the high porosity of OGFC, which prevents air compression and subsequently decreases the generated noise at the pavement-tire interface.

Kowalski et al. used data from three highway sections to evaluate traffic noise properties [53]. These sections were constructed with DGHMA, SMA, and OGFC. Results indicated that OGFC was the quietest, while SMA was the loudest. The OGFC section produced a sound pressure level (SPL) of 75 and 86 dB for passenger and heavy vehicles, respectively. For the SMA, SPL was 5 and 4 dB higher than those of the OGFC for passenger and heavy vehicles, respectively. Similarly, in France, DGHMA produced a noise level of 76 dB when measured by the Statistical Pass-By Method. On the other hand, the same method showed that OGFCs typically reduce highway noise by 3-5 dB compared to DGHMA [54].

In Switzerland, OGFC provided a noise level reduction compared to DGHMA, as illustrated in Figure 7. In the referenced study, noise reduction of OGFC was investigated based on data collected from four pavement sections in which a DGHMA layer was milled and replaced with an OGFC layer. As shown in the figure, in all field projects, OGFC reduced noise levels by 5.2-7.2 dB [2].

Figure 7. Noise reduction on OGFC pavement section in Switzerland [2]

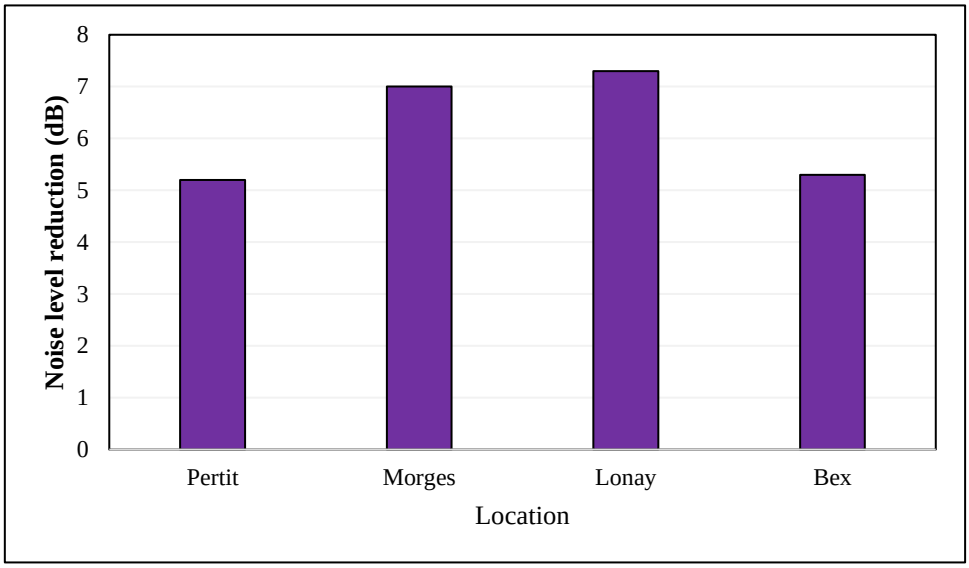

Quality of Water Runoff. Reducing the pollutants in stormwater runoff is another environmental benefit of using OGFC. OGFC can achieve that in two different ways. First, OGFC can retain some of the pollutants in the voids within its structure, which hinders these pollutants from moving to the pavement edge [55]. Second, OGFC reduces or prevents splash and spray, which are known to wash vehicles' engines and bottoms from pollutants; therefore, the use of OGFC may reduce contaminants that are washed from the vehicles [2].

In the Netherlands, pollutant concentrations in runoff water from OGFC and DGHMA pavements were collected and compared [56]. In this study, runoff water samples were collected over a week from a three-year-old OGFC pavement section and a DGHMA pavement section. Results indicated that the concentration of pollutants in OGFC runoff water samples was less than that of the dense-graded pavement, as shown in Table 2.

Table 2. Reduction in runoff water pollutants [56]

Pollutant	% Reduction in concentration
Total Suspended Solids	91
Total Kjeldahl Nitrogen	2
Total Phosphorus	35
Total Copper	40
Total Lead	90
Total Zinc	75
Dissolved Zinc	30

Relation Between Air Voids and Permeability

In NCHRP 1-55, Watson et al. measured the coefficient of permeability of six OGFC mixes and correlated the permeability results to the AV content of each mix [1]. The AVs of all OGFC mixes ranged between 15.7-21.9%, while the permeability values ranged from 80-237 m/day. These data were used to develop a relationship between air AV and the coefficient of permeability for OGFC (K_{OGFC}) mixes. The results indicated a direct relationship between K_{OGFC} and AV (%) content, with a coefficient of determination (R^2) of 0.94. Equation 9 shows the relation between AV content and K_{OGFC}, as reported by Watson et al. [1].

$$K_{OGFC} = 24.87 \times AV - 324.88 \quad (9)$$

Where,
K_{OGFC} = OGFC permeability (m/day); and
AV = air voids content (%).

OGFC Permeability Loss Due to Traffic

Typically, OGFC pavements are designed and constructed to reduce the potential for hydroplaning and minimize splash and spray. However, due to its large AV content, OGFC may be clogged with debris (i.e., dust and soil) over time, resulting in a loss of its permeability [57]. Additionally, other researchers concluded that OGFC experiences a reduction in its permeability due to its densification under traffic loading [57]. Moreover, a reduction in OGFC permeability may be attributed to binder creep (i.e., binder draindown), which starts immediately after construction, especially during the summer months as the binder gets softer [58]. The primary conclusion of all of these studies was that OGFC gradually loses its permeability until a traffic loading of 2×10^6 Equivalent Single Axle Load (ESAL); then, OGFC reaches a plateau in its permeability, at which point the mix resists further densification or clogging [59].

Research Studies on OGFC Durability

Similar to DGHMA, OGFC mix characteristics influence its laboratory and field performance. OGFC should be designed and constructed with a large AV between 18-24% to achieve the primary goal of its construction, which is water permeability. Therefore, a high content of coarse aggregate is typically used to achieve a gap-graded gradation. For this reason, aggregate gradation is the controlling factor of AV in OGFC. Additionally, stiff and flexible binders are desirable for use in OGFC since they promote OGFC long-term durability in terms of raveling, cracking, moisture damage, and permanent deformation

resistance. These characteristics can be attributed to the high bonding properties of stiff binders.

Over the last two decades, numerous studies have been conducted to study the factors that affect the durability of OGFC. Other studies were conducted to develop new generations of OGFC that have enhanced durability compared to existing ones. This section discusses the most noteworthy research efforts that were conducted to enhance OGFC durability. First, research studies that were conducted to evaluate the impacts of aggregate gradation on OGFC performance are discussed. Then, the contributions of different binder additives to the performance of OGFC mixes are reviewed.

Impacts of Air Voids on OGFC Performance

The primary distinctive feature of OGFC is its large AV content [2]. According to NCHRP 9-41, the typical AV content of OGFCs in the United States is between 18-22% [18]. In Louisiana, the AV content of OGFC is required to be in the range of 18-24% [3, 20]. The high AV content of OGFC promotes its functionality by allowing the water to drain horizontally through the interconnected voids which, in turn, prevents hydroplaning and splash and spray [17] [19]. However, the high AV content may have detrimental impacts on the mix's durability. Due to their high AV content, OGFC mixes are easier to be penetrated and are more influenced by water and oxygen [21]. This type of exposure may accelerate the appearance of different types of distress such as raveling, asphalt stripping, and cracking. Therefore, the AV content in OGFC should be controlled adequately in the field to minimize its contribution to durability issues.

Raveling is the primary durability issue with OGFC mixes [18]. Miradi et al. collected and analyzed field data collected from 34 OGFC test sections constructed in the Netherlands to determine the factors that affect OGFC's raveling resistance [60]. The results indicated that binder content is the primary factor that affects OGFC raveling resistance after five years of service. However, AV content was the primary factor that controlled OGFC raveling resistance after eight years. Overall, it was concluded that the optimum AV content is 18.5%.

In a study conducted by James et al., the durability of two OGFC mixes was evaluated [61]. The first mix exhibited adequate field performance after 18 years in service, after which it was replaced due to raveling issues. In contrast, the other mix, which was characterized as a poor mix, was replaced after only eight years due to raveling issues. The original job mix formulas (JMFs) were used to fabricate specimens of these mixes for laboratory evaluation. Both mixes had the same aggregate gradation, except for one sieve (9.50 mm), and the same binder content. Table 3 summarizes the AV content, Cantabro loss, TSR, and number passes in the Hamburg Wheel-Tracking Test (HWT) used for rutting evaluation.

Table 3. Summary of the experimental program conducted by James et al. [61]

Property	Good Mix	Poor Mix
Years in Service	18	8
Reason for Replacement	Raveling	
Road Functional Class	Interstate	
AADT	200,000	50,000
Binder Content (%)	6	6
AV%	15.4	22.2
Cantabro loss	19.3	37.9
TSR	0.78	0.81
No of Passes to Rutting Failure	>20,000	~2,000

Table 3 shows the significant impact of AV content on the performance of OGFC, since all other factors were mostly constant. First, the Cantabro loss percentage of the good and poor mixes was 19.3% and 37.9%, respectively. Further, the AV content was 15.4% and 22.2% for the good and poor-performing mixes, respectively. These results indicate that OGFC mixes with high AV content are more raveling-susceptible compared to OGFC mixes with low AV content. As shown in Table 3, the good mix also showed higher rutting resistance than the poor mix. The good mix required more than 20,000 passes to reach the maximum allowable rutting depth compared to approximately 2,000 passes for the poor mix. With respect to moisture damage resistance, both mixes showed almost the same moisture damage resistance, with a TSR value of approximately 0.80.

Mansour and Putman evaluated the impacts of aggregate gradation and AV content on 10 OGFC mixes [62]. The AV content and Cantabro loss percentages are summarized in Table 4. As shown in Table 4, the binder content ranged from 6.7-7.5%. Additionally, the AV content ranged from 10.0-17.7%. It is noted that mix C had the lowest binder content and the highest AV, which coincided with the highest Cantabro loss, indicating inferior raveling resistance. These results indicate that OGFC's raveling resistance is highly affected by AV and binder contents. Moreover, it is noted that the Cantabro loss percentage of the mixes fabricated with a binder content greater than 7.0% did not exceed 3.5%. However, the mixes prepared with a binder content less than 7.0% showed the highest Cantabro loss compared to the other mixes.

Table 4. Summary of the experimental program conducted by Mansour and Putman [62]

Mix	Binder content (%)	NMAS (mm)	% passing No. 4 (%)	AV (%)	Cantabro Loss (%)
A	7.2	12.5	21.0	17.7	3.4
B	7.3	12.5	15.0	15.6	2.7
C	6.7	12.5	8.0	22.1	13.3
D	7.2	9.5	33.0	18.9	2.7
E	7.3	9.5	22.5	16.4	3.4
F	7.3	12.5	35.0	17.7	3.5
G	7.2	12.5	25.0	17.5	11.5
H	7.5	9.5	48.5	10.0	2.7
I	7.0	12.5	25.0	13.2	5.5
J	7.0	12.5	17.0	12.2	5.6

In NCHRP 1-55, six different OGFC mixes with distinctive field performance were evaluated [1]. Three mixes exhibited good field performance. and the others were classified as poor. Table 5 shows the results obtained from the experimental program, along with the performance indicators used to evaluate the studied mixes. First, the binder content of the mixes with good field performance ranged from 6.0-7.1% compared to 5.8-6.3% for the poor mixes. Additionally, the good mixes showed lower average AV content than the poor mixes. Similar to the results obtained by other researchers [61], the Cantabro loss percentage increased with the increase in AV content and the decrease in binder content. These results indicated that the OGFC raveling resistance can be promoted with either an increase in binder content or a decrease in AV. For moisture damage resistance, both good and poor mixes performed similarly. It is noted that Florida good mixes performed the best in terms of moisture damage resistance, which was attributed to the use of crumb rubber (CR).

For rutting resistance, all the mixes performed well in terms of the maximum allowable rut depth at 20,000 passes, with the exception of the South Carolina poor mix. This mixture exhibited the highest rut depth at 3,200 passes, which corresponds to the highest AV content as presented in Table 5.

Table 5. Summary of the experimental work in NCHRP 1-55 [1]

Mix	NMAS (mm)	Binder Content (%)	AV (%)	Cantabro loss (%)	TSR	Permeability (m/day)	Rut Depth (mm)
Florida–Good	12.5	7.1	17.1	21.9	1.08	80	8.47
Georgia–Good	12.5	6.0	15.7	19.3	0.78	77	8.99
New Jersey–Good	9.5	6.0	19.0	10.21	0.85	186	6.39
Florida–Poor	12.5	6.3	17.7	23.8	0.73	209	6.81
Virginia–Poor	12.5	5.8	21.8	35.1	0.89	107	7.07
South Carolina–Poor	12.5	6.0	22.2	37.9	0.81	237	15.26*

*measured at 3,200 passes

Impacts of Aggregate Gradation on OGFC Performance

The nominal maximum aggregate size (NMAS) is defined as one sieve larger than the first sieve to retain more than 10% of the total aggregate. Most highway agencies in the U.S. use a 12.5 mm NMAS aggregate for OGFC mixes gaped around the 4.75 mm sieve [1]. Additionally, according to a survey conducted on nine highway agencies in the U.S., the percent passing from the 4.75 mm sieve ranges from 10-30%, which results in an adequate AV content [18]. However, many studies showed that using smaller NMAS mixes or increasing the percentage of the aggregate that passes sieve No. 4 may enhance OGFC durability.

Nekkanti et al. examined the impacts of NMAS and percent passing sieve No. 4 on the performance of OGFC mixes [8]. To this end, eight different mixes were fabricated with one granite source and one binder type. The binder was PG 76-22 and was used at a content of 6.0% by weight of the total mix. For moisture damage resistance, hydrated lime was added to the mix at a dosage of 1.0% by the weight of aggregate. The eight mixes were different in two aspects: the NMAS and the percent passing sieve No. 4, and the percent retained on sieve No. 8. Four of these mixes were 12.5 mm NMAS, with percent passing sieve No. 4 ranging from 10-40%. Further, four 9.5 mm NMAS mixes were fabricated with different percent passing sieve No. 4 ranging from 20-50%. The performance of these mixes was evaluated in terms of porosity, indirect tensile strength (ITS), and the Cantabro abrasion test.

For porosity, mixes fabricated with 9.5 mm NMAS aggregate showed lower porosity values than the mixes fabricated with 12.5 mm NMAS aggregate. Additionally, with the increase in percent passing sieve No. 4, the porosity decreased in both mixes. This was expected because more fines were added with the use of 9.5 mm NMAS and more aggregate passing the No. 4 sieve. However, the mixes fabricated with 12.5 mm NMAS aggregate were more sensitive to

the change in percent passing sieve No. 4 than the 9.5 mm NMAS mixes. In terms of ITS, the ITS hit the highest value when the percent passing sieve No. 4 was 30% in both mixes. For the Cantabro test results, all 9.5 mm NMAS mixes exhibited a lower Cantabro loss percentage than the 12.5 mm NMAS mixes. Additionally, with the increase in the percent passing sieve No 4, the Cantabro loss decreased, which indicated enhanced raveling resistance.

The impact of aggregate gradation on the performance of OGFC was also investigated by Hasan et al. [7]. In this study, crushed granite aggregate, one type of binder, and hydrated lime filler were used to prepare OGFC mixes. Three OGFC mixes with different NMAS were investigated in that study: 14, 20, and 25 mm. The performance of each mix was evaluated based on the Cantabro and the ITS tests. Figure 8a compares the results of the AV content and Cantabro loss percentage for the different mixes. The figure shows that the larger the NMAS, the higher the AV content in the mix. Additionally, it can be observed that the Cantabro loss value increased with the increase in AV content in the specimens. Figure 8b shows that AV and Cantabro loss values were highly correlated with an R^2 of 0.91. It was shown that the ITS values decreased when NMAS increased. Additionally, the statistical analysis provided further evidence that the NAMS is a significant factor influencing the tensile strength of OGFC mixes.

Figure 8. Factors affecting Cantabro loss: (a) impact of NMAS on AV and Cantabro loss (b) correlation between AV and Cantabro loss [7]

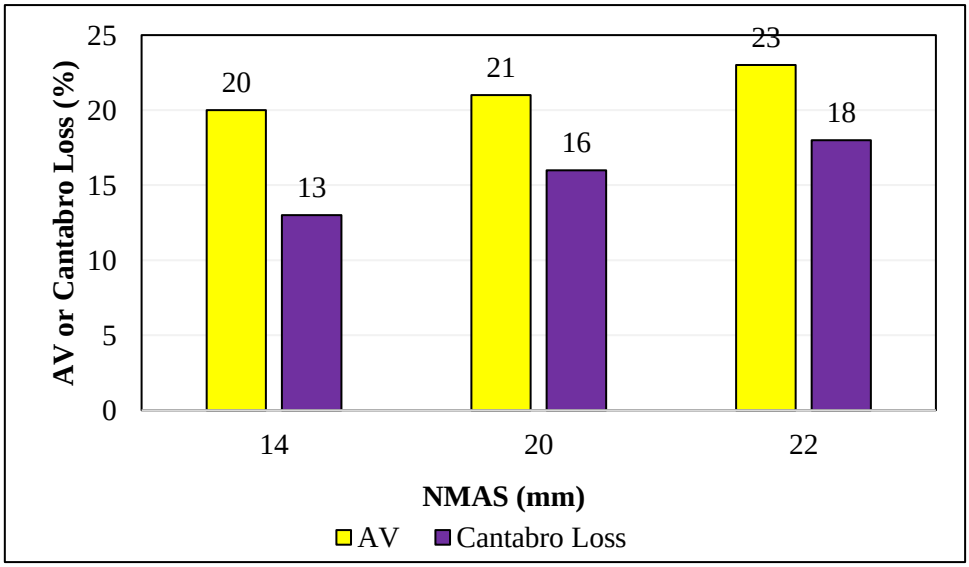

(a)

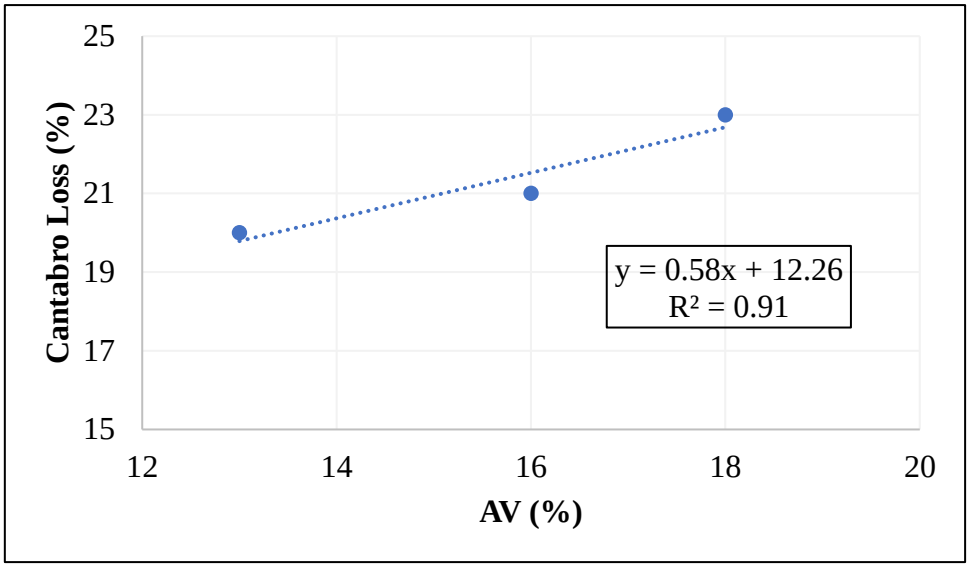

(b)

Chen and Wong evaluated the performance of four OGFC mixes with different aggregate gradations [63]. Two mixes with percent passing sieve No. 4 (4.75 mm) of 30 and 45% were designed. The other two mixes were coarser than the aforementioned mixes, with percent passing sieve No. 4 of 12% and 18%. The percent passing sieve No. 8 (2.36 mm) was kept constant for the four mixes at 7%. The results indicated that the mixes with a high percentage of percent passing sieve No. 4 had lower AV than the other mixes with a low value of percent passing No 4. Additionally, it was shown that an increase in AV caused a corresponding increase in the Cantabro loss percentage, indicating a decrease in OGFC raveling resistance.

Mansour and Putman evaluated 10 OGFC mixes with different aggregate gradations, considering both NMAS and percent passing sieve No. 4 [62]. Among these 10 mixes, three were fabricated with 9.5 mm NMAS aggregate (mixes D, E, and H), and the remaining mixes were prepared with 12.5 mm NMAS aggregate, as presented in Table 4. Similarly, three mixes were prepared with a percent passing sieve No. 4 less than 20%. The remaining mixes were prepared with percent passing sieve No. 4 that ranged from 20-48.5%. Figure 9 presents the impacts of NMAS and percent passing sieve No. 4 on the results of the Cantabro abrasion test. Figure 9a shows the average Cantabro loss value for 9.5 mm and 12.5 mm NMAS mixes. The figure shows that the 9.5 mm NMAS mixes exhibited lower Cantabro loss values than their 12.5 mm counterparts. Similarly, the increase in percent passing sieve No. 4 increased the durability of OGFC in terms of raveling; see Figure 9b. The Cantabro loss values were 4.7% and 7.2% for the mixes fabricated with percent passing sieve No. 4 greater than and lower than 20%, respectively.

Figure 9. (a) Impact of NMAS and AV on Cantabro loss
(b) impact of percent passing No. 4 on AV and Cantabro loss [62]

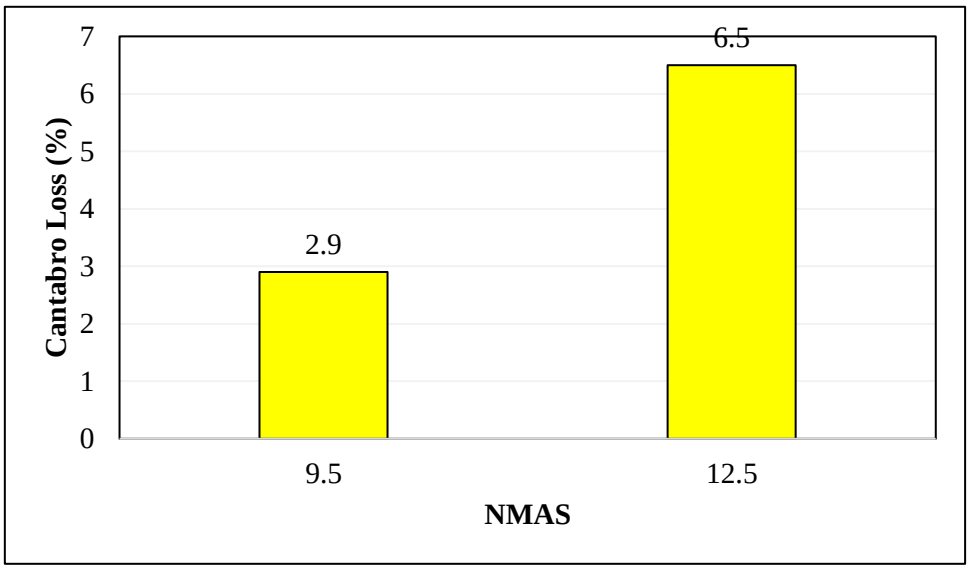

(a)

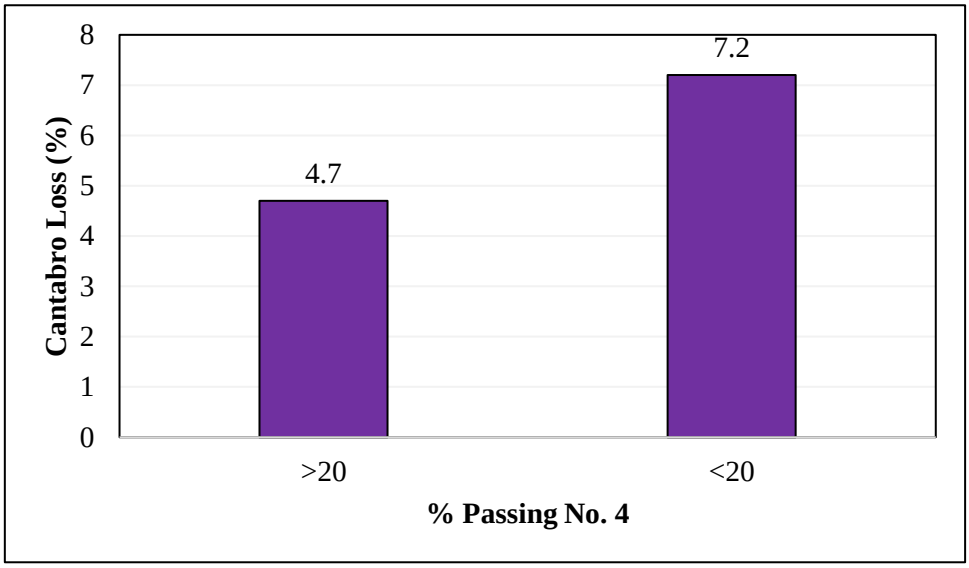

(b)

In NCHRP 1-55, six different OGFC mixes with distinctive field performance were evaluated; see Table 5 [1]. The New Jersey-Good mix was the only mix that was fabricated with a 9.5 mm NMAS gradation. Those mixes were evaluated based on laboratory performance testing. While the New Jersey mix was considered the finest, it did not exhibit the least AV content (19%); see Figure 10. Similar findings were reported by Xie et al., who compared the performance of 12.5 mm and 9.5 mm NMAS OGFC mixes. The AV was 13.8% and 17.1% for the 12.5 mm and 9.5 mm NMAS mixes, respectively [64]. Figure 10 also

shows that the New Jersey mix achieved an acceptable permeability of 186 m/day. Regarding durability, the New Jersey mix showed the highest durability among its counterparts. In terms of raveling resistance, the New Jersey mix exhibited the least Cantabro loss percentage at approximately 10.2%, as shown in Figure 10. Similarly, the 9.5 mm NMAS mix showed the maximum rutting resistance with the least rut depth of 6.39 mm after 20,000 passes of HWT. The New Jersey mix also showed acceptable moisture-damage resistance. The TSR value of the mix was 0.85, which satisfied the minimum requirements of 0.70.

Figure 10. Experimental results of NCHRP 1-55 [1]

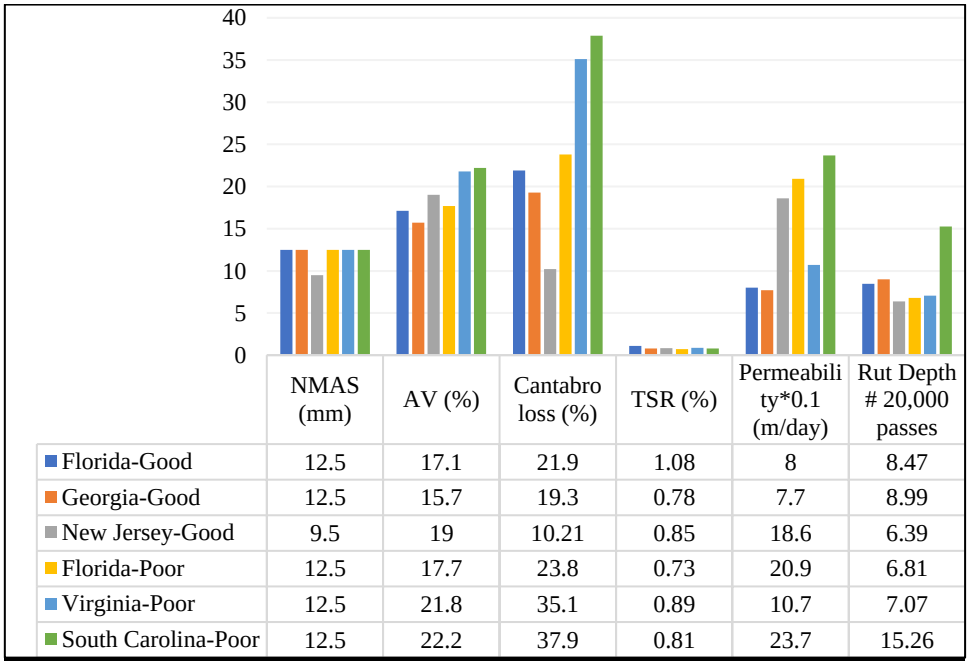

	NMAS (mm)	AV (%)	Cantabro loss (%)	TSR (%)	Permeability*0.1 (m/day)	Rut Depth # 20,000 passes
Florida-Good	12.5	17.1	21.9	1.08	8	8.47
Georgia-Good	12.5	15.7	19.3	0.78	7.7	8.99
New Jersey-Good	9.5	19	10.21	0.85	18.6	6.39
Florida-Poor	12.5	17.7	23.8	0.73	20.9	6.81
Virginia-Poor	12.5	21.8	35.1	0.89	10.7	7.07
South Carolina-Poor	12.5	22.2	37.9	0.81	23.7	15.26

Impact of Percent Passing Sieve #200 on OGFC Performance. In NCHRP 1-55, the impact of percent passing sieve No. 200 on the performance of OGFC was evaluated [1] [61]. In this study, the impact of percent passing sieve No. 200 on the performance of two mixes was assessed. The first mix was classified as a good mix [Georgia-Good (G-G)] and the other was defined as a poor mix [South Carolina-Poor (SC-P)]. These mixtures were modified by adding baghouse fines (BHF) to the original mix at a dosage of 2% and 4%. The control mixes were prepared using one granite aggregate source, a polymer-modified PG 76-22 binder, an anti-stripping agent, and fibers.

Figure 11 summarizes the results obtained in the referenced study. In Figure 11, the number in the legend represents the total percentage of fines in the mix. For example, the mix G-G-2% represents the Georgia-Good mix that was fabricated with 2% fines. As shown in this figure, the AV content decreased with increasing percent passing sieve No. 200 in both mixes. Additionally, the binder film thickness followed the same trend due to the high surface area

of the added BHF. It was expected that with the decrease in binder film thickness, the durability of the OFGC would decrease; however, this was not the case, as shown in Figure 11.

As shown in Figure 11, the Cantabro loss value decreased with increasing percent passing sieve No. 200. For the G-G mix, the Cantabro loss decreased from 19.3 to 9.3% when the percent passing sieve No. 200 was increased from 2 to 6%; see Figure 11. However, Figure 11 shows that the raveling resistance increased noticeably when 2% of BHF was added to the SC-P-1.7 mix. In this case, the Cantabro loss value decreased from 37.9 to 18.9%. Additionally, Figure 11 shows that that the raveling resistance was not significantly enhanced with increasing fine content, at a dosage of 5.6%, for the SC-P mix. In summary, based on the results of the Cantabro abrasion test, it was concluded that the optimum total fine content ranged from 4.5-5.5% [61].

Similarly, OGFC rutting resistance was enhanced by adding more fines to the original mixture. Figure 11 depicts that the original G-G mix showed a rut depth of 8.99 mm after 20,000 passes of HWT, which satisfied the maximum allowable rut depth of 12.5 mm. The rutting resistance of the G-G mix improved with the addition of fines to the original mix. The G-G-3.9% and G-G-6% exhibited rut depth values of 5.54 mm and 5.36 mm after 20,000 passes, respectively.

For the SC-P mix, the rutting resistance was noticeably enhanced by adding fines to the original mix. The original mix (SC-P-1.7%) failed in rutting and exhibited a rut depth of 15.8 mm after approximately 2,540 passes. Yet, by adding 2% fines to the SC-P original mix, almost the same rut depth was measured after 20,000 passes, as shown in Figure 11. Finally, SC-P-5.6% did not fail until it reached pass number 19,202 and hit a rut depth of 12.81 mm after 20,000 passes.

Figure 11. Impacts of percent passing sieve No. 200 on OGFC performance [1]

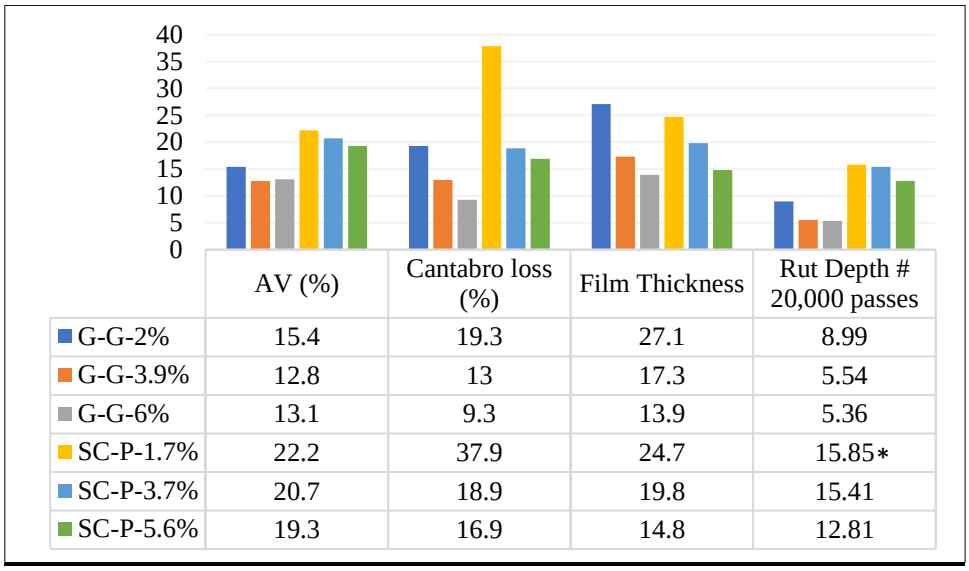

	AV (%)	Cantabro loss (%)	Film Thickness	Rut Depth # 20,000 passes
G-G-2%	15.4	19.3	27.1	8.99
G-G-3.9%	12.8	13	17.3	5.54
G-G-6%	13.1	9.3	13.9	5.36
SC-P-1.7%	22.2	37.9	24.7	15.85*
SC-P-3.7%	20.7	18.9	19.8	15.41
SC-P-5.6%	19.3	16.9	14.8	12.81

*specimens failed at 2,540 passes

Evaluation of the Effects of Binder Modification on OGFC Performance

In this section, the most noteworthy research studies related to the use of binder modification on OGFC were reviewed. This section discusses the following categories of binder modification:

- Polymers;
- Crumb rubber (CR); and
- Warm-Mix Asphalt (WMA) additives.

Evaluation of OGFC Prepared with High Polymer (HP)-Modified Binders. In a research project sponsored by the Florida Department of Transportation (FDOT), the mechanical properties of an OGFC mix fabricated with a high polymer-modified binder were evaluated [65]. Two types of binders and aggregate were used to fabricate four different mixes. Two mixes were fabricated using limestone, of which one was prepared with a conventional polymer-modified binder and the other with a high polymer-modified binder. Further, granite was used to fabricate the two other mixes with the same type of binders. The conventional polymer-modified binder was PG 76-22, which was modified with styrene-butadiene-styrene (SBS) at a dosage of 2-3% by the weight of the binder. The high polymer-modified binder was modified with SBS at a rate of 6-8% HP. Additionally, fibers were added to the mix at a dosage of 0.3% by the weight of the mixture, and a liquid anti-strip was incorporated in the different mixes at a rate of 0.5% by the weight of the binder. The performance of these mixes was evaluated using three mechanical tests: Semi-Circular Bending (SCB), IDEAL-CT, and the Cantabro abrasion tests.

Overall, the results of the SCB test indicated that the mixes that were fabricated with HP showed better fracture resistance than the other mixes; see Figure 12. The SCB test results were used to calculate the flexibility index (FI) and the cracking resistance index (CRI). Both FI and CRI are indicative of the cracking resistance of asphalt mixtures; higher CRI and FI are desirable for adequate cracking resistance. The SCB test was conducted on both unaged and aged samples; aged samples were conditioned in the loose state by placing them in an oven at 95ºC for five days. Overall, FI and CRI results indicated that the use of HP increased the cracking resistance of OGFC mixes.

Figure 12. Impacts of HP on SCB test results [65]

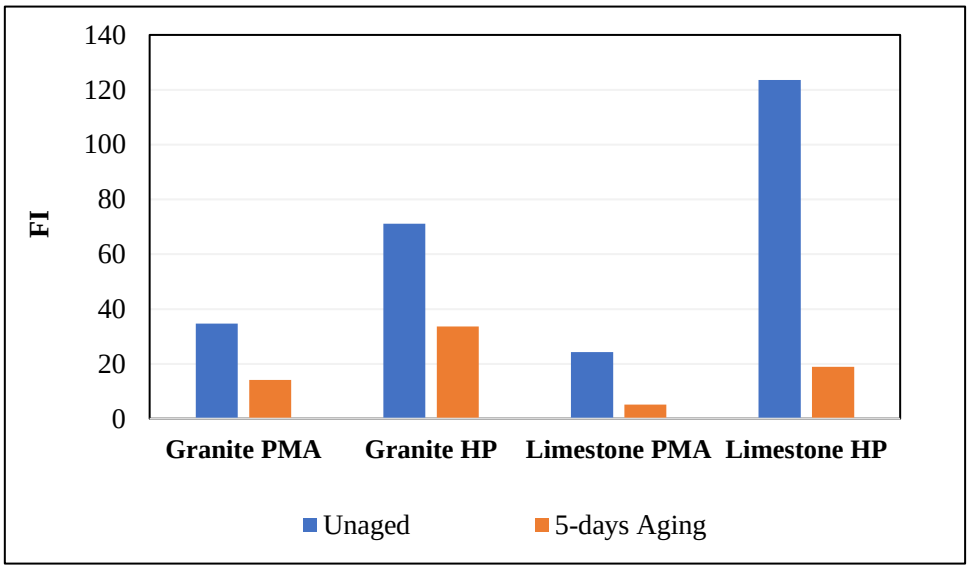

(a)

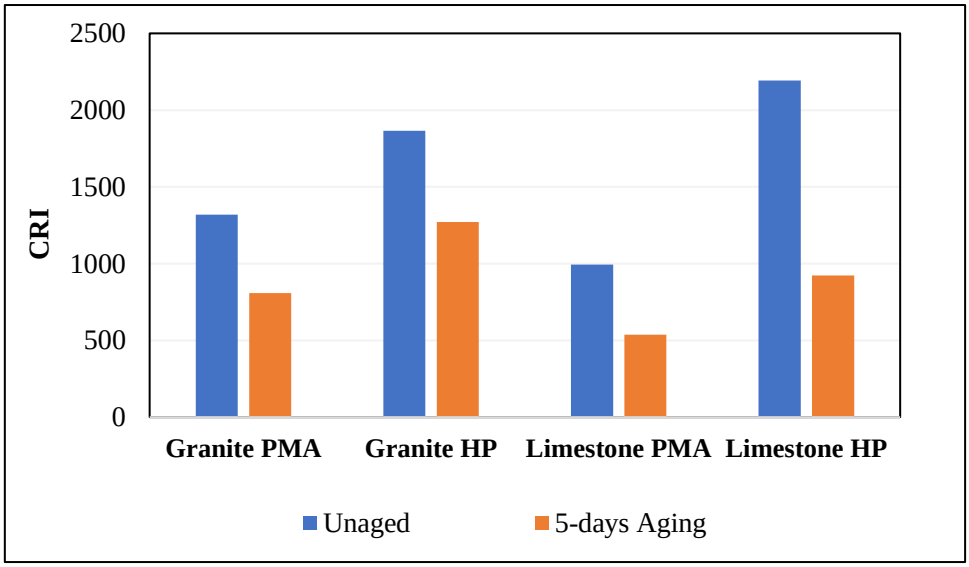

(b)

Similarly, the results of the IDEAL-CT test indicated that HP mixes outperformed other OGFC mixes. IDEAL-CT test results can be analyzed by calculating the CT index, which represents the mixture's resistance to crack propagation; a higher CT index is desirable. As shown in Figure 13, the CT index was 337.4 and 1565.4 for granite-PMB and granite-HP mixes respectively, for unaged samples. Similarly, the crack propagation resistance of unaged limestone-HP was almost four times that of limestone PMB mix. For the aged samples, the same trend was observed, as shown in Figure 13.

Figure 13. Impacts of HP on IDEAL-CT test results [65]

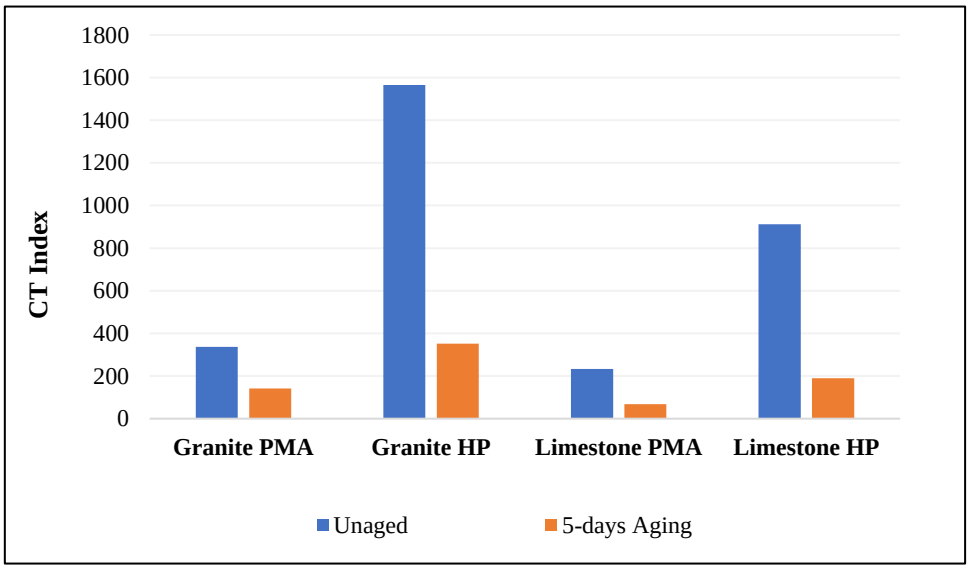

Raveling resistance was evaluated by the Cantabro loss percentage. This test was conducted on samples under three different conditions. The first group of samples was tested unaged. The second and third groups were aged for five and ten days in an oven at 95°C while the mix was loose, respectively. Figure 14 shows that the HP samples were less prone to raveling by showing less weight loss than the other mixes at all aging conditions. Additionally, the results indicated that aging had a significant impact on OGFC raveling resistance.

Figure 14. Impacts of HP on Cantabro test results [65]

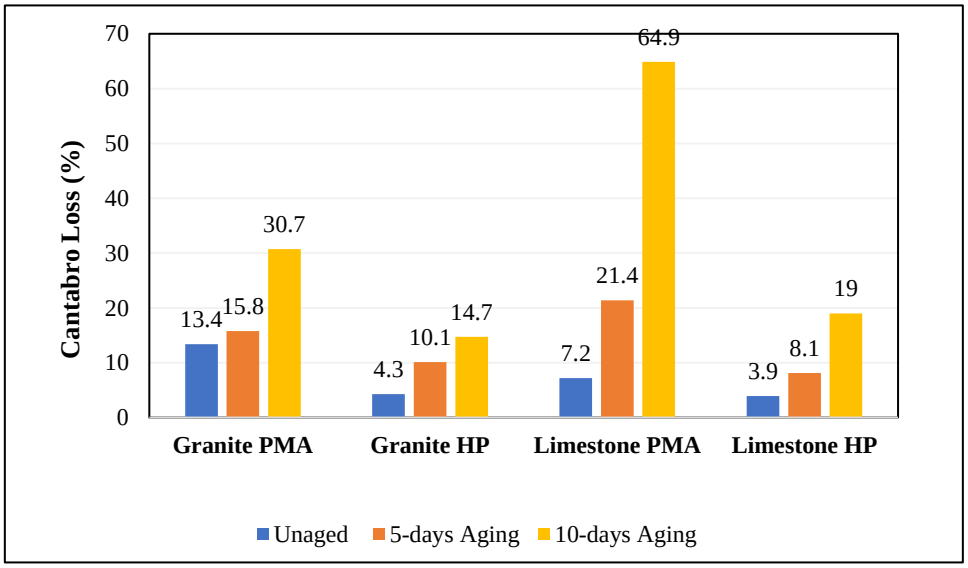

Zhang et al. evaluated the performance of four OGFC mixes with an HP modified binder [12]. Two types of aggregate were used to fabricate the samples. Basalt was used for the coarse aggregate, while limestone was used for the fine aggregate and filler. The base binder was PG 64-22 and was modified with SBS at a rate of 4.5%, 6.0%, 7.5%, and 9.0% by the weight of binder to fabricate the four mixes. Additionally, 0.3% polyester fibers by weight of the aggregate were added to the mixtures to control draindown. The performance of these mixes was evaluated using the Cantabro test, HWT test, and TSR. The Cantabro abrasion test was also used to evaluate the effect of moisture on OGFC raveling resistance. This was achieved by conducting a Cantabro abrasion test on two groups of mixes. The first group was the standard group, which was kept at 20°C for 20 hrs. before testing. The second group was the immersed group, which was immersed in a 60°C bath for 48 hrs. followed by a 20°C bath for 2 hrs., before being tested to simulate moisture damage.

The results indicated that OGFC resistance to raveling increased with the increase in SBS content in the mix. This was observed by the decrease in weight loss in the Cantabro test with the increase in SBS content in both groups. Additionally, the ratio of immersed Cantabro loss to the standard Cantabro loss (i.e., immersed/standard ratio) was used to evaluate the moisture-damage resistance of OGFCs. Further, the results showed that with an increase in SBS, the immersed/standard ratio decreased, indicating better moisture-damage resistance.

In the same study, the HWT test was conducted at three temperatures: 50°C, 60°C, and 70°C. The results of this test were analyzed using two factors. The first factor was the rut depth after a specified number of passes at a predetermined temperature. The second factor was the creep slope, which characterizes the inverse of deformation rate (i.e., wheel passes per 1 mm rut depth) in the creep phase of the deformation curve. For the rut depth, the final rut depth

decreased gradually by adding more SBS to the mix at all test temperatures. Additionally, the creep slope decreased significantly with the addition of SBS, especially at a temperature of 70°C.

For TSR, moisture damage resistance increased gradually with the increase in SBS in the mix. It is noted that the impact of SBS was substantial when it was added to the mix at a dosage up to 7.5%. Beyond that, the effect of SBS was negligible. Therefore, the authors recommended 7.5% as the optimum dosage of SBS in OGFC mixes based on their results.

Chen et al. investigated the impacts of high-viscosity asphalt on OGFC performance [66]. Three binder types were used to fabricate the samples: conventional asphalt (CA), polymer-modified asphalt (PA), and high-viscosity asphalt (HA). The absolute viscosities of CA, PA, and HA at 60°C were 3,560, 16,580, and 326,540 poise, respectively. For mixes containing CA and PA, 0.30% fiber content by weight of asphalt mixture was added to the mixture to control draindown. The performance of these mixes was evaluated in the laboratory using the falling head device, HWT test, Cantabro abrasion test, IDT, and draindown test. The falling head device was used to evaluate the permeability of the prepared mixes. Overall, all of the mixes showed similar permeability values of at least 0.20 cm/sec., which was greater than the minimum acceptable permeability value of 0.01 cm/sec.

The HWT test was conducted on OGFC samples rigidly fixed in a 300x300x50 mm steel frame at a temperature of 60°C, which were subjected to a pressure of 700 kPa to evaluate OGFC resistance to permanent deformation. In this study, OGFC rutting resistance was characterized by dynamic stability (DS), which represents the number of load cycles to induce 1 mm rut depth during the last 15 min. of an hour of testing [67] [68]. Mixtures with high DS values are more stable and durable and would exhibit less rutting depth in the field. DS can be calculated based on Equation 10:

$$DS = \frac{(t_1 - t_2)\, x\, N}{d_1 - d_2} \quad (10)$$

where,
DS = dynamic stability (cycle/mm);
t_1 and t_2 = 45 and 60 min., respectively;
d_1 and d_2 = deformation at t_1 and t_2, respectively; and
N = number of passes/min.

The results of DS showed that OGFC rutting resistance was sensitive to binder type. Mixtures fabricated with PA and HA showed higher DS values than those of CA. Additionally, OGFC samples prepared with PA and fibers showed higher resistance to permanent deformation than the samples prepared with only PA.

To investigate OGFC raveling resistance, Cantabro abrasion test results were used to calculate the weight loss of OGFC samples after the application of a specific number of cycles in the Los Angeles abrasion drum without the steel balls. The results indicated that the samples fabricated with CA were the least resistant to raveling, with a weight loss of more than 30%. However, the samples fabricated with HA and PA + fibers showed the highest resistance to raveling, with weight losses of 7.5 and 10 %, respectively.

The resilient modulus (MR) and IDT test parameters were used to characterize the strength of OGFC in the aforementioned study. The results showed that OGFC samples fabricated with HA and PA + fibers had the highest MR and IDT values compared to the other mixes. Moreover, the measured draindown values showed that the fibers were effective in controlling OGFC draindown. Adding the fibers to CA and PA decreased the draindown significantly. Interestingly, HA mixes with no fibers showed the least draindown among the other mixes.

Evaluation of OGFC Containing Crumb Rubber. Shirini and Imaninasab evaluated the performance of OGFC mixes containing a polymer- and crumb rubber (C) modified binder [69]. In the aforementioned study, five mixes were prepared with limestone aggregate and PG 58-22 binder. The control mix was prepared without any additives. The second mix was prepared with a PG 58-22 base binder modified with 5% SBS. The remaining three mixes were prepared with 10, 15, and 20% by the weight of binder CR modifiers.

The optimum binder content was determined based on the results of the Cantabro abrasion test and AV. The OBC was the binder content that produces a mix with a minimum AV of 18% and a maximum weight loss of 20% for the unaged specimens. The results of the Cantabro abrasion test showed that SBS-OGFC exhibited comparable performance to the control mix at all binder contents (BC). However, the mixes that contained CR showed lower resistance to raveling compared to the control mix at lower BC. At 4.5% BC, CR-OGFC showed a weight loss value higher than that of the control mix. This observation can be attributed to the reduction in BC caused by the addition of CR. With the increase in BC, the difference in weight loss values decreased exponentially until it was negligible at a BC of 6%. Based on these results, the OBC was measured and reported, as shown in Figure 15. Figure 15 shows that the control, SBS, and CR-10% mixes required a BC of 5.3% to satisfy the AV and Cantabro loss requirements. However, with the increase in CR content in the mix, the OBC increased to account for the absorbed binder in the mix due to the addition of CR.

Afterward, a series of laboratory tests were conducted to evaluate the performance of different OGFC mixes. In terms of the draindown test, OGFC mixes containing CR (CR-OGFC) exhibited the lowest draindown values. Additionally, with the increase in CR content in the mix binder, draindown tended to decrease. These results may be attributed to the high

viscosity of the CR-modified binder. It was also noted that OGFC mixes modified with SBS (SBS-OGFC) showed lower binder draindown values than the control mix.

Figure 15. OBC for different mixes [69]

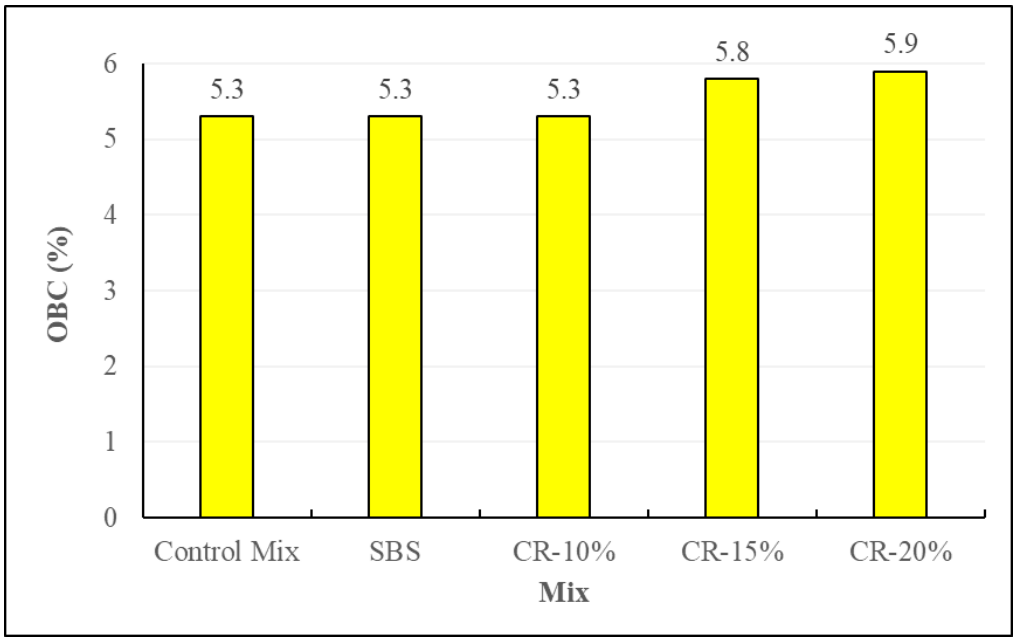

For permeability, the use of CR in OGFC mixes resulted in a gradual decrease in OGFC permeability. For example, the control mix showed a permeability coefficient of 122.9 m/day; however, adding 10%, 15%, and 20% of CR decreased OGFC permeability to 113.9, 85.9, and 54.4 m/day, respectively. Additionally, SBS-OGFC showed lower permeability than the control mix at 107.8 m/day. It is also noted that both SBS-OGFC and CR-10%-OGFC showed similar permeability. However, adding more crumb rubber to the mix decreased OGFC permeability.

TSR and rut depth values were used to compare the performance of the different mixes and assess their durability. TSR results showed that the introduction of CR into OGFC would result in acceptable resistance to moisture-induced damage. OGFC mixtures fabricated with 10 and 15% CR-modified binder showed the highest resistance to moisture damage, with TSR values of 86.2 and 80.9%, respectively. However, the remaining mixtures showed high moisture damage susceptibility, with TSR values of less than 65%. Finally, HWT test results showed substantial improvement with the use of SBS and CR in OGFC. The results indicated that the control mix exhibited a rut depth of 8.5 mm, which was almost three times the rut depth exhibited by the remaining four mixes.

In NCHRP 1-55, Watson et al. compared the performance of three mixes that were prepared with different binder modifiers (e.g., SBS and GTR) without fibers to a control mix prepared

with SBS-modified binder and 0.40% cellulose fibers; see Table 6 [1]. SBS was added at a rate of 2.5% by weight of the binder to the control mix with fiber and to another mix without fiber. CR was blended at a dosage of 12% by weight of the binder (Mix 2). Additionally, a third mix was prepared with 7.5% of SBS (Mix 3). The binder that was used in this study was PG 76-22. The primary objective of this experimental program was to evaluate if fibers are necessary for OGFC mixes containing SBS- and CR-modified binders.

From the results presented in Table 6, it can be concluded that CR-OGFC had the highest OBC of 6.7%. These results were expected since more binder is needed to compensate for the high percentage of CR that was added to the mix. For AV, the removal of fibers increased the AV content in OGFC; however, it did not impact the permeability. Mix 2 and Mix 3 showed AV contents of 13.9 and 14.9%, respectively, and both mixes had the lowest permeability coefficients. For binder draindown, the presence of fiber decreased draindown significantly for the mixes containing SBS (Mix 1, with fibers). OGFC mixes fabricated with 2.5% and 7.5% SBS-modified binder without fibers exhibited 0.3 and 1.0% binder draindown, which was significant. However, Mix 2 (CR-OGFC without fibers) did not show any signs of binder draindown, although it did not contain fibers.

Table 6. Impacts of binder modifications from NCHRP 1-55 [1]

Factor	Mix 1 (2.5% SBS)		Mix 2 (12% CR)	Mix 3 (7.5% SBS)
	w/ fibers	w/o fibers	w/o fibers	w/o fibers
OBC (%)	6.0	6.0	6.7	6.0
AV (%)	15.4	16.3	13.9	14.9
Permeability (m/day)	80	79	33	37
Draindown (180^{o}C)	0	0.30	0	1.00
Cantabro loss (%)	19.3	12.3	12.1	4.7
LWT (@ 20000 passes) (mm)	8.99	10.56	10.84	6.89
TSR (%)	0.78	0.79	0.95	0.88

The durability of the aforementioned mixes was evaluated using the Cantabro abrasion test, HWT test, and TSR. All mixes showed acceptable durability. Mix 3 showed the highest raveling resistance, followed by Mix 2 (CR-OGFC). However, Mix 2 (CR-OGFC) showed the least susceptibility to moisture induced-damage, with a TSR value of 95%. The researchers reported that all mixes satisfied the maximum rut depth after 20,000 passes of HWT.

Sangiorgi et al. investigated the feasibility of using crumb rubber to produce quality OGFC [70]. To this end, two mixes were prepared with an aggregate gradation that conformed to the

Italian specifications. In these mixes, limestone filler was used at a rate of 6% by the weight of the dry aggregate. Additionally, SBS-modified binder was used to fabricate the control mix and crumb rubber modified OGFC mix (CR-OGFC). For CR-OGFC, the crumb rubber was added directly to the heated aggregate at a dosage of 1% by the weight of the aggregate through a dry process. It is worth mentioning that fibers were not added to the mixes in the aforementioned study.

From the aforementioned study, Table 7 shows the impacts of the inclusion of CR on the volumetric properties of OGFC. Overall, the use of crumb rubber in the OGFC mix decreased AV content. The AV content was 14.9% and 18.2% for the CR-OGFC and the control mix, respectively. Consequently, the permeability of OGFC containing CR was 0.96 x 10^{-3} m/s compared to 1.67 x 10^{-3} m/s for the control mix. However, both values satisfied the Italian specifications for the permeability of OGFC.

Table 7. Impacts of CR on the volumetric properties of OGFC [70]

Volumetric Properties (%)	Control Mix	CR-OGFC
VMA	29.0	25.7
VA	18.2	14.9
VFA	37.1	42.1

The results of the aforementioned study also showed that CR-OGFC exhibited high resistance to moisture-induced damage compared to the control mix. The TSR values were 93.7% and 75.4% for the CR-OGFC and control mix, respectively. These results were attributed to the bonding properties of the mastics that contained crumb rubber. The Cantabro abrasion test was used to compare the raveling resistance of both mixes. The results indicated that CR-OGFC samples were more resistant to raveling than the control mix. On average, CR-OGFC and the control mix exhibited weight loss values of 11.4% and 14.7%, respectively.

Jiao et al. investigated the performance of OGFC mixes containing crumb rubber and Tafpack Super (TPS) [71]. First, the effects of adding CR and TPS on the properties of the base binder were evaluated. To this end, different percentages of CR and TPS were added to the base binder, which was a polymer-modified binder. Afterward, the rheological properties of the binder were evaluated. The results indicated that the introduction of TPS and CR improved the consistency and high-temperature stability of the binder. Most importantly, CR and TPS enhanced the viscosity of the binder, which may promote the durability of OGFC. Based on these results, the optimum dosage of CR and TPS was 10% and 8% by weight of the binder, respectively.

To evaluate the impact of CR and TPS additives on the durability of OGFC in the aforementioned study, three mixes were prepared [71]. The first mix was prepared with SBS-modified binder at a rate of 4% by weight of the binder and was defined as the control mix. The control mix was then modified by adding 10% CR and 8% TPS to the mixture. The OBC was determined based on the results of the Cantabro and draindown tests. The OBC of mixes containing SBS, CR/SBS, and TPS/SBS were 4.8%, 5.2%, and 5.0%, respectively. The first observation was that the presence of CR and TPS increased the OBC and consequently increased the binder film thickness, which may result in more durable OGFC mixes.

OGFC rutting resistance was investigated using the HWT test in the aforementioned study [71]. The dynamic stability (DS) parameter was used to analyze the data. The results indicated that the introduction of CR and TPS increased the resistance of OGFC to permanent deformation. The measured DS values were 3684, 5203, and 6428 passes/mm for the control, CR-OGFC, and TPS-OGFC, respectively.

TSR was used to evaluate the resistance of different OGFC mixes to moisture-induced damage. The control mix showed a TSR value slightly above 80%. However, because of the good bonding properties of CR and TPS, the mixes containing 10% CR and 8% TPS showed TSR values that were 7.1% and 11.5% higher than the control mix. These results indicate that CR and TPS can be used to produce quality OGFC mixes that resist moisture-induced damage.

Similar to previous studies, the introduction of CR and TPS reduced the interconnected air voids and subsequently decreased OGFC permeability. The coefficient of permeability of the control mix was 0.295 cm/sec., compared to 0.253 and 0.232 cm/sec. for CR-OGFC and TPS-OGFC, respectively. These results may be attributed to the increase in the binder film thickness and the size of aggregate particles.

Evaluation of OGFC Containing Warm-Mix Asphalt (WMA) Additives. The use of WMA additives has received substantial interest for improving OGFC durability. WMA additives encompass technologies that facilitate asphaltic mixtures to be mixed and compacted at lower temperatures compared to HMA by lowering binder viscosity through the addition of organic or chemical additives or foaming processes [72] [73]. Additionally, WMA has other benefits in terms of workability, cost, and environmental sustainability [73]. WMA additives can be categorized into three broad categories: foaming bitumen technologies, chemical additives, and organic additives [74].

Foaming Bitumen Technologies. Numerous foaming bitumen technologies are available for reducing asphalt binder viscosity through the addition of a small amount of cold pressurized water to preheated asphalt binder [75]. As the temperature of the water-bitumen blend increases, the water evaporates, and the steam is encapsulated in the binder. Steam can

temporarily expand binder's volume and reduce its viscosity, thereby improving asphalt mixture workability. As the expansion gradually dissipates over time, the binder returns to its original characteristics [76]. Foaming bitumen technologies can be grouped into two different categories: water containing additives and water-based technologies. Advera and Aspha-min are examples of water containing additives. These additives are finely crushed powders that have water in their structure. As the temperature increases, the water evaporates, resulting in a foamed binder. In water-based technology, special equipment is used to inject binder with water.

Chemical Additives. WMA chemical additives are among the most recently developed WMA additives. Unlike other WMA additives, chemical additives enhance the ability of the asphalt binder to coat aggregate particles by reducing the frictional forces at the binder-aggregate interface rather than reducing binder viscosity [77]. WMA chemical additives are usually formed by a package of additives such as emulsions, surfactants, polymers, aggregate coating agents, and anti-stripping agents.

Organic Additives. Organic WMA additives are used to reduce asphalt binder viscosity by adding an organic wax to the asphalt binder during mixing [76]. As the temperature decreases, the additive crystalizes resulting in a lattice structure, which in turn enhances asphalt binder stiffness and the resistance to permanent deformation [74]. Typically, organic WMA is formed by a long chain of hydrocarbon atoms, which has a melting point near 212^{o} F (100^{o} C). Therefore, it is usually recommended to select an organic additive with a melting point higher than the in-service temperature; otherwise, a significant reduction in permeant deformation resistance will be experienced [73].

WMA OGFC-Performance Studies. Wurst et al. examined the laboratory performance of OGFC mixes fabricated with WMA technology [78]. Draindown, abrasion resistance, and permeability parameters were evaluated for two WMA mixes (Evotherm and foamed mixes) and compared to traditional HMA OGFC. Five mixes were prepared in this study: two HMA, two Evotherm WMA, and one foamed WMA. HMA and Evotherm WMA mixes were prepared with and without fibers. However, foamed WMA mix was fabricated without fibers. Fibers were added to the mixes at a rate of 0.3% by weight of the mix. The Evotherm used in this study contained a liquid anti-stripping agent (ASA); however, all mixes were prepared with hydrated lime as ASA at a dosage of 1% by weight of the aggregate. Evotherm was added, and water was injected for foamed WMA into the binder at a rate of 0.5% and 2% by weight of the binder.

In the aforementioned study, OBC was determined based on draindown tests. For each mix, two draindown specimens were prepared using a binder content that ranged from 5-7.5% at an interval of 0.5%. The results indicated that the specimens prepared with fibers did not

exhibit any signs of draindown. For specimens prepared without fibers, HMA failed to satisfy the maximum draindown requirement at 6.2% BC, compared to 7.2% for both WMA mixes. Additionally, the analysis indicated that the OBC values for HMA and WMA were 5% and 5.7%, respectively. The higher OBC for WMA indicated the effectiveness of WMA additives to provide OGFC with a thick asphalt film, which may help achieve improved durability in the short and long terms without the need for introducing fibers in the mix.

After the OBC was determined in the aforementioned study, uncompacted samples were prepared to investigate moisture susceptibility using the boiling test. The results indicated that all mixes showed acceptable moisture-damage resistance, regardless of mix type. The author attributed these results to the type of aggregate that showed historically acceptable resistance to stripping and the hydrated lime used in the mixes.

The aforementioned study evaluated the mixes' permeability using the falling head test. The results of the permeability test indicated that the use of fibers in OGFC reduced permeability [78]. The permeability of HMA-OGFC with fibers was almost half that of the HMA-OGFC mixes. Additionally, WMA-OGFC mixes showed comparable permeability values to HMA-OGFC.

Finally, the results of the Cantabro test indicated that HMA fabricated with fibers outperformed HMA fabricated without fibers for aged and unaged conditions [78]. At the OBC, OGFC mixtures containing Evotherm with no fibers showed comparable raveling resistance to HMA mixtures containing fibers under unaged conditions. For aged specimens, OGFC mixes containing both WMA additives showed higher raveling resistance than HMA-OGFC mixes with fibers. These results may be attributed to the higher OBC in WMA mixes compared to HMA mixes. Overall, the results of this study supported the idea of using WMA technology in OGFC, as WMA ensured both the functional and durable performances of OGFC in terms of permeability and raveling resistance [78].

In another study, the performance of OGFC mixes containing an organic warm-mix additive (Sasobit) was evaluated [79]. For this study, two mixtures were fabricated in the laboratory. The first mix was HMA-OGFC and was fabricated with a high viscosity binder at a rate of 5.4% by weight of the mix. Additionally, fibers were used in the mix at a dosage of 0.25% by weight of the binder. The second mix was WMA-OGFC and was fabricated with the same components, but Sasobit was used in the mix at a rate of 2.5% by weight of the binder. The performance of these mixes was evaluated in terms of permanent deformation resistance, reveling resistance, draindown, porosity, and TSR.

For rutting resistance, SGC samples were fabricated at different temperatures to evaluate the impact of mixing temperature on OGFC performance. For HMA-OGFC, the specimens were mixed at 165ºC. However, the mixing temperature of WMA-OGFC varied from 135 to 155ºC

with a 5ºC interval. Results indicated that with the increase in mixing temperature, WMA-OGFC resistance to permanent deformation increased. Below 145ºC, WMA-OGFC showed low permanent deformation resistance compared to HMA-OGFC. However, above 145ºC, both WMA-OGFC and HMA-OGFC exhibited comparable rut depth. Additionally, the results of other performance tests indicated that WMA-OGFC prepared with the organic additive exhibited the same performance as HMA-OGFC; see Table 8.

Results presented in Table 8 show comparable performance for WMA-OGFC and HMA-OGFC. It is noted that WMA-OGFC had a higher porosity than that of HMA OGFC, which increased the permeability of the WMA-OGFC mix. Similar results were reported in a related study [78]. However, WMA-OGFC showed a slight decrease in raveling and moisture damage resistance compared to HMA-OGFC, as indicated by the weight loss percentage and TSR values in Table 8. However, this decrease did not compromise OGFC performance, as TSR and weight loss values were within the acceptable range.

Table 8. Effects of adding Sasobit to OGFC mixes [79]

Performance Factor	HMA-OGFC	WMA-OGFC
Cantabro Loss (%)	14.8	15.6
Draindown	19.0	21.0
Porosity (%)	19.8	20.3
TSR (%)	84.3	83.2

Goh and You prepared four mixes to evaluate the mechanical properties of OGFC containing reclaimed asphalt pavement (RAP) and a WMA additive at a rate of 0.25% by weight of the total mix [10]. These mixes included two HMA-OGFC and two WMA-OGFC mixes, with and without RAP. For HMA-OGFC mixes, mixing and compaction temperatures were 160ºC and 150ºC, respectively, compared to 135ºC and 110ºC for WMA-OGFC mixes. The studied mixes were evaluated based on the Compaction Energy Index (CEI), permeability, ITS, and dynamic modulus |E*|. It was shown that mixtures containing the WMA additive had lower CEI values, indicating lower compaction effort and energy consumption during field compaction. In terms of permeability, HMA mixes showed a higher flow rate compared to WMA-OGFC. However, all mixes satisfied the minimum requirement of OGFC permeability. Additionally, WMA mixes exhibited slightly lower |E*| values than HMA mixes. Finally, ITS was used as an indicator of fatigue cracking resistance. WMA mixes without RAP showed the least resistance to fatigue cracking. However, WMA mixes with RAP showed the highest ITS, indicating their ability to resist fatigue cracking.

Frigio et al. evaluated the volumetric and mechanical properties of two WMA-OGFC mixes [11]. Additionally, an HMA-OGFC mix was prepared as a control mix with 15% RAP. For

WMA-OGFC, two chemical WMA additives designated as C1 and C2 were used at a rate of 0.42% and 0.70% by binder weight. CEI, ITS, Cantabro loss, Semi-Circular Bending, and repeated ITS tests were conducted to compare the performance of the prepared mixes. CEI results indicated that WMA-OGFC mixes had significantly lower CEI values than HMA-OGFC mixes. The ITS test was conducted on dry and wet samples. In the dry condition, all mixtures showed similar ITS values; however, WMA-OGFC showed ITS values that were significantly lower than HMA-OGFC when the test was conducted on wet specimens. These results can be attributed to the low production temperature (i.e., 120ºC) that did not allow the binder to completely coat the aggregate. Similarly, the Cantabro test was conducted on samples in dry and wet conditions. In the dry condition, all mixes showed similar raveling resistance as presented with the same particle loss percentage. However, in wet conditions, WMA-OGFC showed less raveling resistance compared to HMA mixes. Dry and wet samples were also evaluated using the SCB test. In the dry condition, all mixes exhibited almost the same fracture toughness, indicating similar resistance to crack propagation. However, in wet conditions, HMA-OGFC performed better than WMA-OGFC.

Seepage Analysis Using Finite Element Modeling

Since the early 1990s, Finite Element modeling (FEM) has become a powerful tool for solving many complex engineering and scientific problems including pavement structures. Among the existing numerical models, SEEP/W has been extensively used to simulate many drainage problems in pavement engineering due to its accuracy [80]. SEEP/W is a numerical model that can be used to simulate water flow through porous media in real-life applications. In SEEP/W, it is assumed that the flow in the unsaturated soil above the water table follows Darcy's law, similar to the flow in saturated soil [81]. In SEEP/W, the governing formula is Richards' equation, as presented in Equation 10:

$$\frac{\partial}{\partial x}\left(k_x \frac{\partial H}{\partial x}\right) + \frac{\partial}{\partial y}\left(k_y \frac{\partial H}{\partial y}\right) + Q = \frac{\partial \Theta}{\partial t} \quad (10)$$

where,
H = total head;
k_x = hydraulic conductivity in the x-direction;
k_y = hydraulic conductivity in the y-direction;
Q = applied boundary flux;
$\boldsymbol{\Theta}$ = volumetric water content; and
t = time.

Seepage Analysis Using SEEP/W

Mousa et al. utilized the results of a calibrated SEEP/W FE model to introduce guidelines for using crack sealing applications and to minimize water entrapment under cracks for low-volume roads [82]. In the referenced study, SEEP/W was used to model a pavement section in both steady-state and transient analyses. In the steady-state analysis, the calibrated SEEP/W model accurately predicted the volumetric water content (VWC) at the mid-depth of the base layer. Using Ground Penetrating Radar (GPR) data, the VWC at the mid of the base layer was estimated to be 0.30, which was similar to the VWA of SEEP/W at 0.31. Similarly, SEEP/W was able to predict the VWC at mid-depth of the base layer in the transient analysis.

In another study, SEEP/W was used to simulate water flow in flexible pavement using transient analysis [83]. The results of SEEP/W were then compared to the result of DRIP software. Based on the parametric studies conducted, the authors concluded that SEEP/W is an adequate tool to evaluate pavement subsurface drainage systems. However, DRIP software yielded conservative results, as it employs one-dimensional water flow under fully saturated conditions.

Similarly, Yoo et al. utilized SEEP/W to simulate the flood runoff reduction effect of four infiltration facilities [84]. The authors concluded that SEEP/W yielded reasonable results; therefore, SEEP/W was recommended to study water infiltration in such facilities.

Numerical Studies of OGFC Hydraulic Characteristics

Over the last two decades, many studies have evaluated the different factors that contribute to OGFC drainage performance. It has been concluded that OGFC drainage capacity is strongly dependent on its porosity [13] [14]. Additionally, pavement geometric design factors including longitudinal and transverse slope, as well as pavement length are significant factors that affect OGFC hydraulic characteristics [15] [16]. Past studies focused on the impacts of the OGFC layer itself and ignored the impacts of the underlying layers on the drainage properties, which was considered in the present study.

Tan et al. used FE software such as SEEP 3D to investigate the impacts of longitudinal and cross-sectional slope on the design of the thickness of OGFC [85]. To achieve this objective, a SEEP 3D analysis was conducted, considering different cross-sectional and longitudinal slopes. The cross-sectional slopes ranged from 0-4% with an interval of 1%, while the longitudinal slopes included 0%, 2%, 4%, 6%, and 8%. In the referenced study, SEEP 3D was used to calculate the maximum rainfall intensity that would not result in flooding. Results indicated that both cross-sectional and longitudinal slopes affected the drainage performance of the OGFC layer significantly. For example, increasing the cross slope from 0% to 1% increased OGFC drainage capacity by 88%. It is worth noting that a no-flow boundary

condition was applied to the bottom of OGFC, which implies that the underlying layer is impermeable and OGFC is only responsible for draining rainfall water.

Similarly, Nguyen and Ahn utilized numerical analysis to determine the time to reach overflow conditions considering the effects of pavement geometric design and different rainfall intensities [15]. In the study, pavement geometric design parameters included pavement length and cross-sectional slope. Pavement length ranged from 10-30 m, while pavement cross-sectional slope ranged from 0.5-8%. All of these conditions were evaluated under different rainfall conditions, which ranged from 10-120 mm/hr. Results indicated that the time required for water to flow over the pavement increased when the cross-sectional slope increased. However, the increase in pavement length and rainfall intensity decreased the time required for the water to flow over the pavement surface.

In another study, Zhang et al. employed the three-dimensional FE software COMSOL Multiphasic to investigate the impacts of longitudinal slope on OGFC drainage capacity [16]. To achieve the aforementioned objective, a pavement with a width of 10 m and a length of 80 m was simulated using the COMSOL software. OGFC thickness was simulated as a layer of 50 mm in thickness with different longitudinal slopes ranging from 0-6%. Results indicated that the contribution of the longitudinal slope to OGFC drainage capacity was insignificant.

Knowledge Gaps in the Literature

Studies on OGFC Durability

Based on the literature review, studies were conducted to evaluate the concept of WMA-OGFC, crumb rubber, and fillers in recent years. To the best of the authors' knowledge, the literature review revealed the following gaps:

- While a number of studies were conducted to evaluate the impacts of WMA and CR on OGFC laboratory performance, more research is needed to thoroughly investigate the effects of WMA on OGFC durability. Further, most research studies did not address the cracking resistance of WMA-OGFC given the difficulty of testing this property in the laboratory for these types of mixes.
- The laboratory evaluation of OGFC mixes modified with WMA and CR for aggregate types and binder sources used in the South-Central United States has not been conducted to date.
- No previous studies evaluated the impacts of considering the concurrent use of WMA and CR on OGFC durability.

- No previous studies were conducted to evaluate the impact of pozzolanic fillers such as Portland cement and fly ash on OGFC durability.
- In contrast with previous studies, this study evaluated the effects of WMA additives on OGFC properties at three distinct stages: production, construction, and field performance.

Studies on the Seepage Characteristics of OGFC Pavements

Based on the literature review, studies were conducted to characterize the seepage characteristics of OGFC pavements but were limited in scope. To the best of the authors' knowledge, the following gaps were identified based on the literature review:

- No previous studies evaluated the seepage characteristics based on field-collected data.
- No previous studies evaluated the effects of the underlying pavement layers on the hydraulic characteristics of OGFC pavements.
- No previous studies were conducted to investigate the effects of traffic loading on OGFC functionality based on FE modeling.
- The literature revealed that, until now, no quantitative model was developed to simulate the reduction of OGFC pavement functionality with traffic wear.

Objective

The objectives of this study were twofold. First, this study aimed at designing and evaluating a new generation of open-graded friction courses (OGFC) that would provide superior durability while preserving the functional benefits of the mix. To fulfill this objective, current practices including additives and filler types and content were reviewed and comprehensively evaluated in the laboratory. This study also aimed to demonstrate that the new generation of OGFC is environmentally-friendly and cost-effective by evaluating different additives and by-products such as WMA, crumb rubber (CR) from recycled tires, and different pozzolanic fillers, such as Portland cement and fly ash.

Second, this research used FE modeling to simulate the seepage characteristics of a pavement structure constructed with an OGFC surface layer. The objective of the FE modeling was to evaluate the effects of traffic wear and a reduction in permeability on the long-term hydraulic performance of a pavement structure constructed with an OGFC surface layer. Additionally, the effects of OGFC thickness (T_{OGFC}), coefficient of permeability of OGFC (K_{OGFC}), and permeability of the underlying pavements (K_{HMA}) on the seepage behavior of the pavement structure were evaluated under different rainfall intensities (R) using Finite Element Analysis (FEA).

Scope

To fulfill the laboratory objective of the study, different additives were evaluated by modifying an approved and practically-used OGFC mix (control mix). These modifications included three WMA additives, one recycled product (crumb rubber), and two different pozzolanic fillers (Portland cement [F_1] and fly ash [F_2], a by-product from coal-fired electric and steam generating plants). Additionally, a mix with a reduced NMAS of 9.5 mm was evaluated. The newly developed mixes were then evaluated in the laboratory to determine the effects of these modifications on the performance of these mixes at three different stages: production, construction, and field performance.

To achieve the second objective, an FE model was developed to investigate the effects of K_{OGFC}, T_{OGFC}, K_{HMA}, and traffic wear on the seepage characteristics of a pavement structure constructed with an OGFC layer under different climatic conditions. These results were then analyzed statistically to determine the most significant factors that affect the drainage performance of the pavement structure. Afterward, the most significant factors were used to develop an Artificial Neural Network (ANN) model for the prediction of the time to reach overflow conditions without the need for FE modeling. Finally, the developed FE model was used to propose new AV guidelines for OGFC applications in Louisiana.

Methodology

To fulfill the study objectives, the research activities were divided into six tasks. These tasks are described in the following sections.

Task 1: Literature Review

In this task, research studies that describe the local and current state of practice on the design of OGFC mixes were reviewed; the findings of the literature review were previously presented in this report. Local sources included the Louisiana Department of Transportation and Development (DOTD) specifications that guide and control the design of OGFC mixes. Additionally, NCHRP Project 1-55 has introduced innovative procedures for the design of OGFC mixes; the final report of this project was reviewed and synthesized. Further, all available studies that evaluated the different benefits of using OGFC as a surface course layer were reviewed and synthesized. Additionally, recent studies that were conducted to enhance OGFC durability were reviewed. Finally, research studies that were conducted to investigate the seepage characteristics of pavement structures constructed with an OGFC surface layer were reviewed. The literature review included studies that related to the following topics:

- Effects of aggregate gradation and NMAS on the performance and durability of OGFC mixtures;
- Effects of AV content on the performance and durability of OGFC mixtures;
- Effects of various additives and by-products (e.g., WMA and CR) on the performance and durability of OGFC mixtures;
- Effects of design and operating factors (e.g., geometric design, structural design, and local climatic conditions) on the hydraulic characteristics of the OGFC layer; and
- Accuracy and precision of different FE programs that can be used to model the seepage and hydraulic characteristics of pavement structures.

Task 2: Material Selection

The primary objective of this task was to identify and select the OGFC mixture components that were to be considered in the laboratory experimental factorial. In the experimental program, a state-approved JMF of OGFC mix was used to fabricate the control mix (CM). This mix is typically produced using two aggregate types (#78 limestone and #67 sandstone aggregate types) and a PG 76-22 SBS-modified binder at a rate of 6.5% by weight of the total

mix. These materials are typically used in Louisiana in the construction of OGFC [20]. It is noted that #78 limestone and #67 sandstone have different NMAS; therefore, they were batched with varying percentages to satisfy the gradation requirements of OGFC; see Table 9. To resist moisture damage, an anti-stripping agent (ASA) was added to the binder in all mixes before blending with the aggregate at a dosage of 0.60% by weight of the asphalt binder. Additionally, cellulose fibers were incorporated in the mixtures at a specified dosage of 0.2% by weight of the total mix to control draindown.

A number of additives (WMA), by-products (CR), and pozzolanic fillers (Portland cement and fly ash) were used to modify the CM in order to enhance OGFC durability and field performance. The WMA additives included three approved products by DOTD: two chemical additives and one organic additive. Additionally, CR was evaluated in the mixture to investigate its effects on the laboratory performance of OGFC. It is expected that the use of CR will increase both mixing and compaction temperatures; therefore, the incorporation of WMA additives into CR-containing mixtures was investigated to produce more durable OGFC mixes at the same mixing and compaction temperatures as the CM. In this study, Portland cement and fly ash were also evaluated as pozzolanic fillers, F_1 and F_2, respectively, by replacing the percent passing sieve No. 200 with these types of fillers. Adding both pozzolanic fillers may promote adhesion strength between asphalt binder and aggregate particles. For this reason, it is expected that these types of fillers will enhance OGFC durability.

Table 9. Aggregate characteristics

U.S. sieve	% Passing		Mix design	JMF limits
	# 78 limestone	# 67 sandstone		
3/4 in. (19 mm)	100.0	100.0	100	96-100
1/2 in. (12.5 mm)	93.1	88.4	88	84-92
3/8 in. (9.5 mm)	71.3	68.0	69	65-73
No. 4 (4.75 mm)	7.7	26.0	16	12-20
No. 8 (2.36 mm)	2.0	8.0	6	3-9
No. 16 (1.18 mm)	1.6	6.1	5	3-7
No. 30 (0.60 mm)	1.4	5.6	5	3-7
No. 50 (0.30 mm)	1.4	5.4	4	2-6
No. 100 (0.15 mm)	1.3	5.3	4	-
No. 200 (0.075 mm)	1.2	3.2	3.1	1.6-4.6
Bulk specific gravity	2.662	2.581	2.636	-

U.S. sieve	% Passing		Mix design	JMF limits
	# 78 limestone	# 67 sandstone		
Bulk specific gravity (SSD)	2.681	2.615	2.660	-
Apparent specific gravity	2.715	2.672	2.702	-
Absorption	0.74%	1.32%	0.855%	-
Sand Equivalent	100%	100%	100%	>60%
Flat and Elongated Ratio	8.7%	2%	4.26%	<25%
Fine Aggregate Angularity	45%	45%	45%	>45%
Coarse Aggregate Angularity	100%	100%	100%	>90%

Task 3: Preparation of the OGFC Mixes

The objective of this task was to prepare the selected OGFC mixes. The materials described in the previous section were used to fabricate nine mixes (CM and eight modified mixes). The eight modified mixes included one mix with a reduced NMAS (9.5-NMAS) and three mixes containing WMA additives that are referred to as Che1-OGFC, Che2-OGFC, and Org-OGFC, respectively. For WMA-OGFC, the mixing and compaction temperatures were 302ºF and 284ºF, respectively. Additionally, two mixes containing CR were prepared. One of these mixes was prepared by adding the CR to the OGFC mix (CR-OGFC). CR-OGFC was mixed and compacted at 365ºF and 356ºF, respectively. The second CR mix was prepared by modifying the binder through the addition of a WMA additive (Che1) and CR. This mix is referred to as CR+Che1-OGFC. This mix was produced and compacted at the selected temperatures of the CM (325ºF and 311ºF for mixing and compaction, respectively). The remaining two mixes were prepared by replacing the percent passing sieve No. 200 (3.1%) with Portland cement and fly ash to produce F_1-OGFC and F_2-OGFC, respectively. As the binder characteristics of these mixes did not change, the mixing and compaction temperatures of the CM were used as well.

To prepare the selected mixes, laboratory activities started by sampling and acquiring the aggregate, fibers, and additives for fabrication and performance evaluation from Louisiana's contractors. All OGFC mixes were designed following the DOTD specification requirements for OGFC found in Tables 501-1, 501-2, and 501-3. Upon successful materials' preparation, the mixes were fabricated following the requirements of the laboratory performance and durability tests, as detailed below.

Binder Modifications

This section describes the procedures that were used to prepare the modified binders for each selected mix. For the CM, F_1-OGFC, and F_2-OGFC, an anti-stripping agent (ASA) was added at a dosage of 0.6% by the weight of the binder. First, the asphalt binder was heated in an oven until it reached the mixing temperature of 325°F. Next, the anti-stripping agent was added, and a shear mixer was used to mix the blend for 1-2 min. at 1,000 rpm. After adding the anti-stripping agent, the binder was ready for mixing with the aggregate blends.

For WMA-OGFC mixes, Che1, Che2, and organic additives were added at rates of 0.1%, 0.5%, and 2.5% by weight of the binder, respectively. For Che1 and Che2, the specified dosage was added to the binder at the mixing temperature; then, the blend was mixed at 1,000 rpm for 1-2 min., as recommended by the manufacturer. However, the organic WMA was mixed at 3,000 rpm for 45 min [86].

For the CR-OGFC, the following blending procedure was adopted. First, the binder was heated to 325°F. Afterward, the ASA was added to the asphalt binder at a dosage of 0.6% by weight of asphalt. Next, a shear mixer was used to mix the binder and ASA at 1,000 rpm for 1-2 min. Afterward, the blend temperature was raised using a hot plate to 356°F. At this point, the CR was added at a rate of 10% by weight of the asphalt binder. At this stage, the shear mixer was set to 3,000 rpm to mix the CR with the ASA-binder blend for 45 min.

For the CR+Che1-OGFC mix, the procedure followed in the CR-OGFC mix was considered. However, before adding the CR to the ASA-binder blend and once the temperature reached 325°F, Che1 was added to the ASA-binder blend at a dosage of 0.10% by weight of the binder. Next, a shear mixer was used to mix Che1 with the blend at 1,000 rpm for 1-2 min. Afterward, the blend temperature was raised using a hot plate to 356°F. At this point, the CR was added at a rate of 10% by weight of the asphalt binder. At this stage, the shear mixer was set at 3,000 rpm to mix the CR with the ASA-Che1-binder blend for 45 min.

Adding Fibers to the Mixtures

In the experimental program, cellulose fibers were added to the mixtures at a dosage of 0.2% by weight of the total mix using the dry method in all mixes. In this process, the aggregate was heated to the mixing temperature for three hrs. Next, the fibers were manually mixed with the heated aggregate. Finally, using the mechanical mixer, the cellulose fiber was mechanically blended with the aggregate for 1-2 min. to ensure the uniform distribution of fibers throughout the whole mix. Before mixing with the binder, the fibers-aggregate blend was kept in the oven for 30 min. at the target mixing temperature.

Mix Characteristics

Table 10 describes the characteristics of the nine mixes that were prepared as part of the experimental laboratory factorial. As shown in Table 10, the 9.5-NMAS mix was fabricated with the same components and temperatures as the CM but had a NMAS of 9.5 mm.

Table 10. Final experimental factorial

Mix Components	Mix Identification								
	CM	**9.5-NMAS**	**Che1-OGFC**	**Che2-OGFC**	**Org-OGFC**	**CR-OGFC**	**CR+Che1-OGFC**	**F_1-OGFC**	**F_2-OGFC**
Aggregate	78 lime stone + 68 sand stone								
Binder	PG 76-22					PG 67-22		PG 76-22	
ASA	Adhere								
WMA	-	-	Che1	Che2	Org	-	Che1	-	-
CR (10%)	-	-	-	-	-	Yes	Yes	-	-
Passing Sieve No. 200	Limestone and sandstone							F_1	F_2
Mixing Temp.	325°F	325°F	302°F	302°F	302°F	365°F	325°F	325°F	325°F
Compaction Temp.	311°F	311°F	284°F	284°F	284°F	356°F	311°F	311°F	311°F

Task 4: Laboratory Testing

The objective of this task was to evaluate the effects of different additives and modification considered in the experimental factorial on the performance, durability, and physical characteristics of OGFC. The test factorial was designed to investigate the performance of OGFC mixes at three different stages: production, construction, and in-service performance. For the production stage, the draindown test was used to evaluate the impacts of different additives by measuring the amount of asphalt binder that drains out of a loose OGFC mix. More details about the draindown test can be found in the Literature Review portion of this report.

In the construction stage, the Compaction Energy Index (CEI) was used to compare the required compaction effort during construction. The CEI is defined as the area under the curve between the number of gyrations and $\%G_{mm}$ from the eighth gyration to the gyration that corresponds to 92% G_{mm} [87]. It is hypothesized that CEI correlates to the compaction effort applied by the roller in the field to achieve the required density during construction. In the current study, compaction data were used to calculate CEI for each mix type. Since OGFC has a higher AV content compared to conventional HMA, CEI was calculated as the

area under the $\%G_{mm}$ curve from the eighth gyration to the gyration that corresponds to 75% G_{mm}. Figure 16 shows the philosophy of CEI calculations.

Figure 16. CEI philosophy of calculation

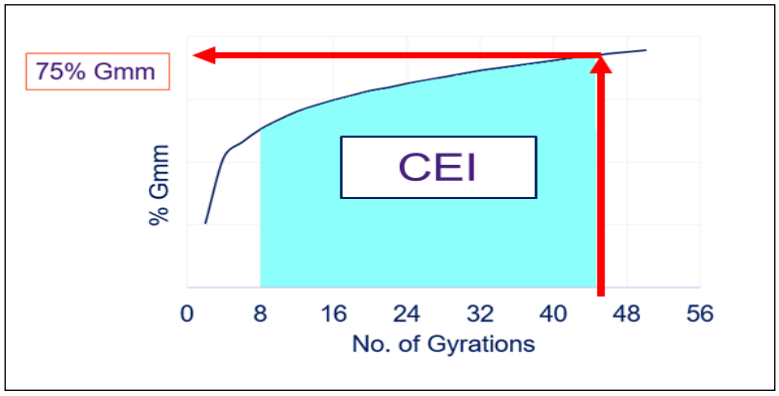

In terms of in-service field performance, the Cantabro test, Hamburg Wheel-Tracking test (HWT), Indirect Tensile Stress (ITS) test, Texas Overlay Test, Tensile Strength Ratio (TSR), and boil test were used to evaluate the mix's resistance to raveling, permanent deformation, fatigue cracking, reflective cracking, and moisture-damage, respectively. For more information about these test procedures, see the Literature Review portion of this report.

It it noted that the primary objective of constructing a pavement with an OGFC layer is to facilitate rainwater drainage. The functionality of each OGFC mix was evaluated in terms of air void (AV) content and permeability. Table 11 summarizes the different test methods, along with the minimum number of test samples required and the number of samples prepared for each test.

As shown in Table 11, the actual number of samples satisfied the minimum number of samples as designated in the specifications. For the Cantabro abrasion test and HWT test, nine and four samples were prepared instead of three and two test samples. For the Cantabro abrasion test, nine SGC samples were prepared for each mix with a diameter of 6 in. and a height of 4.5 ± 0.2 in. These nine specimens were divided into three groups with equal average AV. The first group was tested without any conditioning. The second and third groups were conditioned to evaluate the impact of binder aging and moisture conditioning, respectively, on the abrasion resistance of OGFC mixes. For the second group, three samples were aged in an oven for seven days at 140°F [18]. For the third group, the samples were submerged in a water bath for 24 hr. at 140°F [18]. Afterward, the samples in the second group were left to cool down to room temperature before testing. For the third group, the samples were dried using the core dry machine in accordance with ASTM D 7227, "Standard Practice for Rapid Drying of Compacted Asphalt Mixture Specimens Using Vacuum Drying

Apparatus," before conducting the test [88]. For the HWT test, instead of preparing two samples, four samples were prepared to allow for a robust statistical analysis among the different mixes.

Table 11. Laboratory test factorial

Test	Specification	Purpose	Minimum No. of Samples	Used No. of Samples
Bulk Specific Gravity	ASTM D 6752	AV Content	3	3
Theoretical Specific Gravity	ASTM D 2041		3	3
Draindown test	AASHTO T 305-97	Investigate the amount of binder to drain out during production	3	3
Cantabro Abrasion Test	AASHTO TP 108-14	Raveling resistance	3	9
Hamburg Wheel-Tracking Test	AASHTO T 324	Permanent deformation resistance	2	4
Texas Overlay Test	Tex-248-F	Fatigue and reflective cracking resistance	3	3
Modified Lottman Test	AASHTO T 283	Moisture damage resistance	6	6
Boiling test	DOTD TR 317		3	3

Asphalt Binder Extraction and Testing

The effects of the selected additives and modifications on the binder's rheological properties were evaluated. To this end, asphalt binder was extracted from the prepared OGFC mixes. The binder extraction was performed according to the ASTM D 2172 test method, "Standard Test Methods for Quantitative Extraction of Asphalt Binder from Asphalt Mixtures." In this method, a 1500 g asphalt mix sample was fully immersed into trichloroethylene (TCE) solvent for 60 min. After soaking, the mixture's liquid blend, consisting of binder and TCE, was drained and collected. The soaking and draining processes were repeated until the discharge liquid was clear and had a straw color. Next, the liquid sample was placed in a large centrifuge and allowed to spin for 30 min. at 770 rpm to remove dust particles.

Once the dust materials were removed, the liquid sample was transferred to a large distillation flask for the Abson process, which was used to separate the pure binder from the TCE. In the distillation process, the temperature was gradually increased to 135°C (275°F). At that temperature, the aeration tube was lowered so the bulb could touch the bottom of the

flask and slowly introduce carbon dioxide gas at approximately 100 ml/min. to prevent foaming and provide agitation. Over time, the temperature was raised to between 157-160°C (315-320°F), prompting an increase in carbon dioxide gas flow to approximately 900 ml/min. The gas flow rate was kept constant for 10 min. or until the TCE solvent stopped dripping, and the temperature of the residue in the flask was maintained at 160-166°C (320-330°F) during that time. When all the TCE had evaporated, the residue that remained in the flask was collected as the recovered binder.

After the binder recovery was completed, the physical and rheological properties of the extracted binders were evaluated using performance grading (PG). To assess the effects of the modifications on the binder's aging characteristics, the binders were tested at different aging conditions. Short- and long-term aging were conducted per AASHTO R 28 using the rolling thin film oven (RTFO) and the pressure aging vessel (PAV) devices. A dynamic shear rheometer (DSR) test was conducted according to AASHTO T 315 standard to evaluate the elastic and viscous properties at various temperatures and aging conditions, including unaged, RTFO-aged, and PAV-aged. The DSR test evaluated the binder's resistance to cracking and rutting by measuring $G^*sin\ \delta$, and $G^*/sin\ \delta$, where G^* is the complex modulus of the binders and δ is the phase angle, which is a relative measure of the viscous and elastic properties of the binder. It ranges from 0° for an elastic material to 90° for a viscous material. To assess the ability of the binder to withstand low-temperature thermal cracking, the bending beam rheometer (BBR) test was conducted according to the AASHTO T 313 standard. The BBR test evaluated the performance of the binder at low temperatures based on creep stiffness ($S(t)$) and m-value. The number of replicates tested for all cases was two.

Task 5: Analyze Performance and Durability of OGFC Mixes

The objective of this task was to analyze the results obtained in Tasks 3 and 4 to identify and quantify the effects of the design variables on the performance and durability of OGFC mixes. The results were analyzed statistically using an Analysis of Variance (ANOVA), where the F-statistics and the corresponding P-values were used to assess the statistical significance of the factors investigated in the study. The ANOVA analysis was supplemented with the Tukey's Honest Significant Difference (HSD) test to evaluate if the performance obtained for the combinations of the different variables was statistically different.

Cost-Effectiveness Analysis

A cost-effectiveness analysis was used to provide a quantitative assessment of the benefits gained from the evaluated additives in OGFC. Several strategies are available to evaluate the cost-effectiveness of asphalt mixtures. This study adopted a simple approach that divides the

predicted laboratory performance of the mix by its unit cost. Since the focus of the study is on durability, the results of the Cantabro abrasion test and HWT test were used as indicators of mixture performance. The cost-effectiveness (CE) of any given mixture was calculated as follows:

$$CE_i = \frac{E_i}{C_i} * 100 \quad (11)$$

where,
E_i = expected performance; and
C_i = mixture unit cost (per ton).

The expected performance from laboratory testing, *Ei*, was calculated as follows:

$$\frac{1}{E_i} = \frac{CL_i}{CL_{\min}} + \frac{RD_i}{RD_{\min}} \quad (12)$$

where,
CL_i = mixture Cantabro loss (CL) value;
$CL_{\min}$ = minimum Cantabro loss value obtained from all the mixes;
RD_i = mixture rut depth (RD) value; and
$RD_{\min}$ = minimum rut depth value obtained from all the mixes.

Based on Equation 11, the most cost-effective mixture is the one that provides a greater CE value, or a higher ratio of performance to cost compared to other mixtures. The estimated unit costs per ton with the dosage rates that were used in the experimental program are shown in Table 12.

Table 12. Estimated unit costs

Mix	CM	9.5-NMAS	Che1-OGFC	Che2-OGFC	Org-OGFC	CR-OGFC	CR+Che1-OGFC	F_1-OGFC	F_2-OGFC
Cost ($ per ton)	90.3	90.3	94.7	96.4	92.7	93.4	97.8	94.1	91.1

Task 6: Seepage Analysis Using Finite Element Modeling

The objective of this task was to simulate the seepage behavior of pavement structures constructed with an OGFC surface layer using FEA. The FE model allowed the researchers to evaluate the effects of traffic wear and a reduction in permeability on the long-term hydraulic performance of a pavement structure constructed with an OGFC surface layer. Figure 17 shows the general outlines followed to achieve this task. In this task, a three-dimensional FE model was developed using SEEP/3D, as presented in Figure 17.

Once the model was developed, steady-state analysis was conducted to define the initial conditions. Before proceeding to the transient analysis, the developed model was calibrated, as described in the following sections. Once the model was calibrated, an OGFC layer was added to the model and a series of runs were conducted to evaluate the effects of different factors on the hydraulic characteristics of pavement structures constructed with an OGFC layer as a surface layer. As presented in Figure 17, different factors were varied in the analysis: OGFC layer thickness (T_{OGFC}), OGFC coefficient of permeability (K_{OGFC}), underlying layer coefficient of permeability (K_{HMA}), rain intensity (R), and traffic volume. For the different conditions, SEEP/3D results were used to calculate the time at which water overflow occurs (T_C).

The results of the FE model were statistically analyzed to investigate the factors that significantly affect T_C. The results of SEEP/3D were then used to train and validate an ANN model for the prediction of T_C without the need for FE modeling. Additionally, the results of the developed FE model were used to propose new AV guidelines for OGFC applications in Louisiana.

Figure 17. Research methodology for Task 6

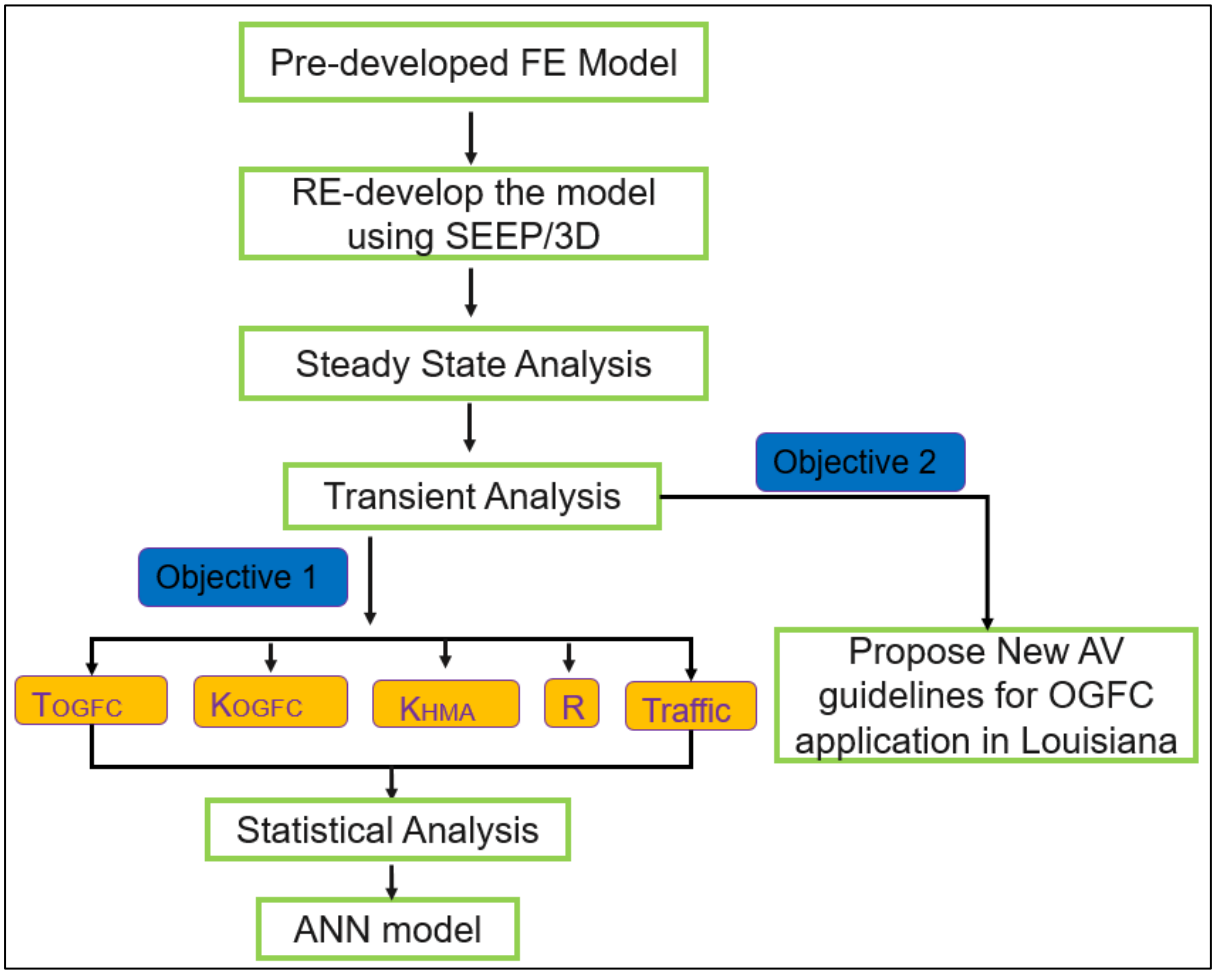

Model Characteristics

The FE model consisted of three layers: a dense-graded hot mix asphalt (DGHMA) layer, a base layer, and a subgrade. The thickness of the DGHMA and base layers was 4.50 and 9.5 in., respectively. The pavement transverse slope and width were 2.5% and 24.0 ft., respectively. Based on a field survey conducted in a previous study by the research team, it was found that the natural soil extended laterally about 36.0 ft. beyond the side ditches [89]. The road had two side ditches, each of which had a width of 5 ft. and a depth of 3 ft.

To describe the unsaturated water flow through the pavement layers, the Soil Water Characteristic Curve (SWCC) and hydraulic conductivity function are required. Table 13 shows the pavement layers' properties as defined in the FE model developed by Elseifi et al. [90]. In the analysis, DGHMA saturated hydraulic conductivity (K_{sat}) was measured in the laboratory according to FM 5-565, "Florida Method of Test for Measurement of Water Permeability of Compacted Asphalt Paving Mixtures," using the falling head permeability test [32]. However, typical K_{sat} values from previous research were assigned for the base

layer and subgrade soil [90]. Similarly, Elseifi et al. used typical Van Genuchten fitting parameters for the DGHMA layer, base layer, and subgrade from previous studies, as presented in Table 13.

Table 13. Material properties [89]

Property	Van Genuchten Fitting Parameters				K_{sat} (m/sec.)
	n	a (KPa)	Residual Moisture Content	Saturated Moisture Content	
DGHMA	1.09	0.489	0.0	0.06	3.45×10^{-8}
Base (Sandy Loam)	1.89	1.31	0.065	0.41	1.22×10^{-5}
Subgrade (Loam)	1.56	2.725	0.078	0.43	2.89×10^{-6}

3-D Model Layout

For this study, SEEP/3D was used to modify the two-dimensional model in the previous study [90], as presented in Figure 18. The model consisted of a total of 45,817 and 7,700 triangular elements and nodes, respectively.

Figure 18. 3-D FE model layout

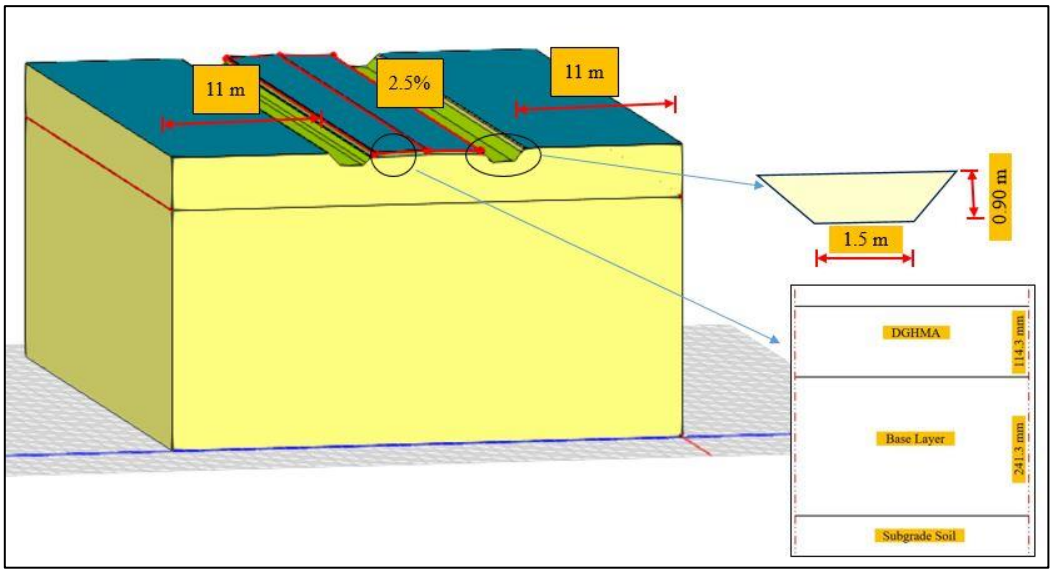

Steady-State Analysis

After developing the model using SEEP/3D, a steady state analysis was conducted to define the initial conditions. Steady-state analysis was conducted under the following boundary conditions [90]:

- Based on the field survey, the water level in the left side ditch was 2.62 ft.; therefore, a total hydraulic head (H) of 64.0 ft. was assigned to the wetted perimeter of the left side ditch (H = ditch bed level (61.38 ft.) + head pressure (2.62 ft.) = 64.0 ft.). More details about the field survey have been presented elsewhere [90].
- Additionally, the water level in the right-side ditch was 0.62 ft.; therefore, a total hydraulic head (H) of 62.0 ft. was assigned to the wetted perimeter of the left side ditch (H = ditch bed level (61.38 ft.) + head pressure (0.62 ft.) = 62.0 ft.).
- To account for the vertical and lateral seepage in the entire system, two lines of zero pressure head were applied at a level of 51.20 ft.

Calibration of the Steady-State Analysis

The steady-state analysis was calibrated using the Volumetric Water Content (VWC) at the mid-depth of the base layer and the ground water table (GWT) level, as presented elsewhere [90]. In the referenced study, VWC was calculated at the mid-depth of the base layer based on a scan obtained using Ground Penetrating Radar (GPR) and the Topp equation [91]. The results indicated that VWC at the mid-depth of the base layer was 0.30. Additionally, the A-scan GPR data showed a strong reflection at 1.97 ft. beneath the pavement surface, which indicated the GWT level. This information was used to validate the steady-state analysis in the 3-D model.

The model was run under steady-state boundary conditions, and VWC was calculated along section 1-1, at the mid-depth of the base layer, as presented in Figure 19a. Results indicated that the average VWC at section 1-1 was approximately 0.20, as shown in Figure 19b. Additionally, the pore water pressure was calculated at section 2-2 to locate the GWT; see Figure 19c. GWT corresponds to the location at which the pore pressure equals zero. Figure 19d indicates that the GWT is located at a depth of 3.94 ft. beneath the pavement surface. The results of the steady-state analysis under the initial boundary conditions revealed that VWC and GWT were not consistent with the GPR A-scan results. It was concluded that inaccurate measurements of the water level in the side ditches may be the primary reason for this inconsistency. Therefore, several runs were conducted after changing the water level in the side ditches. After several trials, the average VWC was 0.30, which was equal to the VWC calculated using the Topp equation; see Figure 19b. Additionally, a pore pressure of zero was observed at a depth of approximately 1.94 ft. Both conditions were satisfied when the total heads of 64 and 63.3 ft. were applied along the wetted perimeter of the left and right-side ditches, respectively.

Figure 19. Calibration of steady-state analysis: (a) section at mid-depth of base layer; (b) VWC at section 1-1 (c) section along model centerline (d) pore water pressure at section 2-2

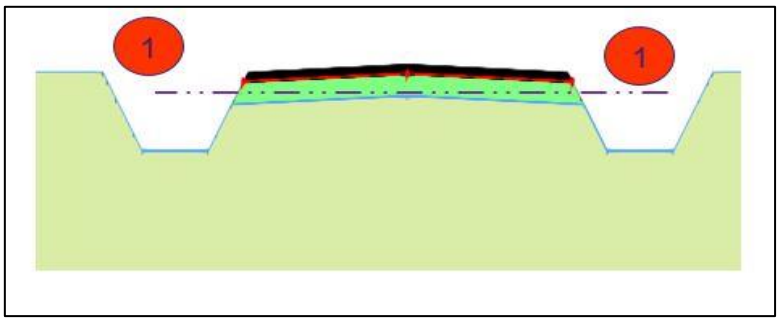

(a)

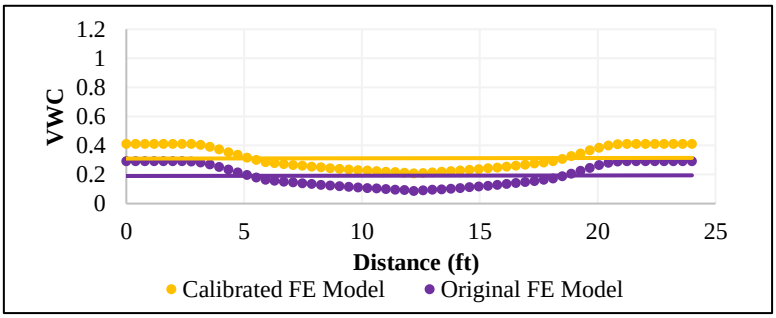

(b)

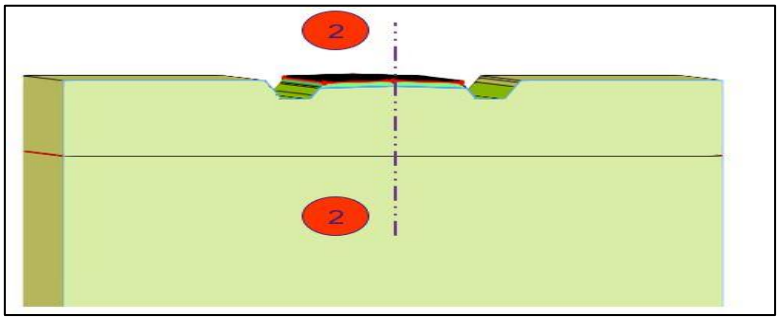

(c)

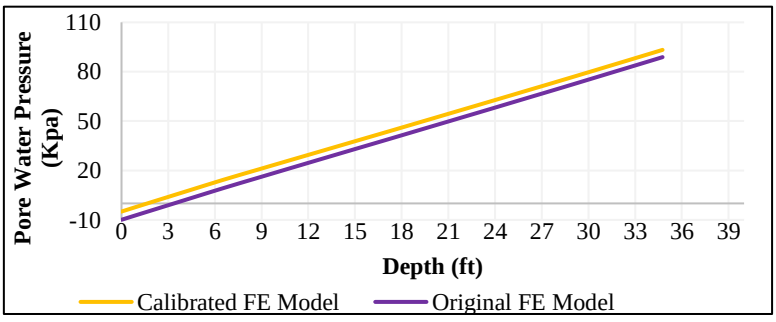

(d)

Transient Analysis

After the model was verified and calibrated, an OGFC layer was added to the model for the purpose of this study. Typical Van Genuchten fitting parameters (*a, n*) were assumed for the OGFC layer based on the results of a previous study [15]. In this study, *a* and *n* were assumed to be 2.23 kPa and 1.63, respectively. Using these inputs, several runs were conducted to evaluate the impacts of K_{OGFC}, T_{OGFC}, K_{HMA}, R, and traffic wear on the seepage characteristics of the pavement structure constructed with an OGFC layer. The following section details the values of K_{OGFC}, T_{OGFC}, K_{HMA}, R, and traffic that were simulated in the analysis.

FE Model Inputs

OGFC Characteristics. In this study, the effects of OGFC permeability (K_{OGFC}) and thickness (T_{OGFC}) on the seepage characteristics of the pavement structure constructed with an OGFC layer were evaluated. For K_{OGFC} values, three OGFC mixes with 12.5 mm NMAS were fabricated in the laboratory, and their coefficients of permeability were measured according to FM 5-565. The results of this test are presented in Figure 20. The results indicate that K_{OGFC} values were 0.06, 0.05, and 0.03 in./sec. for Mix 1, Mix 2, and Mix 3, respectively. It is noted that all mixes satisfied the minimum requirement of OGFC permeability recommended by NCHRP 1-55 [1].

Figure 20. OGFC coefficient of permeability

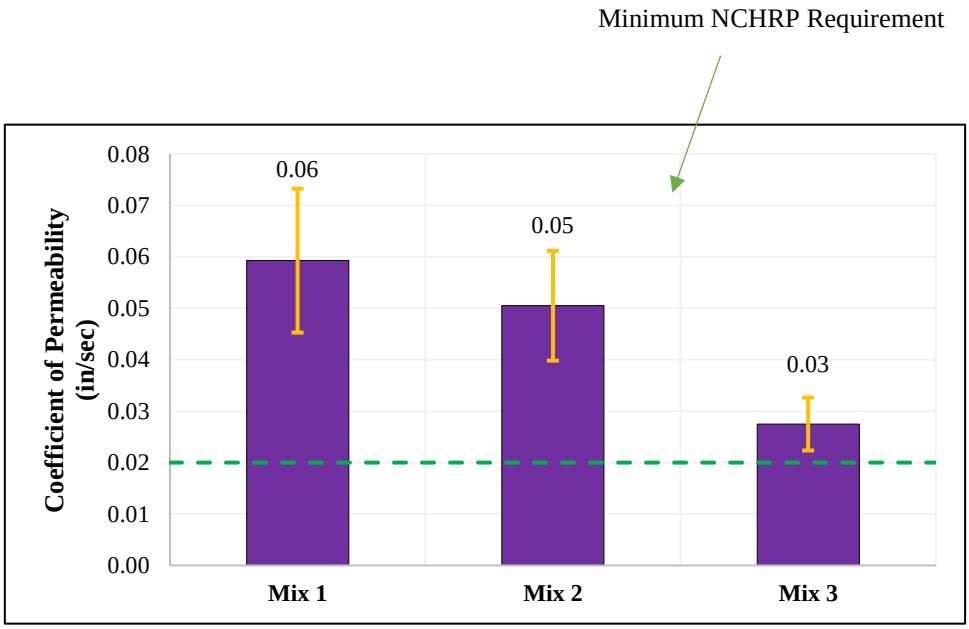

For T_{OGFC}, OGFC is typically constructed with a lift thickness of 0.75 and 1.25 in. in Louisiana [19]. An additional thickness of 1.9 in. was also simulated. The 1.9-in. lift thickness was added for two reasons. First, OGFC is typically placed with a lift thickness of 1-2 in. in Europe [1]. Second, this thickness was considered to generate more simulation data that were used to develop the ANN model. Based on this assumption, three T_{OGFC} were considered in this study: 0.75, 1.25, and 1.90 in.

Underlying Layer Characteristics. The primary shortcoming noted in previous studies was that the effects of the permeability of the underlying layer on the hydraulic characteristics of pavements constructed with OGFC were ignored. In this study, this knowledge gap was addressed. In a previous research study sponsored by LTRC, laboratory permeability tests were conducted on field cores extracted from 17 Superpave projects in Louisiana [92]. The results indicated that the Superpave mixes had a maximum coefficient of permeability of 3.54 x10 $^{-3}$ in./sec. In the present study, these results were incorporated to define the coefficient of permeability of the underlying layer (K_{HMA}) in the developed FE model. Four K_{HMA} values of $1.36x10^{-6}$, 1.18×10^{-3}, 2.36×10^{-3}, and 3.54×10^{-3} in./sec. were used in the simulation.

Rain Intensity. In the simulation, three rain intensities (R) were used based on the climatic conditions in Louisiana. To define the R-values, hourly rain intensity values from the LSU Agricultural Center were reviewed for the period from January 2020 to January 2021. To this end, a total of 8,088 observations were reviewed, with R-values ranging from 0 in./hr. to 1.89 in./hr. In the review, the hours that experienced a rain intensity of 0 in./hr. were removed. A

total of 720 observations of rainy hours were obtained. Afterward, these observations were used to construct a five-number summary table using SAS 9.4 software. Table 14 shows the five-number summary table for the hourly rain intensity for Louisiana from 2020 to 2021. In this study, Q_1, Q_2, and Q_3 were used in the 3D FE model.

Table 14. Rain intensity five-number summary table

Summary Measure	Rain Intensity (in./hr.)
Minimum	0.01
First Quartile (Q_1)	0.02
Second Quartile (Q_2)	0.04
Third Quartile (Q_3)	0.10
Maximum	1.89

Simulation of Traffic Wear. In the simulation, the effect of traffic wear was considered by applying a reduction factor to the initial permeability coefficient of the mixes. As previously discussed in the literature review, due to traffic and other factors, OGFC permeability decreases over time; see Figure 21, which was obtained from field measurements at the National Center of Asphalt Technology (NCAT) test track. In this study and based on the data presented in Figure 21, reduction factors of 1.00, 0.50, 0.36, 0.32, 0.25, and 0.20 were applied to the initial OGFC permeability to simulate the coefficient of permeability at 0, $2x10^6$, $4x10^6$, $6x10^6$, $8x10^6$, and $10x10^6$ Equivalent Single Axle Load (ESALs), respectively. For more details about the loss of OGFC permeability, see [1] and [59]. The AV content that corresponds to each permeability coefficient was then calculated using Equation 9. The verified FE model was then executed to evaluate the impact of traffic wear on the seepage characteristics of pavement constructed with an OGFC layer.

Figure 21. Reduction in OGFC permeability due to traffic [1]

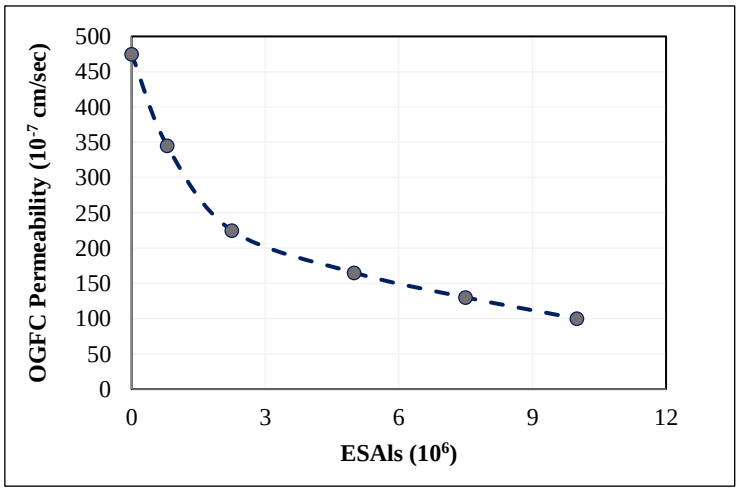

Final Simulation Table. Table 15 presents the details of the different simulation runs performed as part of this analysis. In sum, a total of 648 runs were conducted in this study.

Table 15. Description of simulation runs

Factor	No. of Cases	Values	Units
K_{OGFC}	3	0.03, 0.05, and 0.06	in/sec
T_{OGFC}	3	0.75, 1.25, and 1.90	In
R	3	0.02, 0.04, 0.10	in/hr
K_{HMA}	4	$1.36x10^{-6}$, 1.18×10^{-3} , 2.36×10^{-3}, and 3.54×10^{-3}	in/sec
Traffic	6	0, 2, 4, 6, 8, and 10	10^6 x ESAL
Total	3 x 3 x 3 x 4 x 6 = 648		

Discussion of Results

Laboratory Evaluation

This section introduces the primary results and findings of the laboratory experimental program. Nine mixes were fabricated in this study, as presented in Table 16. The performance of these mixes was evaluated at three different stages: production, construction, and field performance. Additionally, binders extracted from these mixes were evaluated according to AASHTO M 320 using the Performance Grading (PG) system.

Table 16. Description of the evaluated mixes

ID	Mix Abbreviation	Description
1	**CM**	Conventional OGFC mix fabricated with PG 76-22 with a NMAS of 12.5-mm
2	**9.5-NMAS**	Conventional OGFC mix a NMAS of 9.5-mm
3	**Che1-OGFC**	OGFC mix fabricated with PG 76-22 + a chemical WMA (Che1)
4	**Che2-OGFC**	OGFC mix fabricated with PG 76-22 + a chemical WMA (Che2)
5	**Org-OGFC**	OGFC mix fabricated with PG 76-22 + an organic WMA
6	**CR+Che1-OGFC**	OGFC mix fabricated with PG 67-22 + a chemical WMA (Che1)+ 10 % CR
7	**CR-OGFC**	OGFC mix fabricated with PG 67-22 + 10 % CR
8	**F_1-OGFC***	Conventional OGFC mix fabricated with PG 76-22+ F_1 filler
9	**F_2-OGFC***	Conventional OGFC mix fabricated with PG 76-22+ F_2 filler

*Fines in CM were replaced by F_1 and F_2

Results were analyzed statistically using an Analysis of Variance (ANOVA) and Tukey's Honest Significant Difference (HSD) grouping at a 95% confidence level to identify the statistical differences between the characteristics and performance of the different mixes. Statistical differences were identified with letters on the figures: A, B, and C. Different assigned letters indicate that the two groups are statistically different with the letter A assigned to the control mix (CM), followed by the letter B and so on.

Air Voids and Permeability

Figure 22 shows the results of air voids (AV) and permeability measurements for the nine mixes considered in the experimental program. As shown in Figure 22, 9.5-NMAS and crumb rubber mixes showed a significant reduction in AV content. F_1 and F_2, on the other hand, did not affect the AV content compared to the CM. The control mix showed the highest AV content at 20.8% whereas the 9.5-NMAS mix had the lowest AV content at 16.3%. For the 9.5-NMAS mix, these results are attributed to the introduction of additional fine aggregate

particles, which filled the gaps among the large aggregate particles, resulting in a reduction in AV. For mixes produced with CR, the reduction in AV content is due to the increase in asphalt volume caused by CR swelling. Further, ANOVA results indicated that the mixes with F_1 and F_2 showed a negligible reduction in AV content compared to the CM; see Figure 22. However, the incorporation of CR decreased the AV content significantly compared to the CM.

Results in Figure 22a also show that the incorporation of WMA additives decreased the total air voids in OGFC; the Org-OGFC, Che2-OGFC, and CR+Che1-OGFC mixes had similar AV contents of approximately 18.50%. These results can be attributed to the ability of the WMA additives to reduce the viscosity of the binder to a degree that allows the mixture to be compacted to the target density with a lower compaction effort. Despite these changes, all the mixes met the AV content standards of DOTD (18-24%) and NCHRP 1-55 (15% minimum) for OGFC mixes, except the 9.5-NMAS mix, which only satisfied the 15% minimum threshold.

Similarly, WMA additives, 9.5mm NMAS, and CR resulted in a reduction in permeability (k) of the OGFC mixes, as the 9.5-NMAS and CR mixes showed permeability values almost half that of the CM permeability. These results can be attributed to the reduction in the AV content. On the other hand, F_1-OGFC and F_2-OGFC showed similar permeability values compared to the CM. As shown in Figure 22b, CM and Che1-OGFC had a k-value of 426 ft./day and 363 ft./day, respectively. However, Che2-OGFC, Org-OGFC, CR+Che1-OGFC, and CR-OGFC showed almost the same k-values of 198 ft./day. These results are consistent with the findings of NCHRP 1-55, which found a direct relationship between AV content and the coefficient of permeability. Statistically, ANOVA results showed that 9.5-NMAS, Che2-OGFC, Org-OGFC, CR+Che1-OGFC, and CR-OGFC had k values that were significantly different from those of the control mix. However, Che1-OGFC, F_1-OGFC, F_2-OGFC, and CM mixes exhibited statistically equivalent k values. According to NCHRP 1-55, a k value of 164 ft./day is sufficient for OGFC to achieve its functionality [1]. Therefore, all mixes would pass the NCHRP-recommended permeability criterion for OGFC mixes.

Figure 22. OGFC functionality test results: (a) AV (b) coefficient of permeability

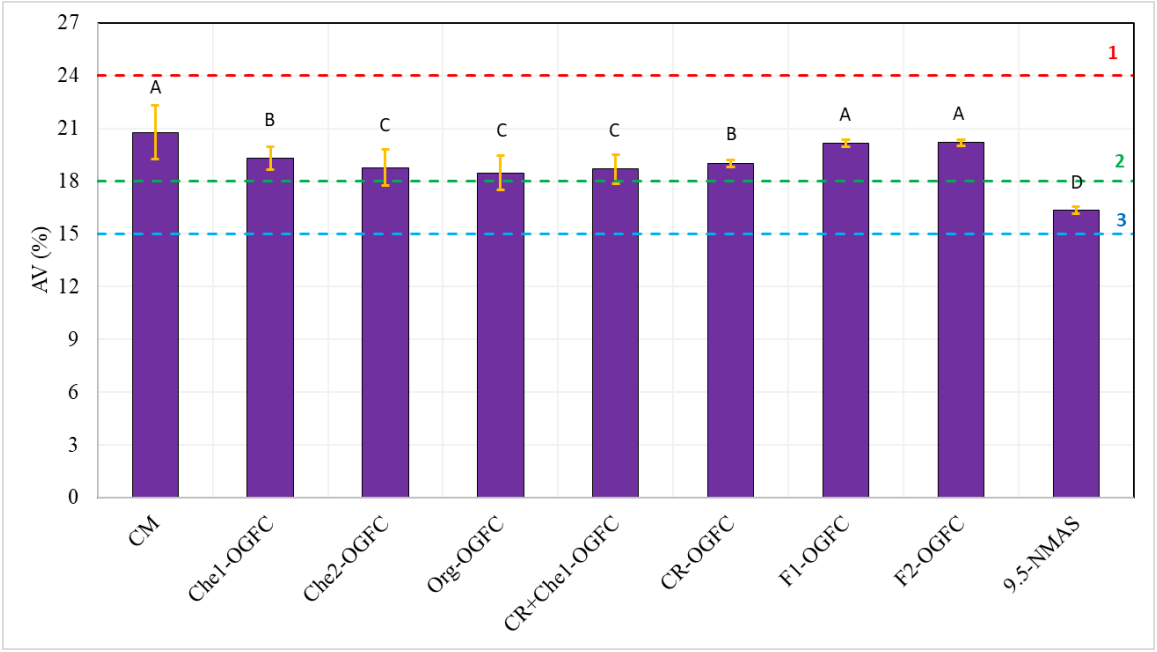

(a)

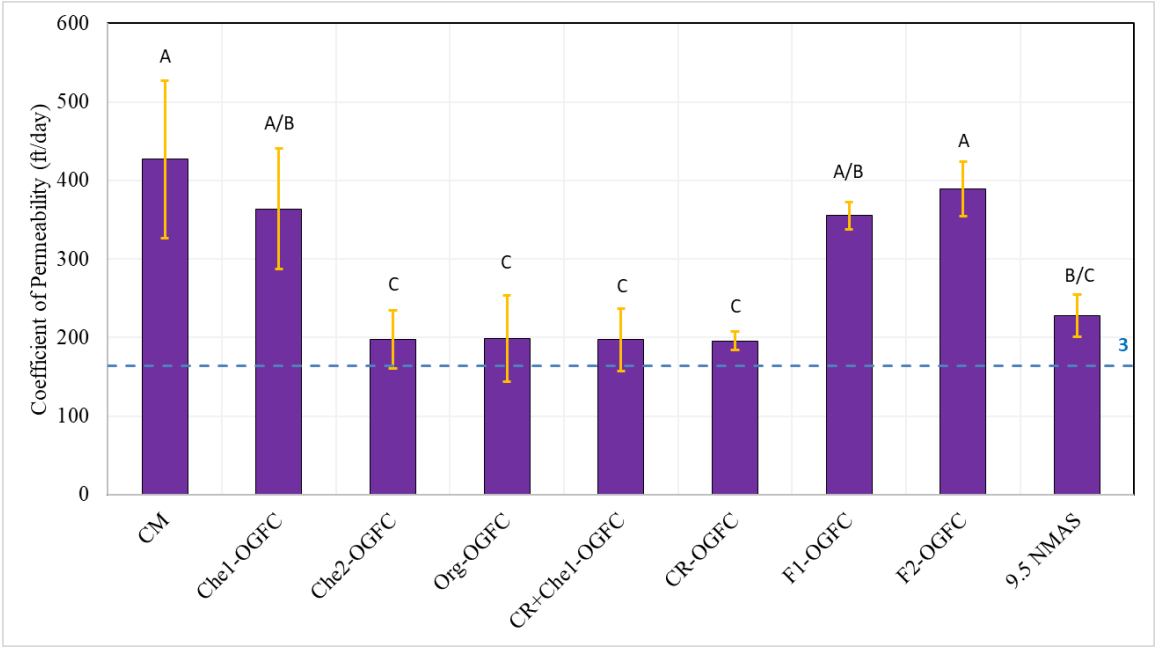

(b)

[1] Maximum DOTD requirement; [2] Minimum DOTD requirement, [3] Minimum NCHRP requirement

Draindown Test Results

Figure 23 compares the results of the draindown test for the nine mixes evaluated in the experimental program. It is noted that all mixes satisfied the DOTD requirement of 0.30% for

draindown. Figure 23 shows that Org-OGFC had the least draindown of 0.01%. In contrast, the Che1-OGFC mix showed the highest draindown value at 0.11%. In statistical terms, Che1-OGFC showed draindown values that were similar to that of the CM. However, the remaining mixes showed draindown values that were significantly smaller than that of the CM. For the WMA mixes, the decrease in draindown values can be attributed to the reduction in mixing temperature. For the CR mixes, crumb rubber increased the viscosity of the asphalt binder; therefore, it was expected that their draindown values would be lower than that of the CM. For F_1-OGFC and F_2-OGFC, the pozzolanic characteristics of both fillers promoted the adhesion properties between the aggregate and binder resulting in a significant reduction in draindown values.

Figure 23. Draindown test results

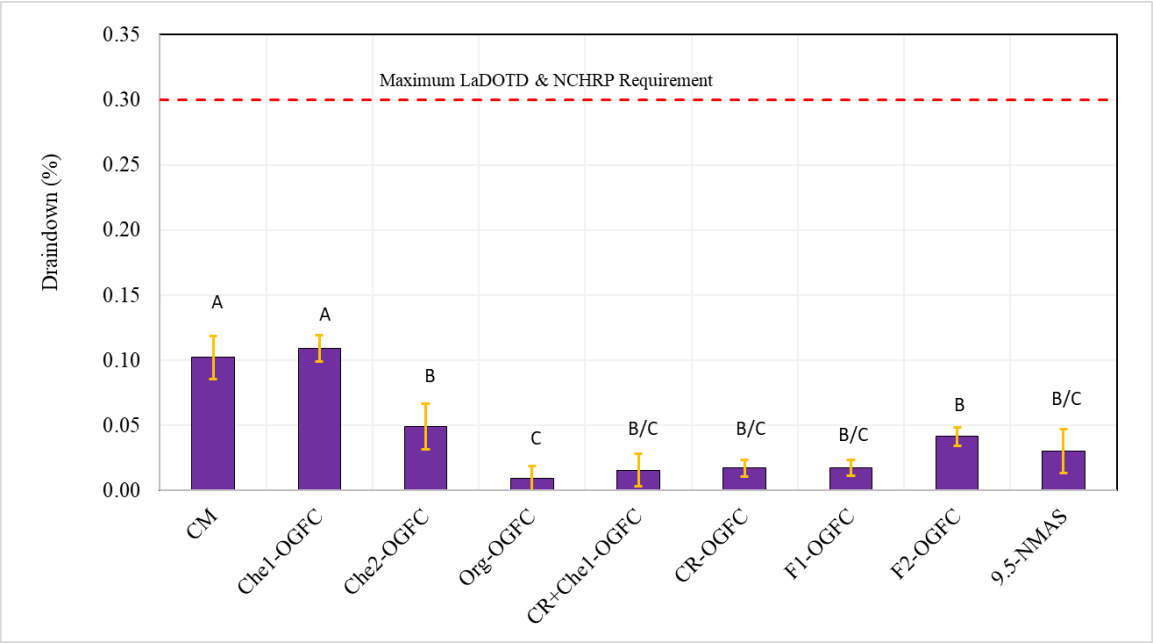

Compaction Energy Index (CEI)

Figure 24 shows the CEI for all mixes evaluated in the experimental program. Overall, the use of WMA additives in the OGFC mix reduced the CEI, which indicates that WMA-OGFC mixes would require less compaction effort and energy consumption during the compaction stage compared to the control mix. Statistically, Che1-OGFC, Che2-OGFC, Org-OGFC, 9.5-NMAS, and CR+Che1-OGFC mixes exhibited CEI values that were significantly lower than that of the CM, as supported by the ANOVA results; see Figure 24. It is noted that the CR-OGFC mix showed the same CEI as compared to the CM, despite the high compaction temperature of 356ºF. These results can be attributed to the increase in binder viscosity due to the use of crumb rubber in the mix, which required a higher compaction effort to compact the mix to the desired density. It is worth mentioning that the CR+Che1-OGFC mix showed

lower CEI compared to the CM, despite the addition of CR in the mix. These results may be attributed to the use of Che1 in the mix, which in turn reduced the frictional forces at the binder-aggregate interface, resulting in a reduction in CEI. Overall, WMA-OGFC and 9.5-NMAS mixes would require a reduced compaction effort in the field compared to conventional CM.

Figure 24. Compaction Energy Index (CEI) results

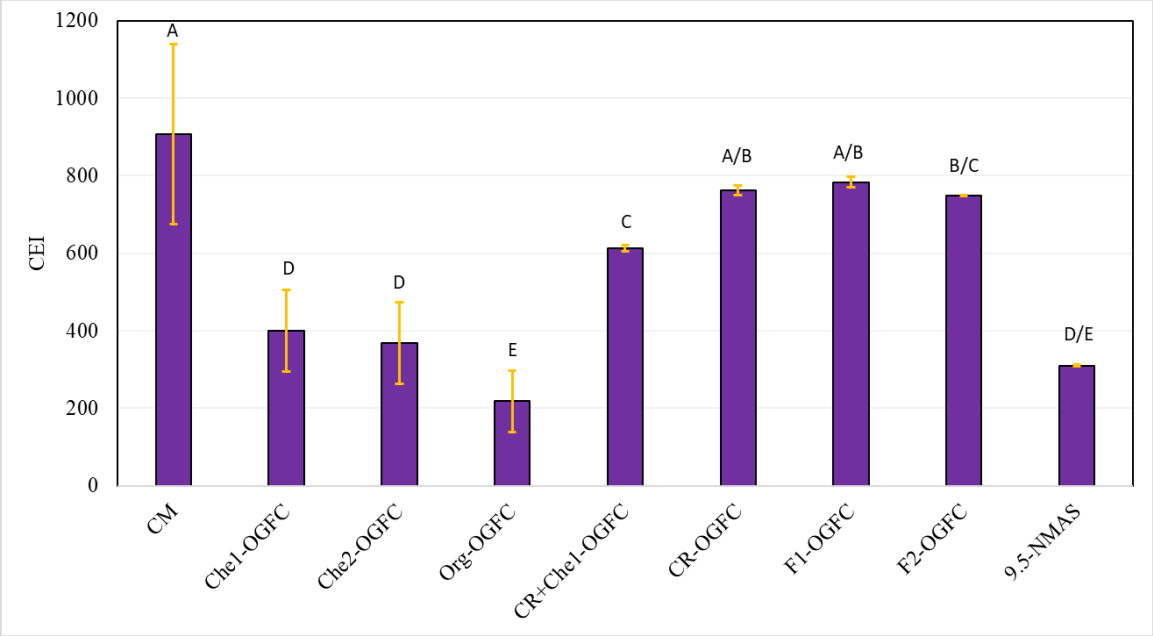

Cantabro Loss Test Results

Figure 25 shows the results of the Cantabro test, which was used to assess the raveling resistance and durability of the OGFC mixtures. In general, all of the evaluated mixes performed adequately in terms of raveling resistance, especially for the test samples that were aged and moisture-conditioned. For the unaged samples, the WMA additives, 9.5-NMAS, and the different fillers enhanced the raveling resistance of the OGFC mixes. However, the use of CR did not improve the raveling resistance of the OGFC mixes.

Figure 25a shows the results of the Cantabro test for the unaged specimens for all mixtures. Under these conditions, the 9.5-NMAS, Che2-OGFC and F_2-OGFC mixes showed the best raveling resistance as indicated by the Cantabro loss values of 6.3%, 7.5%, and 8.7%, respectively. In contrast, the CM mixtures showed the least resistance to raveling, as shown in Figure 25a. The results also indicated that the 9.5-NMAS, Che2-OGFC, Org-OGFC, CR-OGFC, F_1-OGFC, and F_2-OGFC mixes satisfied the allowable Cantabro loss requirement as presented in Figure 25a. While the average Cantabro loss values of CM, Che_1-OGFC, and

CR+Che$_1$-OGFC mixes satisfied the maximum loss requirement, some specimens showed higher Cantabro loss values in these mixtures, as indicated by the error bars in Figure 25a.

For the aged samples, all of the evaluated mixes showed higher raveling resistance compared to the CM; see Figure 25b. The 9.5-NMAS, F_1-OGFC, and Che2-OGFC mixes showed the best raveling resistance with Cantabro loss values of 4.5%, 5.9%, and 10.7%, respectively. Additionally, the results of the ANOVA test indicated that all the proposed mixes exhibited a significant improvement in raveling resistance compared to the control mix.

For moisture-conditioned samples, all of the mixtures considered in this study satisfied the maximum Cantabro loss requirements, except the CM; see Figure 25b. The CM exhibited a Cantabro loss value of 43.9% when the Cantabro abrasion test was conducted on the moisture-conditioned samples, indicating poor raveling resistance. Additionally, Figure 25b shows that the CM was the only mix that exceeded the maximum allowable Cantabro loss value for the moisture-conditioned samples. The aforementioned observations were supported by the results of the statistical analysis. As presented in Figure 25b, the CM showed Cantabro loss values that were significantly greater than those of the remaining mixes. These results imply that the modified OGFC mixes would provide superior raveling resistance compared to the CM even after the pavement is exposed to rainfall or flooding conditions.

Figure 25. Cantabro loss results: (a) unaged samples (b) aged and moisture conditioned samples

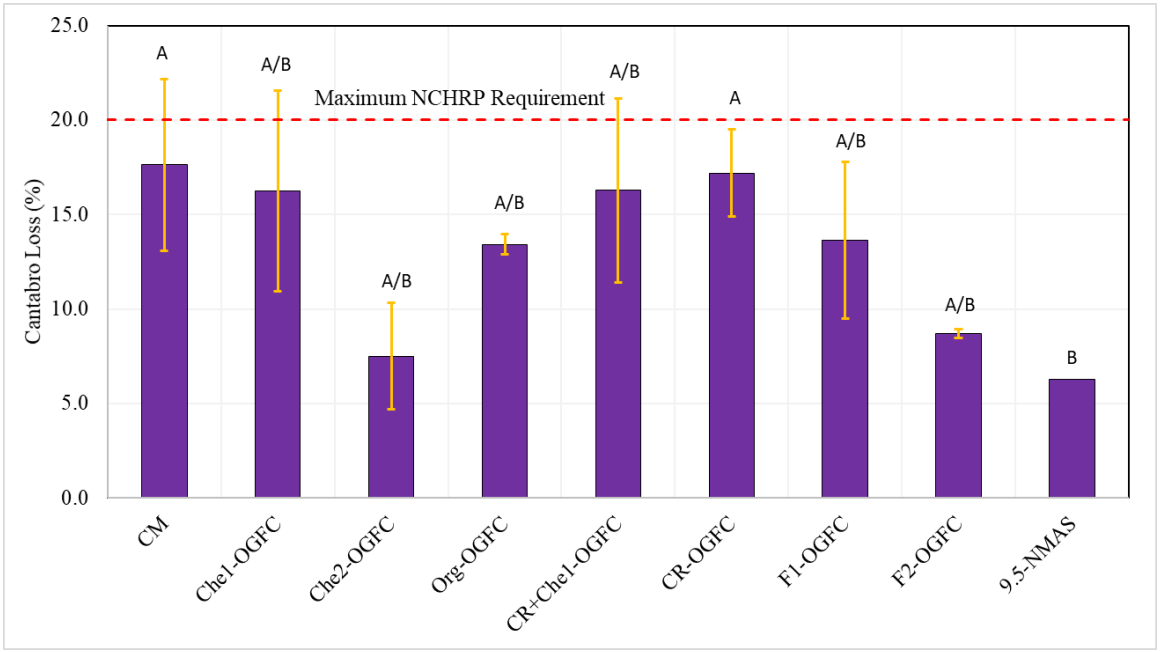

(a)

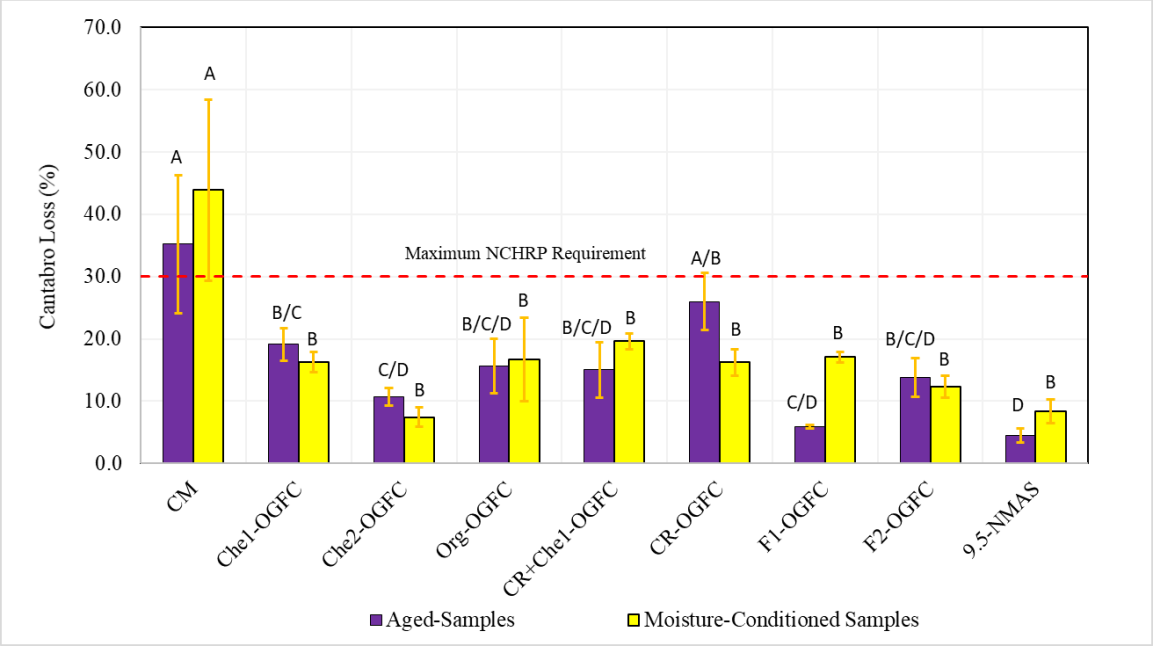

(b)

Rutting Performance Test Results

Figure 26 summarizes the results of the rutting performance test using the HWT. In general, compared to the CM, OGFC mixes containing WMA showed comparable permanent deformation resistance. However, 9.5-NMAS, crumb rubber, and filler-modified mixes enhanced the OGFC permanent deformation resistance.

Figure 26a shows the rut depth results of the OGFC mixes at 5,000 passes. While Org-OGFC had the smallest rut depth of 0.16 in. after 5,000 passes, the CM showed the largest rut depth of 0.31 in. after 5,000 passes. Figure 26a indicates that both Che1-OGFC and Che2-OGFC had a rut depth of 0.27 in. after 5,000 passes. For the remaining mixes (9.5-NMAS, CR-OGFC. F_1-OGFC, and F_2-OGFC), HWT test results indicated a permanent deformation of about 0.20 in. after 5,000 passes.

Tukey's HSD results showed that Org-OGFC, CR-OGFC, F_1-OGFC, F_2-OGFC, and 9.5-NMAS had permanent deformation values that were significantly lower than that of the CM. Compared to the CM, the rut depth values of 9.5-NMAS, F_1-OGFC, and F_2–OGFC mixes were reduced by 39.0%, 30.0%, and 31.0%, respectively. For the Org-OGFC, as the temperature decreased, the organic WMA additive crystalized resulting in a lattice structure, which in turn enhanced asphalt binder stiffness and subsequently improved asphaltic mixture permanent deformation resistance [85]. For the CR-OGFC mix, the crumb rubber increased the stiffness of the asphalt binder; subsequently, the permanent deformation resistance improved when CR was incorporated into OGFC mixes. For F_1-OGFC and F_2-OGFC, adding cement and fly ash is expected to increase the adhesive bond between the aggregate and the

binder within the mixture; therefore, the permanent deformation resistance was improved. It is noted that all mixes satisfied DOTD requirements of 0.50 in. after 5,000 passes, as presented in Figure 26a.

In Figure 26b, the rut depth values of all mixes at 20,000 passes were compared to the maximum allowable rut depth recommended by NCHRP 1-55. From Figure 26b, Org-OGFC, 9.5-NMAS, CR-OGFC, F_1-OGFC, and F_2-OGFC satisfied NCHRP 1-55 requirements after 20,000 passes. However, CM, Che1-OGFC, Che2-OGFC and CR+Che1-OGFC did not meet the NCHRP criterion with rut depths of 0.70, 0.51, 0.65, and 0.69 in., respectively.

The statistical analysis results indicated that Org-OGFC, 9.5-NMAS, CR-OGFC, F_1-OGFC, and F_2-OGFC achieved a significant reduction in rut depth compared to the CM. In contrast, the remaining mixes did not show any significant enhancement in permanent deformation resistance compared to the CM; see Figure 26b.

Figure 26. HWT results: (a) rut depth @ 5,000 passes (b) rut depth @ 20,000 passes

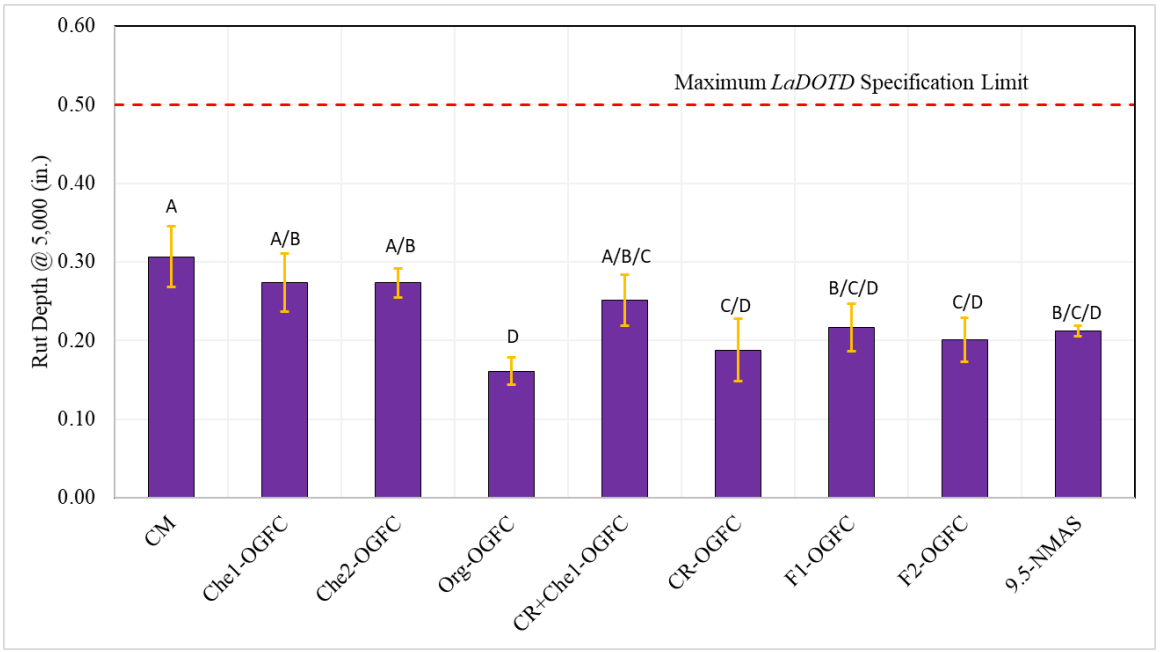

(a)

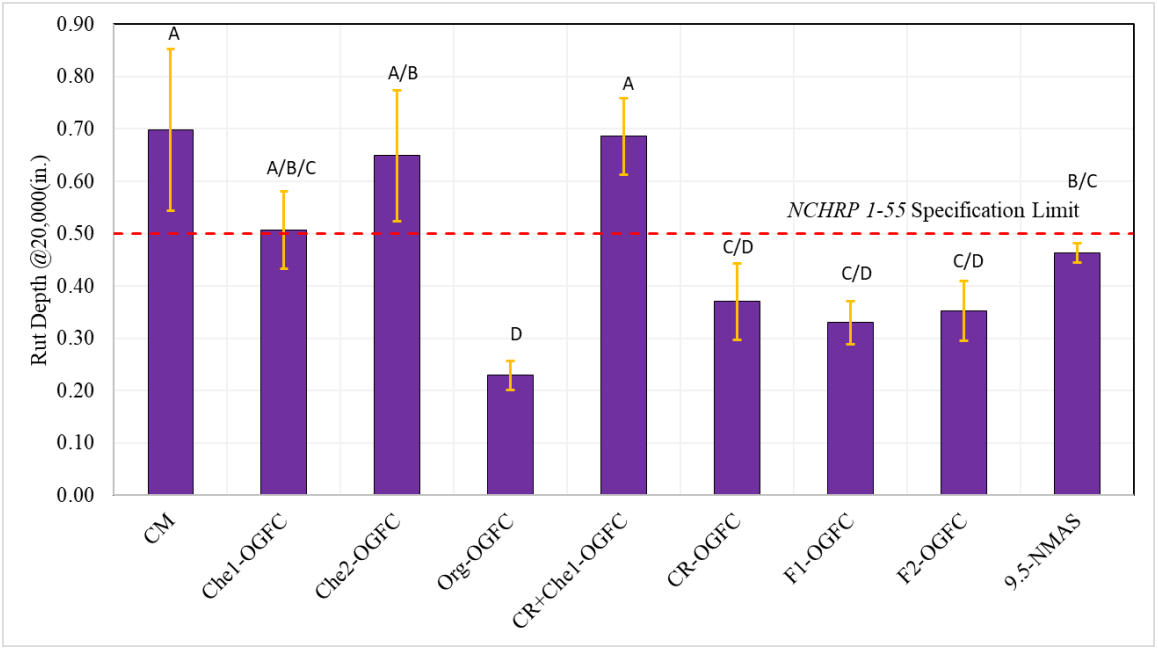

(b)

Texas Overlay Tester Results

Figure 27 shows the results of the Texas Overlay Tester (TOT). Overall, all mixes showed acceptable resistance to cracking. The results of GC are presented in Figure 27a. From the figure, it can be concluded that all mixes performed adequately in the test; however, Che1-OGFC showed the least resistance to crack initiation with a GC value of 0.5 lb.-in./in^2, which is less than the minimum acceptable value of 1.0 lb.-in./in^2. Additionally, the figure indicates that the CR+Che1-OGFC mix did not satisfy the minimum acceptable value of GC with a GC value of 0.97 lb.-in./in^2. In contrast, the remaining mixes showed GC values that ranged from 1.0 to 2.2 lb.-in./in^2, which indicated acceptable cracking resistance. Among the mixes evaluated, F_1-OGFC showed the highest crack initiation resistance with a GC value of 2.2 lb.-in./in^2. Additionally, the ANOVA results showed that F_1 significantly enhanced OGFC performance in terms of cracking resistance compared to the control mix. However, the use of Che1 resulted in a reduction in the resistance to crack initiation compared to the control mix, as presented in Figure 27a.

Figure 27b shows the results of the Crack Propagation Rate (CPR). This parameter was used to evaluate OGFC's ability to delay crack propagation once the crack has initiated. From the figure, it can be concluded that all mixes satisfied the maximum allowable CPR value of 0.50. Additionally, Figure 27b indicated that CR-OGFC has the highest CPR at 0.40; however, most OGFC mixes had a CPR value of 0.24. ANOVA results showed that the CPR values of the mixes fabricated with CR were significantly different compared to the CM.

However, the observed statistical differences among the CPR values of the remaining mixes were negligible compared to the CM, as presented in Figure 27b.

Figure 27c presents the cracking interaction plot, which can be used to evaluate the mixture cracking characteristics based on both GC and CPR values. To this end, GC and the corresponding CPR values were plotted and compared to the allowable range of GC and CPR. Ideally, a mixture with acceptable crack resistance should be located in the soft-crack resistant zone, as illustrated in Figure 27c. From the figure, it can be concluded that all mixes were located in the soft-crack resistant zone, indicating an acceptable crack resistance. However, OGFC mixes fabricated with Che1 (Che1-OGFC and CR+Che1-OGFC) were outside the recommended crack resistance zone.

Figure 27. TOT results: (a) critical facture energy results (b) crack propagation rate results (c) cracking interaction plot

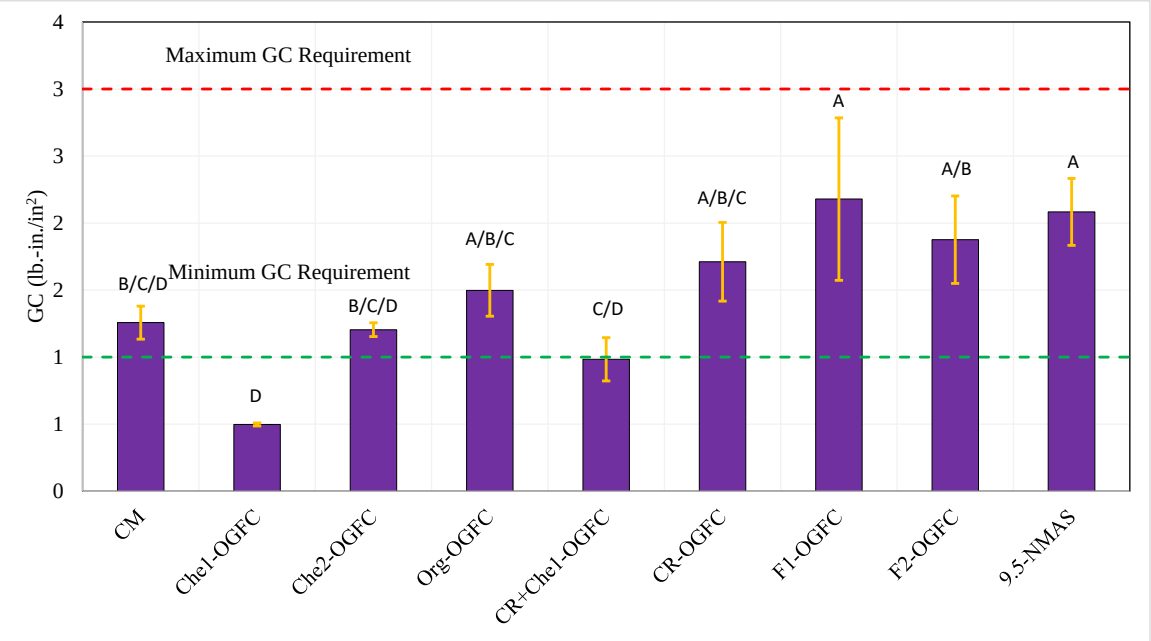

(a)

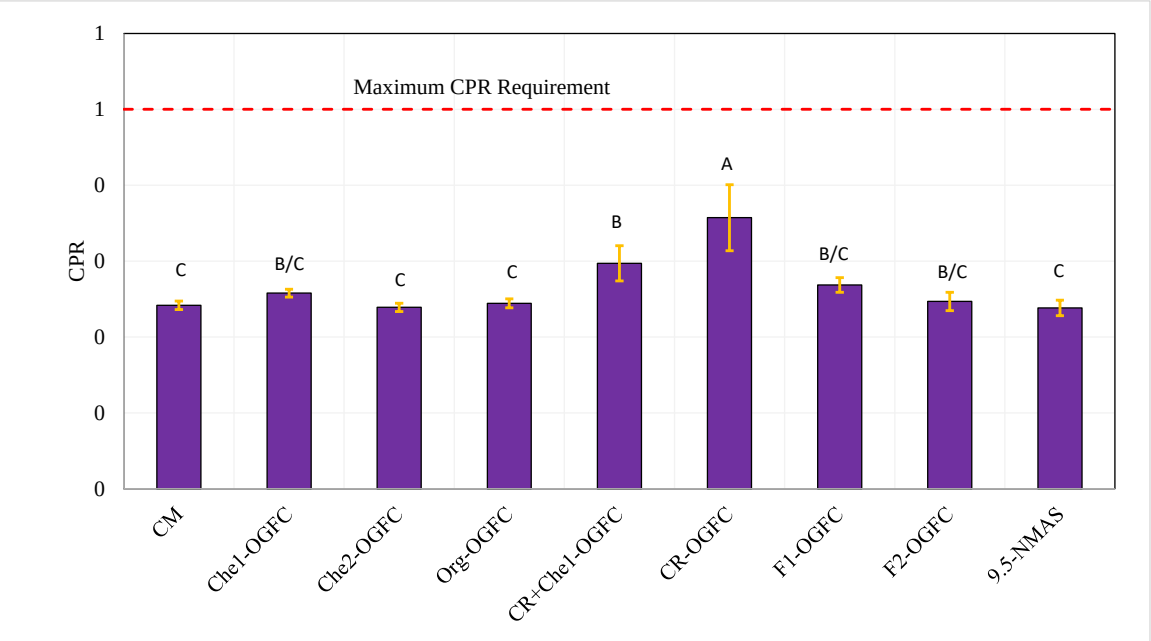

(b)

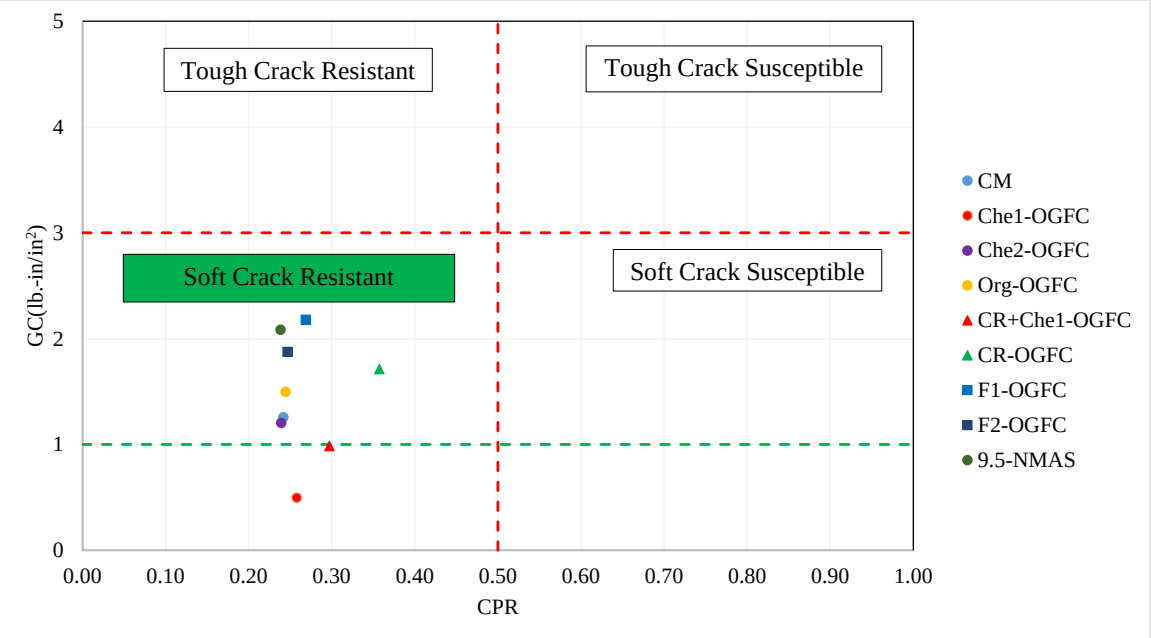

(c)

Modified Lottman Test Results

Figure 28 presents the results of the Modified Lottman test. Modified Lottman test results were analyzed in terms of unconditioned (dry) ITS, conditioned ITS, and TSR. The results of the unconditioned ITS are presented in Figure 28a. In general, dry ITS value decreased when Che1 and Che2 were used in the mix, as well as the CR+Che1-OGFC mix. However, the

incorporation of the organic WMA, CR (without WMA additive), 9.5-NMAS, F_1, and F_2 into the OGFC increased the dry ITS. Since dry ITS value is typically used as an indication of fatigue crack resistance, it may be inferred that the organic WMA, CR only, 9.5-NMAS, F_1, and F_2 improved the fatigue cracking resistance of OGFC.

Statistically, the effect of WMA additives on OGFC fatigue crack resistance was insignificant. However, the use of organic WMA in OGFC resulted in dry ITS values that are larger than the minimum acceptable values of 70 psi, as recommended in NCHRP 1-55 [1]. Therefore, it can be concluded that among the WMA mixes, the Org-OGFC may exhibit a superior fatigue crack resistance compared to the CM. Additionally, the statistical analysis indicated that CR-OGFC, 9.5-NMAS, F_1-OGFC, and F_2-OGFC showed significant improvement in fatigue cracking resistance compared to the CM; see Figure 28a. Further, these mixes satisfied the minimum dry ITS values of 70 psi recommended by NCHRP 1-55 [1].

The results of conditioned ITS values are presented in Figure 28b. The results indicated that F_1-OGFC and F_2-OGFC mixes showed the highest conditioned ITS value of approximately 81 psi. The figure also indicates that Org-OGFC, 9.5-NMAS, and CR-OGFC showed increased wet ITS values of 26.4%, 35.5%, and 23.5% compared to the CM. However, the remaining mixes exhibited comparable conditioned ITS values. According to NCHRP 1-55, the acceptable conditioned ITS value for OGFC applications should be more than 50 psi. The results presented in Figure 28b indicated that the CM, Org-OGFC, CR-OGFC, 9.5-NMAS, F_1-OGFC, and F_2-OGFC mixes satisfied the NCHRP requirements, while the other mixes did not.

TSR values are presented in Figure 28c.The TSR value is typically used to evaluate the moisture-damage resistance of asphalt mixes. According to NCHRP 1-55, a TSR value of 0.70 is the minimum value for OGFC mixes. According to Figure 28c, it can be concluded that all mixes satisfied the minimum TSR values of OGFC. The results of TSR showed that all mixes had similar moisture resistance and stripping performance. This may be due to the use of an ASA in all OGFC mixes prepared in this study.

Figure 28. Modified Lottman test results: (a) unconditioned ITS (b) conditioned ITS (c) TSR

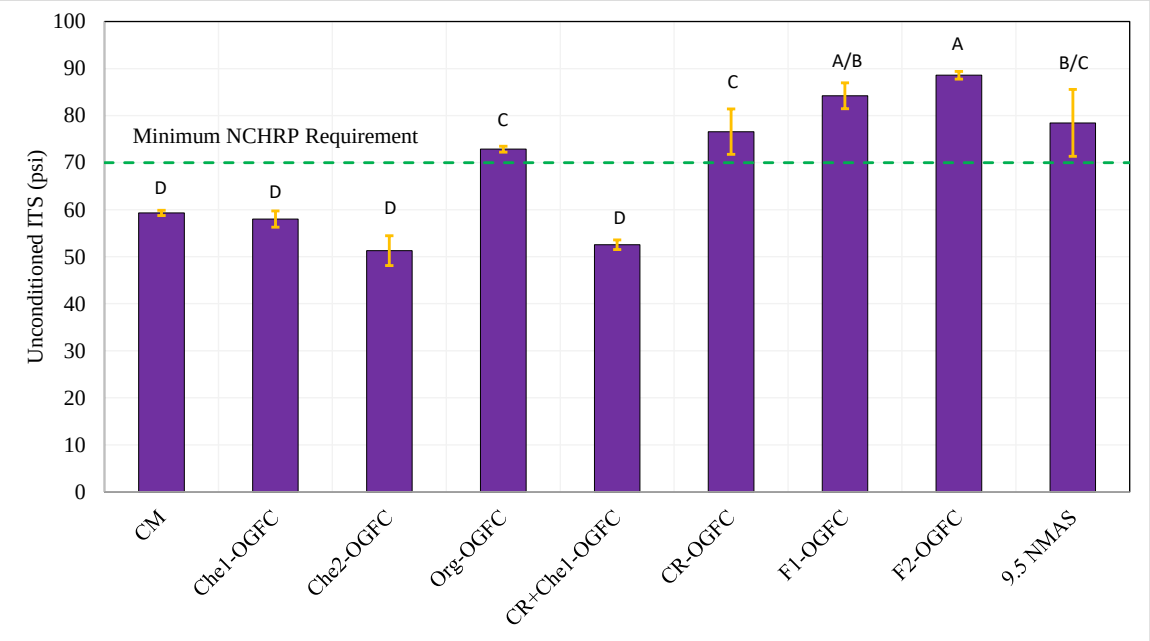

(a)

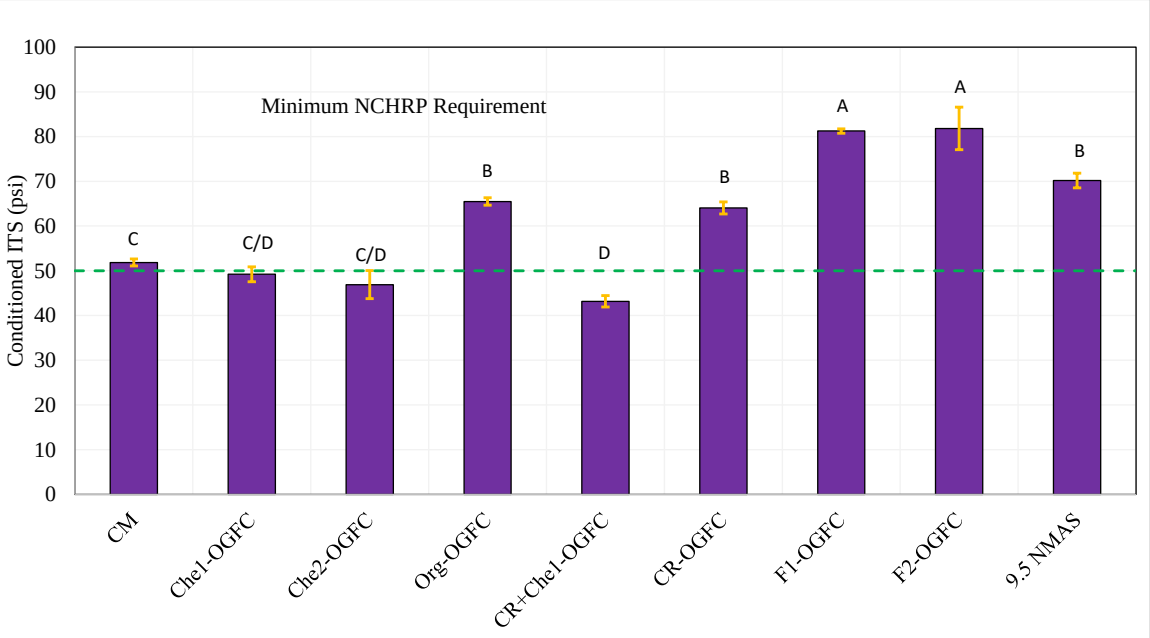

(b)

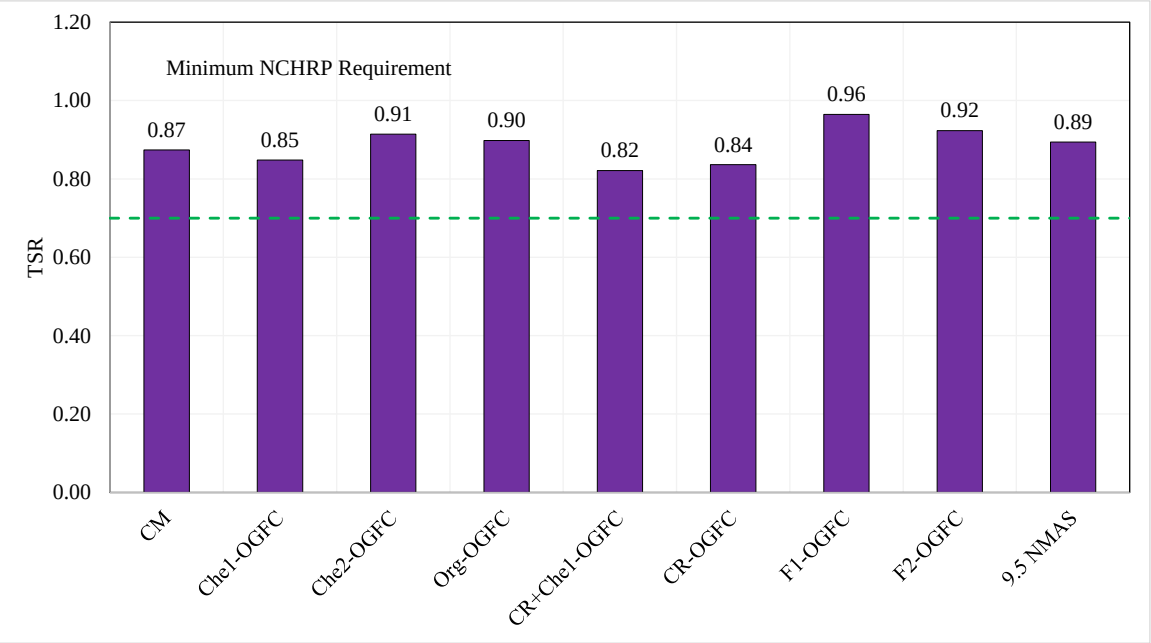

(c)

[1] Minimum NCHRP 01-55 requirement

Boil Test

Figure 29 shows the results of the boil test. It compares the condition of the loose mix specimens for the different mixes after a 10-min. boiling period. Regardless of the mixture type, the visual inspection indicated that no stripping has occurred to the aggregate in all mixes, predicting acceptable moisture damage resistance for all mixes. These results may be explained as follows. First, the high viscosity of PG 76-22 used in the current study promoted the adhesive strength, which in turn enhanced OGFC moisture damage resistance. Second, the use of WMA additives enhanced the ability of the asphalt binder to coat aggregate particles by reducing the frictional forces at the binder-aggregate interface, resulting in adequate adhesion strength for moisture damage resistance [77]. For mixes that were fabricated with CR, adding CR to the binder increased its viscosity, which in turn increased the ability of the binder to adhere to the aggregate particles promoting stripping resistance. Similarly, the use of pozzolanic materials such as Portland cement and fly ash enhanced the adhesive strength between the binder and aggregate particles, resulting in acceptable stripping damage resistance. Lastly, all the mixes were fabricated with an ASA, which helped promote OGFC stripping resistance.

Figure 29. Boil Test Results for (a) CM (b) Che1-OGFC (c) Che2-OGFC (d) Org-OGFC (e) CR+Che1-OGFC (f) CR-OGFC (g) F_1-OGFC (h) F_2-OGFC (i) 9.5-NMAS

(a)

(b)

(c)

(d)

(e)

(f)

(g)

(h)

(i)

Binder Testing Results

The extracted binders' rheological properties were measured in order to evaluate the effects of the selected additives and modifications on the binder. Table 17 presents the results of binder laboratory testing conducted using the dynamic shear rheometer and the bending beam rheometer. In the DSR test, the permanent deformation of the binder residues was analyzed using $G^*/\sin\delta$, where G^* is the complex shear modulus of the binder and δ is the phase angle. Binders with higher $G^*/\sin(\delta)$ are predicted to demonstrate enhanced resistance against permanent deformation. Based on these results, it was found that 9.5-NMAS and F_1-OGFC provided superior resistance to permanent deformation with a high temperature grade of 82, followed by CR+Che1-OGFC, F_2-OGFC, and CM. The worst performing binders at high temperatures were Org-OGFC, Che2-OGFC, and Che1-OGFC, which were WMA binders. Interestingly, the best performance mixture against rutting was Org-OGFC; see Figure 26. These results may indicate that the binder's rheological properties had little influence on the mix's rutting resistance when comparing the mix rutting performance to the binder rheological results.

According to the BBR test results, 9.5-NMAS, CR+Che1-OGFC, and F_1-OGFC exhibited the highest resistance against low-temperature cracking, followed by CM, Che2-OGFC, and CR-OGFC. A lower creep stiffness value indicates greater resistance to thermal stresses and a higher m-value suggests a faster stress relaxation rate. These results indicate that the binder's resistance to permanent deformation and low temperature cracking was improved for the binder extracted from mixes 9.5-NMAS and F_1-OGFC. However, since the binder used in CM and 9.5-NMAS was the same, it may indicate that the binder extraction process did not successfully remove all the filler materials from the sample. On the other hand, the low-temperature grade of CM, Che1-OGFC, Che2-OGFC, Org-OGFC, CR-OGFC, and F_2-OGFC was found to be the same at -16°C, and their relaxation slope (m-value) was similar, indicating a similar level of performance at low temperatures.

Table 17. Summary of rheological test results

Test	Specifications	Temp.	CM	9.5-NMAS	C1-OGFC	C2-OGFC	O-OGFC	CR-OGFC	CR+C1-OGFC	F_1-OGFC	F_2-OGFC
	Original										
DSR G*/Sin(δ), kPa	>1.0 kPa	52°C	---				1.170				
DSR G*/Sin(δ), kPa	>1.0 kPa	58°C					0.590				
DSR G*/Sin(δ), kPa	>1.0 kPa	64°C			1.320	1.395		1.415			
DSR G*/Sin(δ), kPa	>1.0 kPa	70°C	1.305		0.777	0.835		0.748			
DSR G*/Sin(δ), kPa	>1.0 kPa	76°C	0.781						1.645		1.285
DSR G*/Sin(δ), kPa	>1.0 kPa	82°C		1.305					0.886	1.475	0.824
DSR G*/Sin(δ), kPa	>1.0 kPa	88°C		0.782						0.875	
	RTFO										
DSR G*/Sin(δ), kPa	>2.20 kPa	58°C					3.675				
DSR G*/Sin(δ), kPa	>2.20 kPa	64°C			3.840		2.010	3.530			
DSR G*/Sin(δ), kPa	>2.20 kPa	70°C	3.280		1.705	3.310		1.685			
DSR G*/Sin(δ), kPa	>2.20 kPa	76°C	1.815			1.950					
DSR G*/Sin(δ), kPa	>2.20 kPa	82°C		3.060					3.175	3.500	
DSR G*/Sin(δ), kPa	>2.20 kPa	88°C		1.755					1.645	2.055	3.650

Test	Specifications	Temp.	CM	9.5-NMAS	C1-OGFC	C2-OGFC	O-OGFC	CR-OGFC	CR+C1-OGFC	F_1-OGFC	F_2-OGFC
DSR G*/Sin(δ), kPa	>2.20 kPa	94°C									1.730
	PAV										
DSR G*Sin(δ), kPa	<5000 kPa	01°C					5867				
DSR G*Sin(δ), kPa	<5000 kPa	04°C					4725				
DSR G*Sin(δ), kPa	<5000 kPa	07°C			5769			6066			
DSR G*Sin(δ), kPa	<5000 kPa	10°C	6449		4564	5610		4675			
DSR G*Sin(δ), kPa	<5000 kPa	13°C	3768			4312					
DSR G*Sin(δ), kPa	<5000 kPa	16°C									
DSR G*Sin(δ), kPa	<5000 kPa	19°C		5721					6742		
DSR G*Sin(δ), kPa	<5000 kPa	22°C		4686					4859	6004	6751
DSR G*Sin(δ), kPa	<5000 kPa	25°C								4222	4969
BBR, S, MPa	<300 MPa	-6°C	33	----	28	27	16	34	----	----	95
BBR, S, MPa	<300 MPa	-12°C	62	189	48	55	26	77	134	139	172
BBR, S, MPa	<300 MPa	-18°C	----	271	----	----	----	----	294	301	----
BBR, m-value	>0.300	-6°C	0.319	----	0.308	0.317	0.302	0.308	----	----	0.331
BBR, m-value	>0.300	-12°C	0.294	0.304	0.265	0.275	0.258	0.262	0.325	0.333	0.279
BBR, m-value	>0.300	-18°C	----	0.258	----	----	----	----	0.279	0.273	----

Property	CM	9.5-NMAS	C1-OGFC	C2-OGFC	O-OGFC	CR-OGFC	CR+C1-OGFC	F_1-OGFC	F_2-OGFC
PG Grading	70-16	82-22	64-16	64-16	52-16	64-16	76-22	82-22	76-16
Continuous PG grade	73.1-20.5	85.2-22.5	67.1-17.1	67.9-18.4	53.4-22.2	67.3-17.0	80.8-25.3	86.5-25.3	79.4-19.6
Useful temperature interval (UTI)	93.64	107.66	84.2	86.28	75.6	84.3	106.08	111.76	98.96

CM= control mix**;** C1= Che1; C2= Che2; O= Org, CR= crumb rubber, CR+C1-OGFC= CR+Che1-OGFC, F_1= Portland cement; F_2= fly ash.

Summary of Laboratory Test Results

Table 18 shows a summary of the experimental results obtained in this study. The table indicates that the control mix had some durability issues as demonstrated by the Cantabro abrasion, HWT, and Modified Lottman test results. These issues would negatively impact OGFC performance and subsequently reduce its cost-effectiveness. The table also shows that the use of WMA additives generally enhanced OGFC durability. However, some durability issues may be encountered when chemical WMA additives are used in the mix. The results also indicate that the organic additive (Org-OGFC) was the most effective WMA additive evaluated in the study and has the potential to prevent durability issues in OGFC.

Table 18 shows that the use of 9.5-mm NMAS, CR only, and fillers (F_1 and F_2) significantly enhanced the performance of OGFC, as all test results satisfied local and national requirements. However, the use of Che1 and CR concurrently in the OGFC mix did not achieve the desired performance. These results may be attributed to two primary factors. First, the dosage of 0.1% of Che1 may be insufficient when used with crumb rubber. In other words, other dosages should be investigated in future studies. Second, the production temperature of 325^{o}F may be too low for the rubberized binder to reach the appropriate viscosity required for mixing. In future studies, more research should be conducted to evaluate and identify the optimum mixing and compaction temperatures with crumb rubber-modified WMA mixes.

Table 18. Summary of the laboratory mix test results

Test Properties / Mix ID	AV	Permeability	Draindown	Cantabro			Hamburg Wheel-Tracking Test		Texas Overlay Test		Modified Lottman Test			Boiling Test
				Unaged	Aged	Moisture Conditioned	5,000 passes	20,000 passes	GC	CPR	ITS dry	ITS wet	TSR	
CM	P*	P	P	F**	F	F	P	F	P	P	F	P	P	P
9.5-NMAS	P	P	P	P	P	P	P	P	P	P	P	P	P	P
Che1-OGFC	P	P	P	F	P	P	P	F	F	P	F	F	P	P
Che2-OGFC	P	P	P	P	P	P	P	F	P	P	F	F	P	P
Org-OGFC	P	P	P	P	P	P	P	P	P	P	P	P	P	P
CR+Che1-OGFC	P	P	P	F	P	P	P	F	F	P	F	F	P	P
CR-OGFC	P	P	P	P	P	P	P	P	P	P	P	P	P	P
F_1-OGFC	P	P	P	P	P	P	P	P	P	P	P	P	P	P
F_2-OGFC	P	P	P	P	P	P	P	P	P	P	P	P	P	P

*P = Pass and **F= Fail

Cost-Effectiveness

Figure 30a and 30b illustrates the cost effectiveness results for the nine OGFC mixes evaluated in this study based on Equations 11 and 12. As previously noted, the cost-effectiveness analysis expressed the durability of the mixes based on the Cantabro abrasion and the rutting test results from the HWT. Further, the rutting test results were considered at 5,000 passes, which is currently specified by DOTD, and 20,000 passes, which was recommended based on the findings of NCHRP 1-55 [1].

As shown in Figure 30a and based on the 5,000 pass rutting test results, the most cost-effective OGFC mixes were 9.5-NMAS, F_2-OGFC, Che2-OGFC, and Org-OGFC, in this order. On the other hand, considering the rutting performance at 20,000 passes, the most cost-effective OGFC mixes were F_2-OGFC, 9.5-NMAS, Org-OGFC, and F_1-OGFC, in this order. These results support the idea that the aforementioned mixes have the potential to enhance OGFC performance with a little to negligible increase in cost. This performance enhancement is in addition to the energy savings and environmental benefits during production and mix compaction widely documented for WMA mixes. To assess the overall cost effectiveness of the additives over the entire pavement service life, additional research is needed to include field performance, maintenance costs, and end-of-life options.

Figure 30. Cost-effectiveness analysis results considering (a) rutting performance at 5,000 passes and (b) rutting performance at 20,000 passes

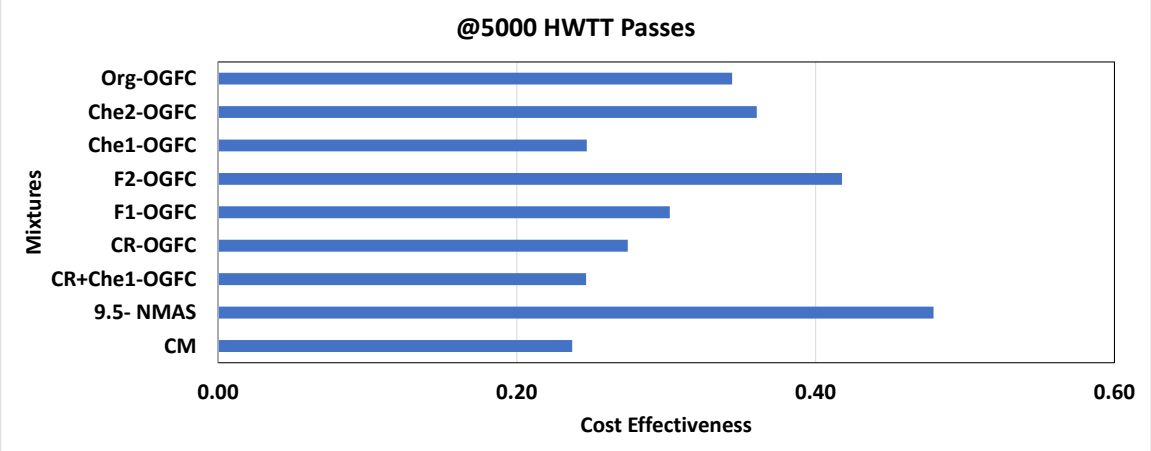

(a)

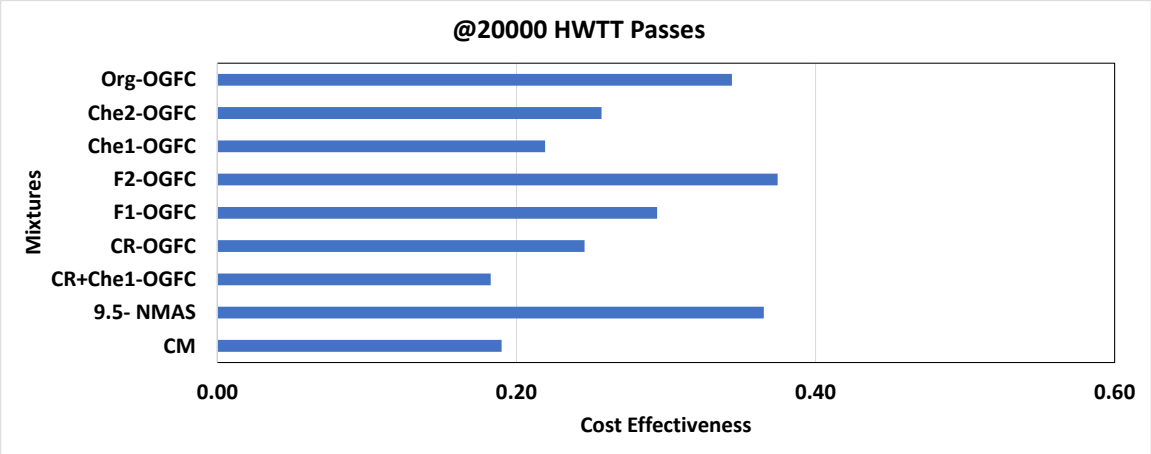

(b)

Results of the Seepage Analysis

This section presents the results of evaluating the effects of K_{OGFC}, T_{OGFC}, K_{HMA}, and traffic volume on the seepage characteristics of pavement structures constructed with an OGFC layer under rain conditions in Louisiana. These effects were evaluated in terms of the time (T_C) at which a point on the OGFC surface reaches overflow or saturated conditions. First, the location at which T_C should be calculated was determined. Second, the effects of the aforementioned factors on the seepage characteristics of the OGFC layer were evaluated. Third, a statistical analysis was conducted to identify the significant factors that affect T_C. Next, an ANN model was trained and validated for the prediction of T_C using the most significant factors while avoiding the need for FE modeling. The results of the developed FE model were then used to propose new guidelines for AV content for OGFC applications in Louisiana.

Critical Location

In this step, the critical location on the surface of OGFC was identified based on the analysis of SEEP/3D. Two initial locations were investigated in the current study: left and right wheel paths. These locations were selected because of their frequent exposure to traffic compared to other locations on the pavement surface. A line located at 2.5 ft. from the pavement centerline was identified as the left wheel path. On the other side, a line at a distance of 3 ft. represented the right wheel path from the shoulder-lane interface [93]. To identify the critical location, the calibrated FE model was executed using the following conditions:

- K_{OGFC} = 0.06 in./sec.;
- T_{OGFC} = 0.75 in.;
- K_{HMA} = 2.36 x 10^{-3} in./sec.;
- Rain Intensity (R) = 0.02, 0.04, and 0.1 in./hr.; and
- Traffic volume = 0 ESAL.

Figure 31 compares the T_C values in the left and right wheel paths for different rain intensities using R-values. These results indicated that the T_C value in the right wheel path was always shorter than the T_C in the left wheel path at all R-values. Therefore, a location in the right wheel path would reach its saturation stage before a similar point in the left wheel path. These results may be attributed to the fact that rainwater always moves towards the shoulder due to gravitational forces. Therefore, the total amount of water that would be induced in the right wheel path would be greater than the amount induced in the left wheel path. Based on these results, all the remaining analyses were conducted based on the T_C values in the right wheel path.

Figure 31. Critical locations in OGFC pavement surface

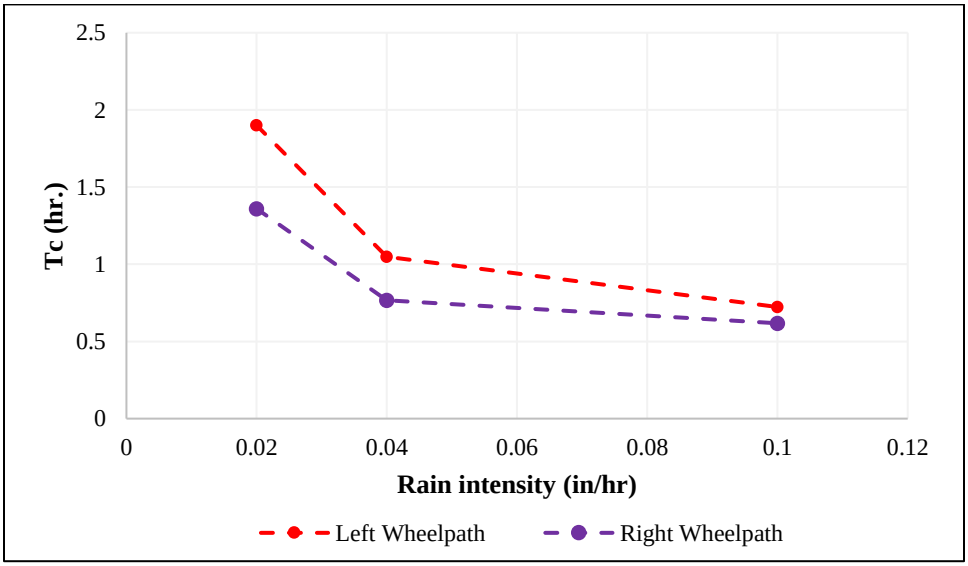

Effects of OGFC Thickness

Figure 32 shows the effect of OGFC thickness on the hydraulic characteristics of the OGFC layer. These results were obtained by executing the calibrated FE model under the following conditions:

- K_{OGFC} = 0.05 in/sec/;
- T_{OGFC} = 0.75. 1.25, and 1.90 in.;
- K_{HMA} = 1.18 x 10^{-3} in./sec/;
- R = 0.02, 0.04, and 0.1 in./hr.; and
- Traffic volume = 0 ESAL.

The results indicate that for all rain conditions, the time required to achieve saturated conditions increased with increasing T_{OGFC}; see Figure 32. For example, T_C increased from 1.26 hr. to 2.70 hr. when the OGFC thickness was increased from 0.75 to 1.90 in. These results can be attributed to the increase in the water storage capacity of the OGFC layer with the increase in thickness.

Figure 32. Impacts of OGFC thickness on OGFC hydraulic characteristics

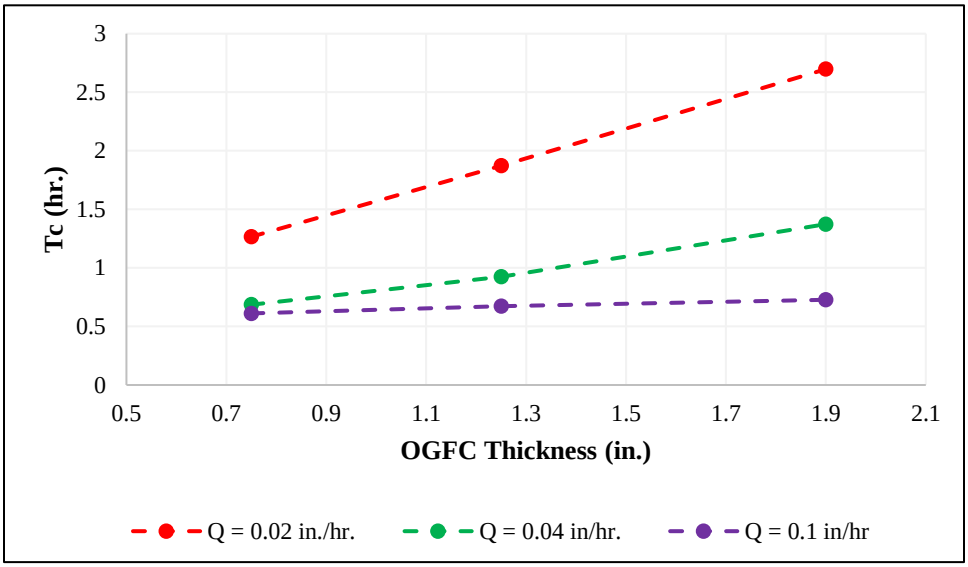

Effects of OGFC Permeability

Figure 33 illustrates the effects of K_{OGFC} on the hydraulic characteristics of the OGFC layer. These results were obtained by executing the FE model under the following conditions:

- K_{OGFC} = 0.06, 0.05, and 0.06 in./sec.;
- T_{OGFC} = 1.25 in.;
- K_{HMA} = 1.18 x 10^{-3} in./sec.;
- R = 0.02, 0.04, and 0.1 in./hr.; and
- Traffic volume = 0 ESAL.

Figure 33 indicates that K_{OGFC} had a minor positive contribution to the overall hydraulic performance of the pavement. The higher the K_{OGFC} value, the longer it takes to reach overflow conditions. For example, T_C increased slightly from 1.80 to 1.86 hr. when K_{OGFC} was increased from 0.03 to 0.06 in./sec at R = 0.02 in./hr. These results may be attributed to the increase in the interconnected AV content and permeability, which contributed to the increase in the water storage capacity of the OGFC layer.

Figure 33. Impacts of OGFC permeability coefficient on OGFC hydraulic performance

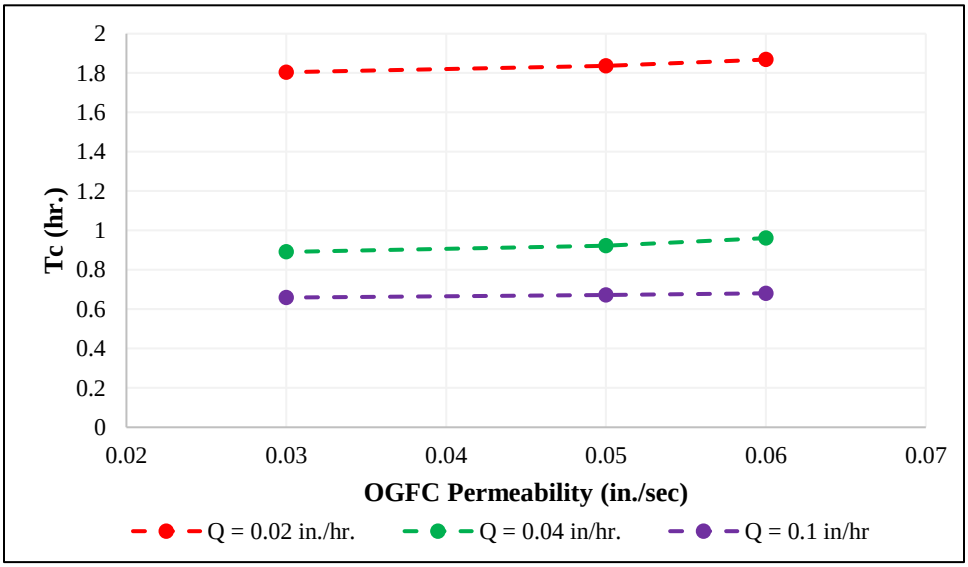

Effects of HMA Permeability

Figure 34 presents the effects of K_{HMA} on the overall hydraulic performance of the OGFC layer. Simulation runs were conducted to identify the controlling trend using the following conditions:

- K_{OGFC} = 0.06 in./sec.;
- T_{OGFC} = 1.25 in.;
- K_{HMA} = 1.18 x 10^{-3}, 2.36 x 10^{-3}, and 3.54 x 10^{-3}in./sec.;
- R = 0.02, 0.04, and 0.1 in./hr.; and
- Traffic volume = 0 ESAL.

The results presented in Figure 34 indicate that as K_{HMA} increased, the time to reach the overflow point increased. At R of 0.02 in./hr., for example, T_C increased by 0.2 hr. (12 min.) when K_{HMA} was increased from 1.36 x 10^{-6} to 3.54 x 10^{-3} in./sec. These results imply that the underlying layers may have a significant role in controlling the drainage of rainfall water in a pavement constructed with an OGFC layer.

Figure 34. Impacts of HMA permeability coefficient on OGFC hydraulic characteristics

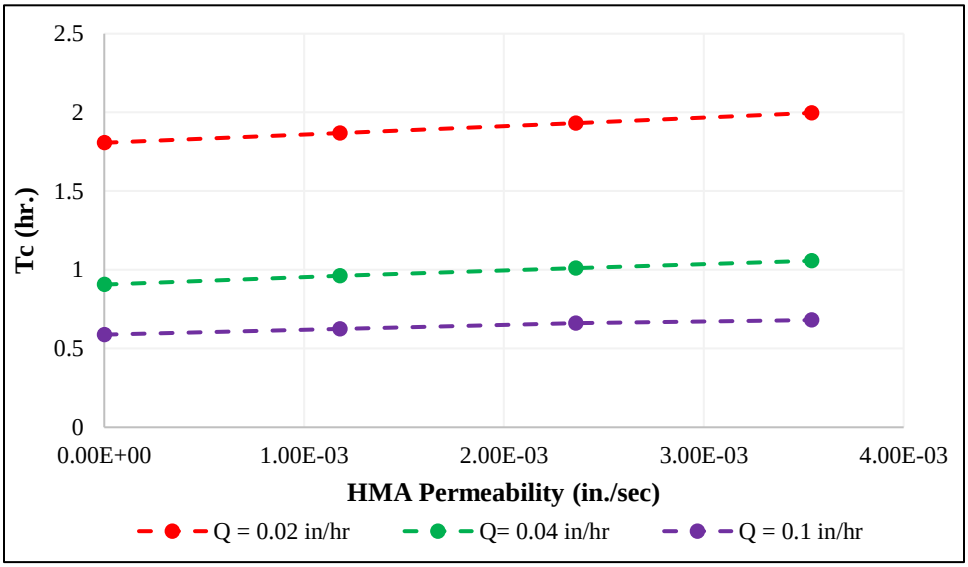

Effects of Rain Intensity

Figure 35 presents the effects of rain intensity (R) on the overall hydraulic performance of a pavement structure constructed with an OGFC surface layer. Simulation runs were conducted using the following conditions:

- K_{OGFC} = 0.05 in./sec.;
- T_{OGFC} = 1.25 in.;
- K_{HMA} = 2.36 x 10^{-3}in./sec.;
- R = 0.02, 0.04, and 0.1 in./hr.; and
- Traffic Volume = 0 ESAL.

Figure 35 shows an inverse relationship between R and T_C. As the rain intensity increased, the time for the OGFC layer to reach saturation decreased. For example, T_C decreased from 2.04 hr. to 0.98 hr. when the rain intensity was increased from 0.02 in./hr. to 0.04 in./hr.

Figure 35. Impacts of rain intensity on the seepage characteristics of OGFC pavements

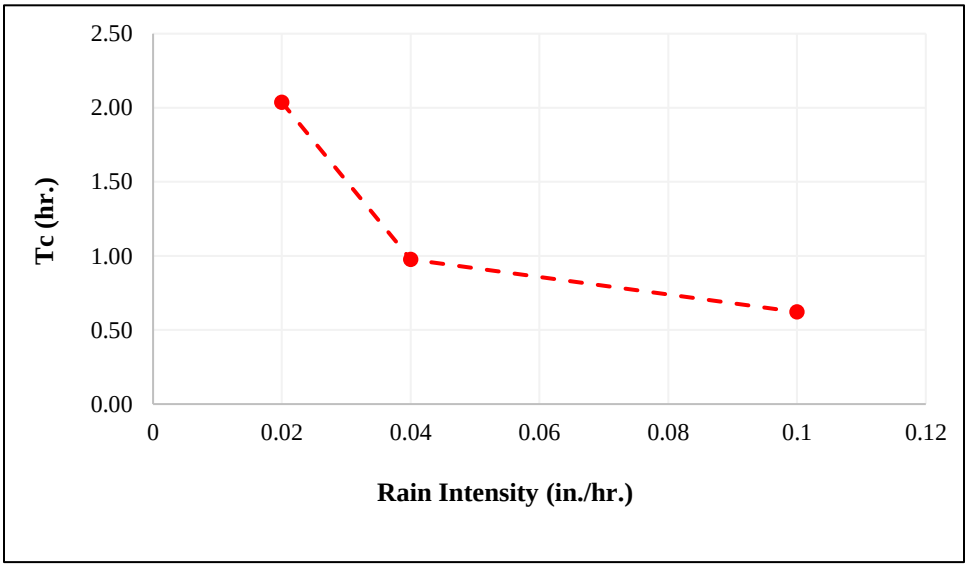

Effects of Traffic Wear

Figure 36 shows the effects of traffic wear on the seepage characteristics of a pavement structure constructed with OGFC. Simulation runs were conducted to simulate traffic wear using the following conditions:

- K_{OGFC} = 0.05 in./sec.;
- T_{OGFC} = 0.75 in.;
- K_{HMA} = 1.18 x 10^{-3}in./sec.;
- R = 0.04 in./hr.; and
- Traffic Volume = 0, 2, 4, 6, 8, and 10 x 10^6 ESAL.

Results shown in Figure 36 indicated that, similar to rain intensity, the relationship between T_C and traffic volume is inverted, especially in the early stage of a pavement service life. As the pavement experienced more traffic, the time to reach overflow conditions decreased. For example, the time to reach overflow condition decreased from 1.37 hr. to 0.80 hr. when the pavement carried a traffic volume of 2x10^6 ESALs.

Figure 36. Impacts of traffic levels on the seepage characteristics of OGFC pavements

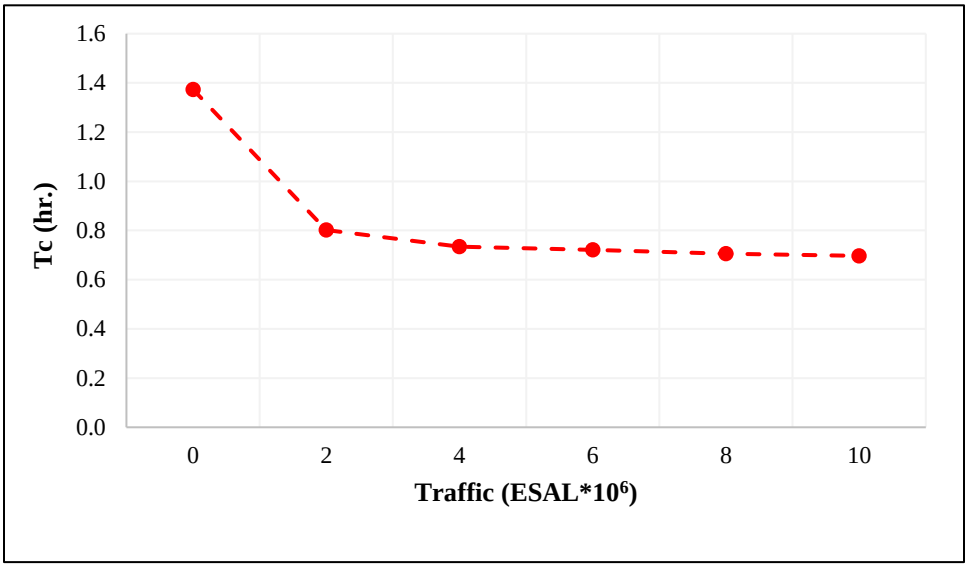

Development of an ANN and XG-BOOST Models for T_C Prediction

In this section, two AI models were developed. An ANN model was developed to predict the time to reach overflow conditions (T_C) for a pavement structure constructed with an OGFC layer. Additionally, an XG-BOOST model backed with a regression model was developed. The primary objective of developing such models was to develop a tool that can predict T_C without the need for FE modeling. To develop these models, it was necessary to determine which parameters are significant in predicting T_C.

Correlation Matrix between TC and FE Model Inputs. SAS 9.4 was used to construct a correlation matrix between T_C and all the inputs of the FE model considered in this study. Next, an ANOVA test was conducted to evaluate the statistical significance of each FE model input on T_C by examining the following hypothesis at a 0.05 confidence level (α).

- H_o (null hypothesis): $\beta_1 = 0$;
- H_1 (alternative hypothesis): $\beta_1 \neq 0$.

where, H_o and H_1 are the null and alternative hypotheses, respectively, β_1 is the slope of the regression line between each input and T_C.

Table 19 shows the correlation among T_C and the different factors considered in the analysis. The results indicated that T_C had a positive correlation with T_{OGFC}, K_{OGFC}, and

K_{HMA} as measured by Pearson correlation coefficients of 0.32, 0.02, and 0.41, respectively. Conversely, both R and traffic volume had an inverse correlation with $T_{C,}$ with a Pearson correlation coefficient value of -0.52 and -0.35, respectively. These results agree with the trends presented in Figures 32 to 36.

Table 19. Correlation matrix between T_C and FE model inputs

Variable	FE Model Inputs	Correlation Coefficient	Prob>|ρ|
Tc (hr.)	T_{OGFC} (in)	0.32	<0.0001
Tc (hr.)	K_{OGFC} (in/sec)	0.02	0.63
Tc (hr.)	K_{HMA} (in/sec)	0.41	<0.0001
Tc (hr.)	R (in/hr.)	-0.52	<0.0001
Tc (hr.)	Traffic	-0.35	<0.0001

Table 19 also shows the results of the ANOVA test. Based on these results, H_o can be rejected for T_{OGFC}, K_{HMA}, R, and traffic volume because the P-value is less than 0.05. Therefore, it can be concluded that there is sufficient evidence at a 0.05 significance level that a linear relationship exists between T_C and T_{OGFC}, K_{HMA}, R, and traffic volume. In contrast, the results indicated that H_o cannot be rejected in the case of K_{OGFC} because the P-value was greater than 0.05. Therefore, it can be concluded that a linear correlation does not exist between T_C and K_{OGFC} at a 0.05 significance level. These results were expected due to the fact that all mixes considered in this study satisfied the minimum requirement of permeability, as shown in Figure 20. Based on the previous results, T_{OGFC}, K_{HMA}, R, and traffic volume were considered inputs for the ANN, while K_{OGFC} was not included in the predictive model.

ANN Model Structure and Inputs. In this study, a multi-layered feed-forward backprop ANN with a LOGSIG transfer function and TRAINGDX training function was developed. The input layer consisted of four neurons, while the output layer consisted of one neuron, as shown in Figure 37. The remaining two layers were hidden layers and consisted of eight neurons each. The ANN model was developed to predict T_C using T_{OGFC}, K_{HMA}, R, and traffic volume as input parameters. This model can be used as a practical and simple tool for the prediction of T_C without the need for conducting FE modeling.

Figure 37. Components of the ANN model

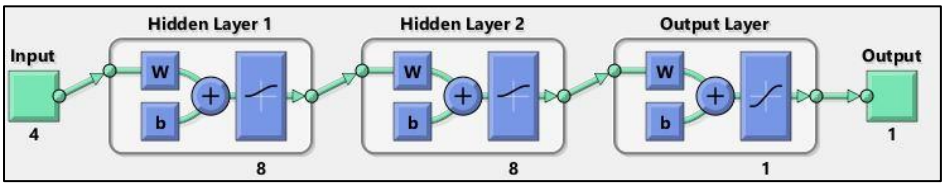

Training and Validation of the ANN Model. In this study, a dataset that included 648 data points was used to develop and validate the ANN model. This dataset was divided into two groups. The first group contained 80% of the data (520 data points), which were used to train the model. The data in the first group were divided into three subsets: 70%, 15%, and 15% for training, testing, and validation, respectively. These percentages were adopted since they resulted in the best performance of the proposed model. The second group consisted of 20% (128 data points) of the whole data, which were used to validate the trained ANN model using a separate independent dataset. It is noted that the data points in each subset were selected randomly. Additionally, the training of the developed ANN model was terminated when the validation error was leveled to avoid overfitting.

Results of ANN Model Training. Figure 38 shows the results of training the ANN model. In general, Figure 38a illustrates that the developed model can predict T_C accurately with a coefficient of determination (R^2) and root mean square error (RMSE) values of 99% and 5.02%, respectively. Additionally, the figure shows that ANN model predictions were precise as presented by the slope (β_1) and intercept (β_o) of the regression line between the ANN and FE outputs. The regression line had a slope (β_1) of 0.99, which is close to unity, indicating a strong linear relationship between the ANN and FE values. Similarly, the regression line exhibited an intercept (β_o) of 0.01, which is close to zero confirming the unbiased prediction, especially at smaller T_C values. Moreover, the error analysis presented in Figure 38b indicates that the errors are randomly distributed. The figure also shows that there is no systematic error trend between the residuals and the predicted values. Further, Figure 38b indicates that the error between the FE and ANN values had an average and standard deviation (Std.) of 0.003 and 0.047 hr., respectively.

For further evaluation, SAS 9.4 was used to conduct a two-tailed t-test to compare the means of T_C produced by ANN and FE by testing the following hypotheses at $\alpha = 0.05$.

- H_o: the average of T_C_ANN = the average of T_C_FE; and
- H_1: the average of T_C_ANN ≠the average of T_C_FE.

The results indicated a p-value of 0.926; therefore, H_o cannot be rejected indicating that the average T_C_ANN = average T_C_FE. Based on these results, it can be concluded that the average critical time predicted by the ANN was statistically equal to the average critical time obtained from the FE model at $\alpha = 0.05$.

Figure 38. Results of the ANN model in the training stage (a) comparison between T_C calculated using FE and ANN (b) relation between the TC_ANN values and the residuals

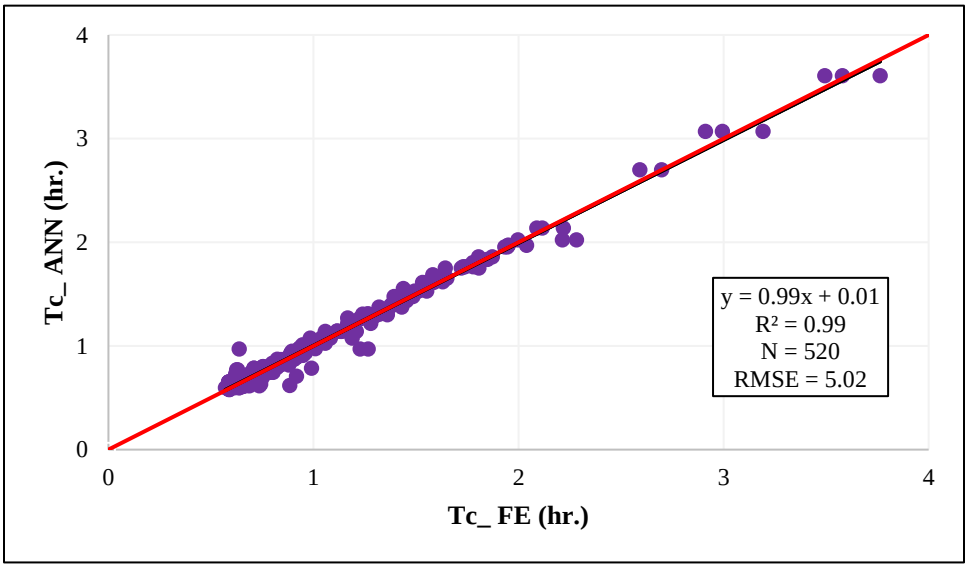

(a)

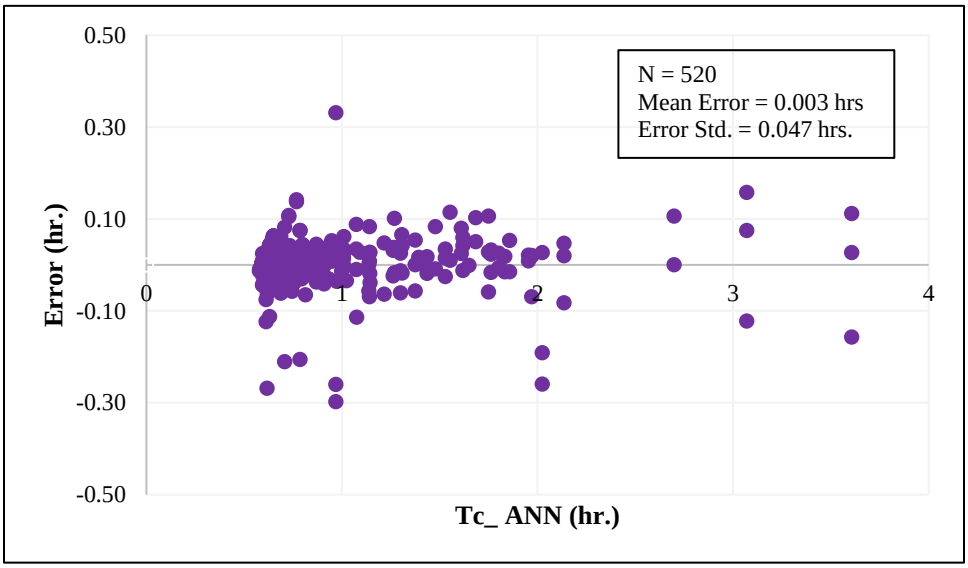

(b)

Results of ANN Model Validation. A separate dataset consisting of 128 data points was used to validate the ANN model. The T_C values obtained from the ANN model were compared to those calculated by the FE model. Figure 39a shows the T_C_ANN compared to the T_C_FE. As presented in the figure, the ANN model predicted T_C accurately. Figure 39 indicates that the ANN model predicted T_C with R^2 and RMSE of 98% and 0.31%, respectively, compared to the FE model T_C values. Additionally, the figure illustrates a minimum level of bias as presented by β_1 (0.98) and β_o (0.02). Further, the error analysis presented in Figure 39b indicates that the ANN model can accurately predict T_C with an average error of 0.00001 hrs.

SAS 9.4 was also used to conduct a two-tailed t-test to compare the means of T_C produced by ANN and FE at $\alpha = 0.05$. The results indicated a p-value of 0.99; therefore, the null hypothesis cannot be rejected. Consequently, it can be concluded that at $\alpha = 0.05$, the average T_C values predicted by the ANN using a separate dataset were equal to the average Tc values obtained by the FE model. Based on the aforementioned results, it can be concluded that the developed ANN model can be used as an alternative tool for the calculation of the time to overflow conditions for pavement structures constructed with an OGFC layer.

Figure 39. Results of the ANN model in the validation stage (a) comparison between T_C calculated using FE and ANN (b) relation between the TC_ANN values and residuals

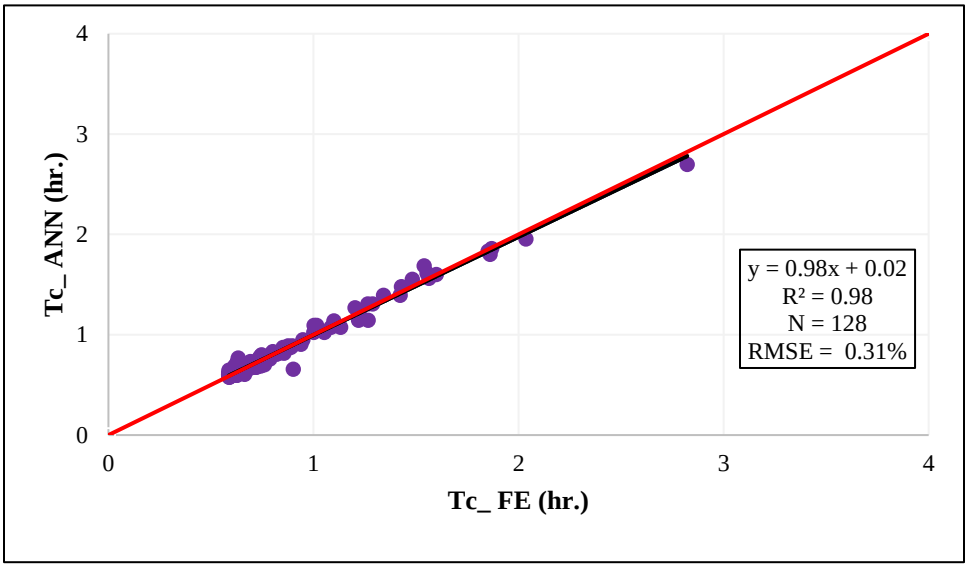

(a)

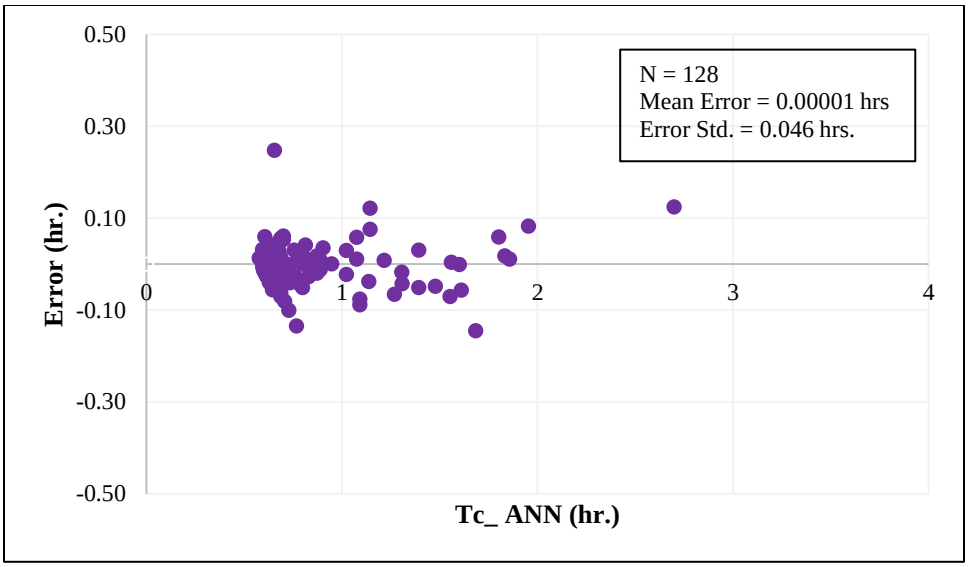

(b)

Results of XGBOOST Model Training and Validation. Fitting the XGBOOST model backed with a regression model achieved adequate statistical fits. In the validation phase, the XGBOOST model achieved an RMSE = 0.0381 and a coefficient of determination (R^2) of 0.9845. The advantage of the XGBOOST model over the ANN model is that it is able to predict the time to reach overflow conditions (T_c) for heavy rain conditions not originally considered in the FE model.

Real-Life Application of the Developed Model. Over time, OGFC layers may become clogged due to dust, binder creep, and consolidation due to traffic. Therefore, routine maintenance (e.g., vacuum sweeping) for the OGFC layer is necessary to maintain its functional benefits. To the best of the authors ' knowledge, there is no available tool or model for predicting the functional service life of pavement structures constructed with an OGFC layer. The developed ANN model presented in this study can fill this gap.

To illustrate this application, the verified FE model developed in this study was used to calculate T_C for the two cases described in Table 20 over its entire service life. The ANN was also used to calculate T_C for the same cases. The T_C values produced by both approaches were compared.

Table 20. Inputs to FE and ANN models for real-life applications

Factor	Case 1	Case 2	Unit
K_{OGFC}	0.05		in./sec
T_{OGFC}	1.25	1.90	in
R	0.04		in./hr.
K_{HMA}	3.54×10^{-3}		in./sec
Traffic	0, 2, 4, 6, 8, and 10		10^6 x ESAL

Figure 40 compares the T_C values predicted by the ANN and FE models for cases 1 and 2. Results indicated that the time to reach the overflow condition decreased over the pavement service life due to the clogging of the interconnected voids in the OGFC. Additionally, the ANN model predicted T_C accurately with RMSE values of 4.11% and 4.95% for cases 1 and 2, respectively, compared to the FE model. These results imply that the developed ANN model can be used to predict the deterioration in the functional performance of OGFC mixes over their service lives. With the use of this model, state highway agencies can predict the time at which routine maintenance should be conducted for roadway segments constructed with an OGFC layer.

Figure 40. Comparison between ANN and FE models T_C values over time (a) case 1 (b) case 2

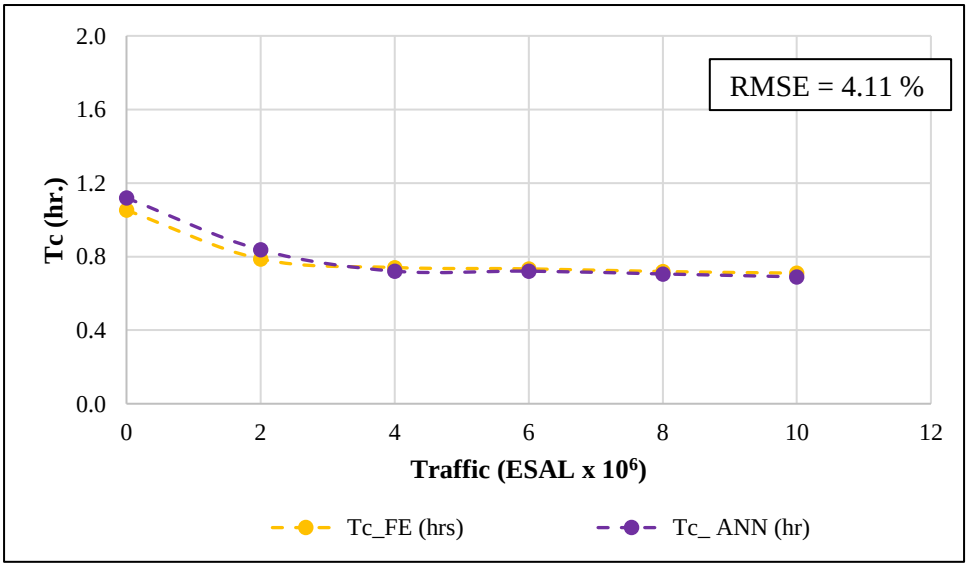

(a)

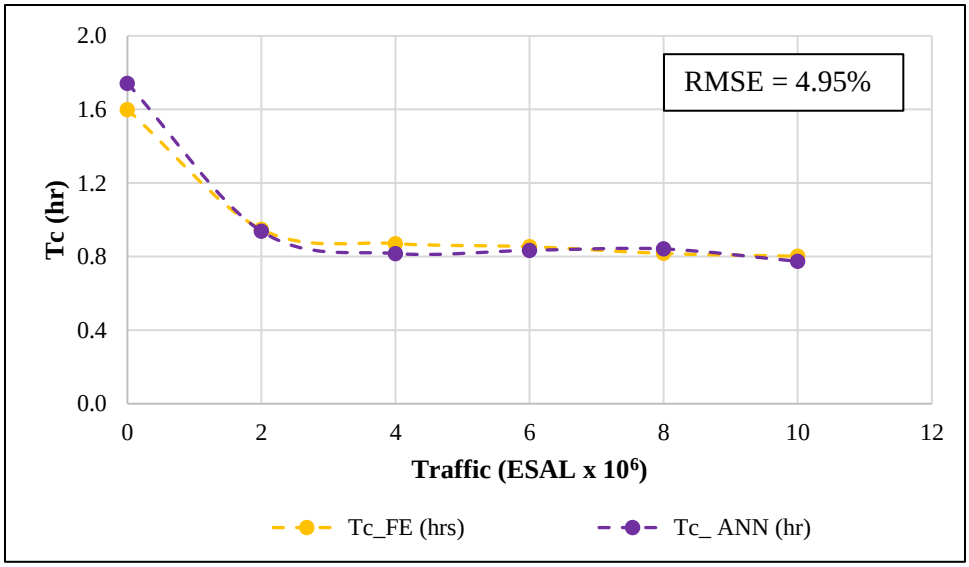

(b)

New AV Guidelines for OGFC Mixes in Louisiana

In this section, the developed XGBOOST model was used to propose more effective air voids (AV) guidelines for OGFC applications in Louisiana. As previously demonstrated, high AV content has a negative effect on OGFC durability [69, 70, 1]. In Louisiana, OGFC mixes are usually placed with an AV content between 18-24%, which is higher than the AV content recommended by other states [1]. Therefore, the XGBOOST model developed in this study was used to investigate whether the current AV guidelines in Louisiana for OGFC mixes can be revised (i.e., decreased) based on local rainfall intensity.

To achieve this objective, the developed XGBOOST model was used to calculate the time to reach overflow conditions in the right wheel path at R ranging between 0.01 and 3 in./hr. (0.01, 0.1, 0.5, 1, 2, and 3 in./hr.). The T_c was calculated for pavement structures constructed with an OGFC layer with different AV contents (14%, 16%, 18%, 20%, 22%, and 24%). Additionally, the effect of traffic wear was considered by applying the reduction factors previously presented in this report. Table 21 shows the inputs of the XGBOOST model that were used in this analysis.

Table 21. Inputs of the FE model for new AV guidelines

Factor	Factor Values	Unit
OGFC AV Content	14, 16, 18, 20, 22, and 24	%
K_{OGFC}	0.01, 0.03, 0.06, 0.08, 0.1, and 0.12	in./sec.
T_{OGFC}	1.25	in
R	0.01, 0.1, 0.5, 1, 2, and 3	in./hr.
K_{HMA}	$1.36x10^{-6}$	in./sec.
Traffic	10	10^6 x ESAL

Time to Reach Overflow Conditions. Figure 41 shows the time to reach overflow conditions of the pavement structure modeled with different AV contents at different rainfall intensities. In general, as the AV content increased, the time to reach overflow conditions also increased across all levels of air voids. For instance, at 0.1 in/hr., overflow occurs between 35-60 min., while at 3 in/hr., it drops to approximately 10-13 min., regardless of the air void level. As shown in this figure, higher rainfall intensities overwhelm the system faster, leading to quicker saturation.

Figure 41. Time to reach overflow conditions for different rainfall intensities

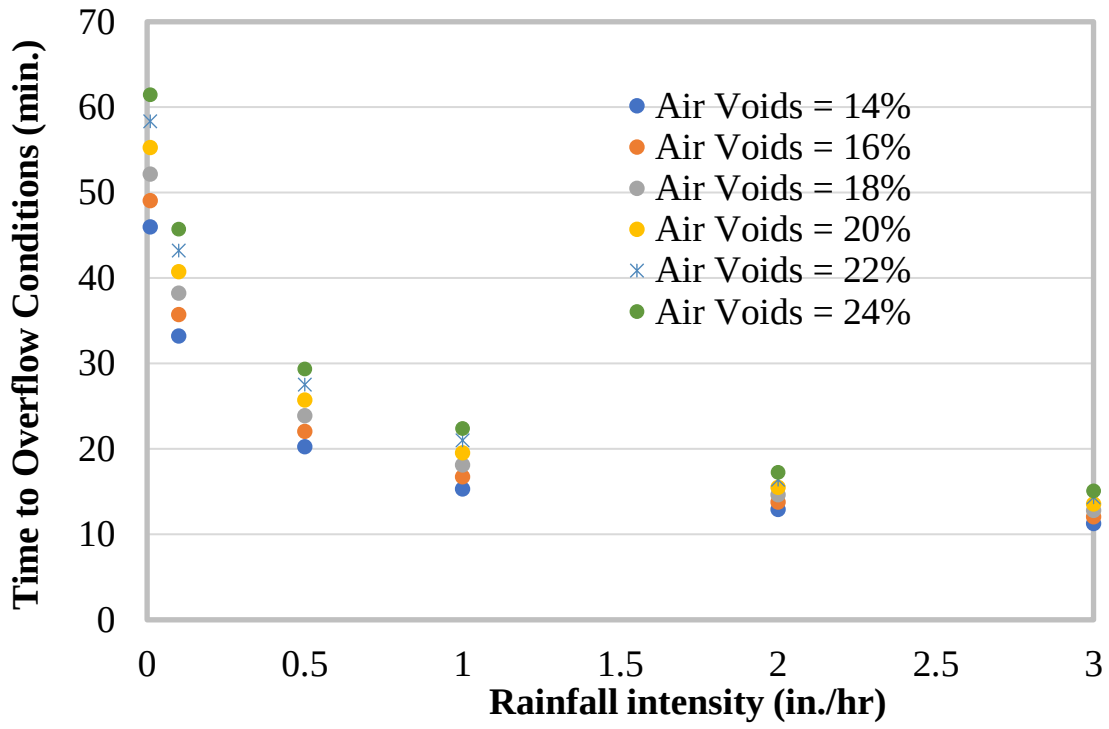

Recommendations for New AV Guidelines. The results presented in Figure 41 indicate that under the current AV guidelines, OGFC layers do not demonstrate significantly better performance compared to those with lower AV contents, particularly at high rainfall intensities. At a rainfall intensity of 3 in./hr, the difference in time to reach overflow conditions between 14-24% air voids was only 4 min. Therefore, it is reasonable to conclude that OGFC mixes produced with AV contents between 18-24% do not offer additional functional benefits during heavy rainfall events. Conversely, OGFC mixes with air void contents of 14-16% may provide notable improvements in durability and overall performance. Therefore, it is recommended to change the AV content specifications for OGFC mixes to 16% minimum and 20% maximum.

Conclusions

This study was conducted to fulfill four major objectives. First, it aimed to improve the durability of the current OGFC mix in Louisiana through the use of additives and other by-products, and by reducing the NMAS of the mix. To fulfill this objective, nine mixes were fabricated in the laboratory, and their performance was thoroughly evaluated. These mixes included a control mix, three mixes modified with WMA additives, two mixes fabricated with crumb rubber (CR), two mixes produced with fillers, and one mix prepared with reduced NMAS (9.5 mm NMAS). The test factorial was designed so that the performance of each mix would be evaluated at three different stages: production, construction, and field performance.

The second objective was to investigate the effects of selected factors on the seepage characteristics of pavement structures constructed with an OGFC layer. For this purpose, a three-dimensional finite element (FE) model was developed and calibrated based on GPR measurements. The results of the FE model were used to investigate the impacts of OGFC layer thickness, OGFC coefficient of permeability, underlying layer coefficient of permeability, rain intensity, and traffic wear on the seepage characteristics of OGFC layers. Based on these results, the third objective was to develop an ANN model to model the deterioration in the functional performance of pavement structures constructed with an OGFC layer.

The fourth objective was to propose new guidelines for AV contents for OGFC mixtures in Louisiana. The developed FE model was used to investigate the ability of an OGFC layer with an air void content ranging from 10-24% to drain rainfall water without reaching overflow conditions. Based on the results presented in this study, the following conclusions may be drawn.

Laboratory Performance of New OGFC Mixes

- WMA additives, 9.5 mm NMAS, and CR reduced the total AV content of the OGFC mix, which in turn reduced the coefficient of permeability. Nevertheless, all of the mixes satisfied the requirements of both AV content and the coefficient of permeability, per the NCHRP 1-51 study.

- Che1, Che2, CR, F_1, F_2, and 9.5 mm NMAS enhanced the raveling resistance of OGFC mixes compared to the CM based on the Cantabro abrasion loss test that was conducted on unaged samples.
- For aged and moisture-conditioned test samples, Cantabro loss test results indicated that all of the additives and the 9.5 mm NMAS significantly enhanced the raveling resistance of the OGFC mixes compared to the CM, which failed to satisfy the maximum allowable loss requirement.
- In terms of permanent deformation, all of the mixes satisfied the maximum allowable requirement at 5,000 passes, including the CM. The results also showed that organic WMA, CR, 9.5 NMAS, F_1, and F_2 significantly enhanced the permanent deformation resistance of OGFC mixes after 5,000 passes. At 20,000 passes, the mixes that contained organic WMA, CR, F_1, F_2, and 9.5 NMAS satisfied the permanent deformation requirement.
- For cracking resistance, Texas Overlay Test results indicated that the mixes that contained organic WMA, Che 2, F_1, F_2, and 9.5 NMAS performed satisfactorily against cracking.
- The organic WMA, CR (without Che1), F_1, F_2, and 9.5 NMAS significantly enhanced the cracking resistance of OGFC compared to the CM based on the ITS (dry and wet) test results. The results of the tensile strength ratio (TSR) and boil test also showed that all mixes were predicted to provide acceptable moisture damage resistance.
- Given the notable reduction in production temperature (23°F), WMA-OGFC mixes achieved the target density at a lower compaction energy effort compared to the CM.
- Based on the results of the Cantabro test and HWT rut depth at 5,000 passes, the most cost-effective OGFC mixes were 9.5 NMAS, F_2-OGFC, Che2-OGFC, and Org-OGFC, in this order. On the other hand, considering the results of the Cantabro test and rutting performance at 20,000 passes, the most cost-effective OGFC mixes were F_2-OGFC, 9.5 NMAS, Org-OGFC, and F_1-OGFC, in this order.

Factors Affecting Seepage Characteristics of OGFC Pavements

- Results indicated that as the thickness of OGFC, the permeability coefficient of OGFC, and the permeability coefficient of the underlying layer increased, the time it took for the system to reach the overflow condition (T_C) also increased.

- Conversely, the time it took to reach saturated (i.e., overflow) conditions decreased with increasing rain intensity and traffic wear.
- All of the aforementioned factors were statistically significant in controlling the seepage characteristics of OGFC pavement, except the permeability coefficient of OGFC.

Development of a Tool for the Prediction of OGFC Functional Performance Deterioration

- The results of the developed FE model (648 data points) were used to train and validate an Artificial Neural Network (ANN) model and an XGBOOST model for the prediction of T_C.
- The inputs of this model included the thickness of OGFC, the permeability coefficient of the underlying layer, and rain intensity.
- Results showed that the developed ANN model was able to predict T_C accurately with R^2 values of 99% and 98% in the training and validation phases, respectively.
- Statistical analysis showed that the T_C values generated by the ANN model were statistically equivalent to those predicted by the FE model.
- The developed ANN model showed good accuracy in predicting the deterioration rate of OGFC pavement functionality with a minimal Root Mean Square Error (RMSE) of less than 5%.

New Guidelines of OGFC Air Void Content for Louisiana Roads

- At a rainfall intensity of 3 in./hr., the difference in time to reach overflow conditions between 14-24% air voids was only 4 min. Therefore, it is reasonable to conclude that OGFC mixes produced with AV contents between 18-24% do not offer additional functional benefits during heavy rainfall events. Conversely, OGFC mixes with AV contents of 14% and 16% may provide notable improvements in durability and overall performance, as demonstrated by the results of the 9.5 NMAS OGFC mix.

Recommendations

Based on the results presented in this report, it is recommended to:

- Allow and encourage the use of 9.5 mm NMAS OGFC in Louisiana while changing the AV content specifications for OGFC mixes to 16% minimum and 20% maximum.
- Implement the use of the WMA additives, Portland cement, and fly ash in OGFC mixes for enhanced durability without significantly reducing their functionality.
- Construct road segments with the recommended OGFC mixes to evaluate their field performance under real-life traffic and climatic conditions.
- Evaluate the developed ANN model based on field-collected data.
- Design and place an OGFC mix with an AV content of 16% to assess its functional performance under real-life rainfall conditions.
- Evaluate different additive percentages and identify optimum dosages.

Acronyms, Abbreviations, and Symbols

Term	Description
AADT	Annual Average Daily Traffic
AASHTO	American Association of State Highway and Transportation Officials
AC	Asphalt Concrete
ACC/MVK	Accidents per Million Vehicles per Kilometer
ANN	Artificial Neural Networks
ANOVA	Analysis of Variance
ASA	Anti-Stripping Agent
ASTM	American Society for Testing and Materials
AV	Air Voids
DGHMA	Dense-Graded Hot-Mix Asphalt
DOS	Degree of Saturation
CA	Coarse Aggregate
CE	Cost-Effectiveness
CEI	Compaction Energy Index
CR	Crumb Rubber
DOT	Department of Transportation
DOTD	Louisiana Department of Transportation and Development
ESAL	Equivalent Single Axle Load
FA	Fine Aggregate
FE	Finite Element
FEA	Finite Element Analysis
HMA	Hot-Mix Asphalt
HSD	Honest Significant Difference
HWT	Hamburg Wheel-Tracking
ITS	Indirect Tensile Strength
JMF	Job-Mix Formula
LTRC	Louisiana Transportation Research Center

Term	Description
NCHRP	National Cooperative Highway Research Program
NMAS	Nominal Maximum Aggregate Size
OBC	Optimum Binder Content
OGFC	Open-Graded Friction Course
PAV	Pressure Aging Vessel
PG	Performance Grade
RTFO	Rolling Thin Film Oven
SCB	Semi-Circular Bending
TOT	Texas Overlay Tester
TSR	Tensile Strength Ratio
TxDOT	Texas Department of Transportation
WMA	Warm-Mix Asphalt

References

[1] D. Watson, N.H. Tran, C. Rodezno, A.J. Taylor and T.M. James, "Performance-Based Mix Design of Porous Friction Courses," NCHRP Report 877, Project 01-55, National Academy of Sciences, Transportation Research Board, 2018.

[2] H. Wu, J. Yu , W. Song, J. Zou, Q. Song and L. Zhou, "A critical state-of-the-art review of durability and functionality of open-graded friction course mixtures," *Construction and Building Materials*, vol. 237, 2020.

[3] W. King, M.S. Kabir, S.B. Cooper and C. Abadie, "Evaluation of Open Graded Friction Course (OGFC) Mixtures," Louisiana Transportation Research Center, Baton Rouge, LA, 2013.

[4] F. Gu, D. Watson, J. Moore and N. Tran, "Evaluation of the benefits of open graded friction course: Case study," *Construction and Building Materials*, vol. 189, pp. 131-143, 2018.

[5] E.R. Brown, P.S. Kandhal, F.L. Roberts, Y.R. Kim, D.Y. Lee and T.W. Kennedy, "Special Mixtures, Recycling, and Additives," in *Hot Mix Asphalt Materials*, *Mixture Design and Construction*, pp. 519-598, Lanham, MD, 2009.

[6] P.S. Kandhal and R.B. Mallick, "Open-Graded Friction Course: State of the Practice," Transportation Research Board, National Research Council, Washington, D.C., 1998.

[7] M.R.M. Hasan, J.Y. Eng, M.O. Hamzah and J. Voskuilen, "The effects of break point location and nominal maximum aggregate size on porous asphalt properties," *Construction and Building Materials*, vol. 44, no. 2013, pp. 360-367, 2013.

[8] H. Nekkanti, B.J. Putman and B. Danish, "Influence of Aggregate Gradation and Nominal Maximum Aggregate Size on the Performance Properties of OGFC Mixtures," *Transportation Research Record*, vol. 2673, no. 1, pp. 240-245, 2019.

[9] R.B. Mallick, P.S. Kandhal, L.A. Cooley and D.E. Watson, "Design, Construction, and Performance of New Generation Open-Graded Friction Courses," *Association of Asphalt Paving Technologists*, vol. 69, pp. 391-423, 2000.

[10] S.W. Goh and Z. You, "Mechanical Properties of Porous Asphalt Pavement Materials with Warm Mix Asphalt and RAP," *Journal of Transportation Engineering*, vol. 138, no. 1, pp. 90-97, 2012.

[11] F. Frigio, A. Stimilli, A. Virgili and F. Canestrari, "Performance Assessment of Plant-Produced Warm Recycled Mixtures for Open-Graded Wearing Courses," *Transportation Research Record*, vol. 2633, no. 2017, pp. 16-24, 2017.

[12] J. Zhang, W. Huang, G. Hao, C. Yan, Q. Lv and Q. Cai, "Evaluation of open-grade friction course (OGFC) mixtures with high content SBS polymer modified asphalt," *Construction and Building Materials*, vol. 270, no. 2021, 2020.

[13] A.E. Alvarez, A.M. Epps and C. Estakhri, "Connected Air Voids Content in Permeable Friction Course Mixtures," *Journal of Testing and Evaluation*, vol. 37, no. 3, Available online at: www.astm.org.

[14] F.G. Praticò and A. Moro, "Permeability and Volumetrics of Porous Asphalt Concrete," *Road Materials and Pavement Design*, pp. 799-817, 2007.

[15] T.H. Nguyen and J. Ahn, "Numerical Study on the Hydrologic Characteristic of Permeable Friction Course Pavement," *Water*, vol. 13, no. 843, 2021.

[16] Q. Zhang, T. Ji, Z. Wang and L. Xiao, "Experimental Study and Calculation of a Three-Dimensional Finite Element Model of Infiltration in Drainage Asphalt Pavement," *Materials*, 2020.

[17] M.A. Hernandez-Saenz, S. Caro, E. Arámbula-Mercado and A.E. Martin, "Mix design, performance and maintenance of Permeable Friction Courses (PFC) in the United States: State of the Art," *Construction and Building Materials*, vol. 111, no. 2016, pp. 358-367, 2016.

[18] L.A. Cooley, J.W. Brumfield, R.B. Mallick, W.S. Mogawer, M. Partl, L. Poulikakos and G. Hicks, "Construction and Maintenance Practices for Permeable Friction Courses," Transportation Research Board, Washington, D.C., 2009.

[19] M.S. Kabir, W. King, C. Abadie, P. Icenogle and S.B. Cooper, "Louisiana's Experience with Open-Graded Friction Course Mixtures," *Transportation Research Record*, vol. 2295, pp. 63-71, 2012.

[20] Louisiana Department of Transportation and Development, Louisiana Standard Specifications for Roads and Bridges, Baton Rouge, LA, 2016.

[21] M. Hu, L. Li and F. Peng, "Laboratory investigation of OGFC-5 porous asphalt ultra-thin wearing course," *Construction and Building Materials*, vol. 219, no. 2019, pp. 101-110, 2019.

[22] AASHTO, "Standard Practice for Materials Selection and Mixture Design of Permeable Friction Courses (PFCs)," AASHTO PP 77, 2014.

[23] A.E. Alvarez, A.E. Martin and C. Estakhri, "A review of mix design and evaluation research for permeable friction course mixtures," *Construction and Building Materials*, vol. 25, no. 11, pp. 1159-1166, 2011.

[24] ASTM, "Standard practice for open-graded friction course (OGFC) mix design," ASTM D 7064/D 7064 M-08, West Conshohocken, PA, 2008.

[25] E. Mahmoud, E. Masad and S. Nazarian, "Discrete Element Analysis of the Influences of Aggregate roperties and Internal Structure on Fracture in Asphalt Mixtures," *Journal of Materials in Civil Engineering*, vol. 22, no. 1, 2010.

[26] H.F. Hassan, S. Al-Oraimi and R. Taha, "Evaluation of Open-Graded Friction Course Mixtures Containing Cellulose Fibers and Styrene Butadiene Rubber Polymer," *Journal of Materials in Civil Engineering*, vol. 17, no. 4, pp. 416-422, 2005.

[27] A.E. Alvarez, A. Epps-Martin, C. Estakhri and R. Izzo, "Evaluation of durability tests for permeable friction course mixtures," *International Journal of Pavement Engineering*, vol. 11, no. 1, pp. 49-60, 2010.

[28] ASTM, "Standard Practice for Open-Graded Friction Course (OGFC) Mix Design," ASTM D7064-08, West Conshohocken, PA, 2013.

[29] G. Lefebvre, "Porous Asphalt," Permanent International Association of Road Congresses, 1993.

[30] P. S. Kandhal, "Design, Construction, and Maintenance of Open-Graded Asphalt Friction Courses," National Asphalt Pavement Association Information Series 115, 2002.

[31] L.A. Cooley, E.R. Brown and D.E. Watson, "Evaluation of Open-Graded Friction Course Mixtures Containing Cellulose Fibers," *Transportation Research Record*, vol. 2000, no. 1096, pp. 13-25, 2000.

[32] Florida Department of Transportation, "Florida Method of Test for Measurement of Water Permeability of Compacted Asphalt Paving Mixtures," 2015.

[33] AASHTO, "Hamburg Wheel-Track Testing of Compacted Hot Mix Asphalt (HMA)," 2019.

[34] Texas Department of Transportation, "Test Procedure for Overlay Test," 2007.

[35] V.M. Garcia, A. Miramontes, J. Garibay, I. Abdallah and S. Nazarian, "Assessing Crack Susceptibility of Asphalt Concrete Mixtures with Overlay Tester," *Journal of Testing and Evaluation*, vol. 46, no. 3, pp. 924-933, 2018.

[36] AASHTO, "Resistance of Compacted Bituminous Mixture to Moisture-Induced Damage," 2014.

[37] ASTM, "Standard Practice for Open-Graded Friction Course (OGFC) Asphalt Mixture Design," West Conshohocken, PA, 2021.

[38] R. Chapuis and A. Gatien, "Temperature dependent tensile strength of asphalt mixtures in relation to field cracking data," Proceedings of the Symposium on Engineering Properties of Asphalt Mixtures and the Relationship to Their Performance, pp. 180-193, 1995.

[39] Louisiana Department of Transportation and Development, "Water Susceptibility of Asphaltic Concrete Materials," Baton Rouge, LA, 2021.

[40] B.A. Hamilton, "Ten-Year Averages from 2005 to 2014," Retrieved from Road Weather Management Program, NHTSA, 2016.

[41] P.A. Pisano, L.C. Goodwin and M.A. Rossetti, "U.S. Highway Crashes in Adverse Road Weather Conditions," HWA Road Weather Management Program Publications, 2008.

[42] Y. Ding and H. Wang, "Evaluation of Hydroplaning Risk on Permeable Friction Course using Tire–Water–Pavement Interaction Model," *Transportation Research Record*, vol. 2672, no. 40, pp. 408-417, 2018.

[43] W. Jayasooriya and M. Gunaratne, "Evaluation of Widely Used Hydroplaning Risk Prediction Methods Using Florida's Past Crash Data," *Transportation Research Record*, no. 2457, pp. 140-150, 2014.

[44] L. Titus-Glover and S.D. Tayabji, "Assessment of LTPP Friction," Federal Highway Administration, U.S. Department of Transportation, Washington, D.C, 1999.

[45] X. Chen, H. Zhu, Q. Dong and B. Huang, "Case Study: Performance Effectiveness and Cost Benefit Analyses of Open-Graded Friction Course Pavements in Tennessee," *International Journal of Pavement Engineering*, 2017.

[46] S. Shimeno, A. Oi and T. Tanaka, "Evaluation and Further Development of Porous Asphalt Pavement with 10 Years Experience in Japanese Expressways," in 11th International Conference on Asphalt Pavement, Nagoya, Aichi, 2010.

[47] G. Huber, "NCHRP Synthesis of Highway Practice 284: Performance Survey on Open-Graded Friction Course Mixes," Transportation Research Board, National Research Council, Washington, D.C., 2000.

[48] G.W. Flintsch, "Assessment of the Performance of Several Roadway Mixes Under Rain, Snow, and Winter Maintenance Activities," Virginia Transportation Research Council, Charlottesville, VA, 2004.

[49] A.P. Greibe, "Porous Asphalt and Safety," in Proceedings of the Ninth International Conference on Asphalt Pavements, Copenhagen, Denmark, 2002.

[50] NCHRP Synthesis 49, "Open-Graded Friction Courses for Highways," Transportation Research Board, National Research Council, Washington, D.C., 1978.

[51] P.R. Donavan, Exterior Noise of Vehicles, New Jersey, John Wiley & Sons Inc., 2007.

[52] Q. Lu and J. T. Harvey, "Laboratory Evaluation of Open-Graded Asphalt Mixes with Small Aggregates and Various Binders and Additives," *Transportation Research Record*, no. 2209, pp. 61-69, 2011.

[53] K.J. Kowalski, R.S. McDaniel, A. Shah and J. Olek, "Long-Term Monitoring of Noise and Frictional Properties of Three Pavements," *Transportation Research Record*, no. 2127, pp. 12-19, 2009.

[54] Y. Brousseaud and F. Anfosso-Lédée, "Silvia Project Report: Review of Existing Low Noise Pavement Solutions in France," Sustainable Road Surfaces for Traffic Noise Control, European Commission, 2005.

[55] M. Barrett, P. Kearfott, J. Malina, H. Landphair, M.H. Li and F. Olivera, "Pollutant Removal on Vegetated Highway Shoulders," Texas Center for Transportation, Austin, TX, 2006.

[56] M.E. Barrett, P. Kearfott and J.F. Malina, "Stormwater Quality Benefits of a Porous Friction Course and Its Effect on Pollutant Removal by Roadside Shoulders," *Water Environment Research*, vol. 78, pp. 2177-2185, 2006.

[57] J. Chen, H. Li, X. Huang and J. Wu, "Permeability Loss of Open-Graded Friction Course Mixtures due to Deformation-Related and Particle-Related Clogging: Understanding from a Laboratory Investigation," *Journal of Materials in Civil Engineering*, vol. 27, no. 11, 2015.

[58] M.O. Hamzah, N.H. Abdullah, J.L. Voskuilen and G.V. Bochove, "Laboratory simulation of the clogging behavior of single-layer and two-layer porous asphalt," *Road Materials and Pavement Design*, vol. 14, no. 1, pp. 107-125, 2013.

[59] R. West, D. Timm, B. Powell, M. Heitzman, N. Tran, C. Rodezno, D. Watson, F. Leiva, A. Vargas, R. Willis, M. Vrtis and M. Diaz, "Phase V NCAT Track Findings," NCAT Report 16-04. NCAT, Auburn University, 2018.

[60] M. Miradi, A.A. Molenaar and M.F. van de Ven, "Performance Modeling of Porous Asphalt Concrete using Artificial Intelligence," *Road Materials and Pavement Design*, vol. 10, pp. 263-280, 2009.

[61] T. James, D. Watson, A. Taylor, N. Tran and C. Rodezno, "Improving cohesiveness of porous friction course asphalt mixtures," *Road Materials and Pavement Design*, vol. 18, no. S4, pp. 256-272, 2017.

[62] T.N. Mansour and B.J. Putman, "Influence of Aggregate Gradation on the Performance Properties of Porous Asphalt Mixtures," *Journal of Materials in Civil Engineering*, vol. 25, no. 2, pp. 281-288, 2013.

[63] M.J. Chen and Y.D. Wong, "Gradation design of porous asphalt mixture (PAM) for low-strength application in wet environment," *International Journal of Pavement Engineering*, vol. 19, no. 7, pp. 611-622, 2018.

[64] Z. Xie, N. Tran, D.E. Watson and L.D. Blackburn, "Five-Year Performance of Improved Open-Graded Friction Course on the NCAT Pavement Test Track," *Transportation Research Record*, vol. 2673, no. 2, pp. 544-551, 2019.

[65] E. Arámbula-Mercado, S. Caro, C.A.R. Torres, P. Karki, M. Sánchez-Silva and E. S. Park, "Evaluation of FC-5 with PG 76-22 HP TO Reduce Ravelling," Florida Department of Transportation, Tallahassee, FL, 2019.

[66] J.S. Chen, C.T. Lee and Y.Y. Lin, "Influence of Engineering Properties of Porous Asphalt Concrete on Long-Term Performance," *Journal of Materials in Civil Engineering*, vol. 29, no. 4, 2016.

[67] X. Chen, B. Huang and Z. Xu, "Correlating Loaded Wheel Testing Dynamic Stability with Asphalt Pavement Analyzer Rut Depth," in Airfield and Highway Pavements 2006, 2006.

[68] X. Ma, Q. Li, Y.C. Cui and A.Q. Ni, "Performance of porous asphalt mixture with various additives," *International Journal of Pavement Engineering*, vol. 19, no. 4, pp. 355-361, 2018.

[69] B. Shirini and R. Imaninasab, "Performance evaluation of rubberized and SBS modified porous asphalt mixtures," *Construction and Building Materials*, vol. 107, no. 2016, pp. 165-171, 2016.

[70] C. Sangiorgi, S. Eskandarsefat, P. Tataranni, A. Simone, V. Vignali, C. Lantieri and G. Dondi, "A complete laboratory assessment of crumb rubber porous asphalt," *Construction and Building Materials*, vol. 132, no. 2017, pp. 500-507, 2017.

[71] Y. Jiao, Y. Zhang, L. Fu, M. Guo and L. Zhang, "Influence of crumb rubber and tafpack super on performances of SBS modified porous asphalt mixtures," *Road Materials and Pavement Design*, 2019.

[72] P. Mirzababaei, "Effect of zycotherm on moisture susceptibility of Warm Mix Asphalt mixtures prepared with different aggregate types and gradations," Construction and Building Materials, vol. 116, no. 2016, pp. 403-413, 2016.

[73] L. Mohammad, A. Raghavendra, M. Medeiros, M. Hassan and W. King, "Evaluation of Warm Mix Asphalt Technology in Flexible Pavements," Baton Rouge, LA, 2018.

[74] S.D. Capitão, L. Picado-Santos and F. Martinho, "Pavement engineering materials: Review on the use of warm-mix asphalt," *Construction and Building Materials*, vol. 36, no. 2012, pp. 1016-1024, 2012.

[75] M.F.C. van De Ven, K.J. Jenkins, J.L.M. Voskuilen and R.V.D. Beemt, "Development of (half) warm foamed bitumen mixes: state of the art," *International Journal of Pavement Engineering*, vol. 8, no. 2, pp. 163-175, 2007.

[76] A. Behnood, "A review of the warm mix asphalt (WMA) technologies: Effects on thermo-mechanical and rheological properties," *Journal of Cleaner Production*, vol. 259, no. 2020, 2020.

[77] X. Li, H. Wang, C. Zhang, A. Diab and Z. You, "Characteristics of a Surfactant Produced Warm Mix Asphalt Binder and Workability of the Mixture," *Journal of Testing and Evaluation*, vol. 44, no. 6, pp. 2219-2230, 2015.

[78] J.E. Wurst and B.J. Putman, "Laboratory Evaluation of Warm-Mix Open Graded Friction Course Mixtures," *Journal of Materials in Civil Engineering*, vol. 25, no. 3, pp. 403-410, 2013.

[79] Q. Zhu, G. Hu, Y. Zhang and Y. Zhuang, "Laboratory evaluation of warm-mix open graded friction course mixtures with Sasobit," *Advanced Materials Research*, vol. 780, no. 2013, pp. 311-314, 2013.

[80] M. Asadi, R. Mallick and S. Nazarian, "Numerical modeling of post-flood water flow in pavement structures," *Transportation Geotechnics*, vol. 27, no. 2021, 2021.

[81] S. Rabab'ah and R.Y. Liang, "Finite Element Modeling of Field Performance of Permeable Bases Under Asphalt Pavement," *Transportation Research Record*, pp. 163-172, 2007.

[82] M.R. Mousa, M.A. Elseifi, Z. Zhang and K. Gaspard, "Evaluation of Moisture Damage under Crack-Sealed Asphalt Pavements in Louisiana," *Transportation Research Record*, vol. 2673, no. 3, pp. 460-471, 2019.

[83] R.Y. Liang and M. Taamneh, "Design of Effective Subsurface Drainage for Flexible Pavement," GeoFlorida 2010: Advances in Analysis, Modeling & Design, pp. 2631-2640, 2010.

[84] C. Yoo, J.M. Ku, C. Jun and J.H. Zhu, "Simulation of infiltration facilities using the SEEP/W model and quantification of flood runoff reduction effect by the decrease in CN," *Water Science & Technology*, pp. 118-129, 2016.

[85] S.A. Tan, T.F. Fwa and K.C. Chai, "Drainage Considerations for Porous Asphalt Surface Course Design," *Transportation Research Record*, vol. 1868, pp. 142-149, 2004.

[86] S. Yang, K. Yan, W. He and Z. Wang, "Effects of Sasobit and Deurex additives on asphalt binders at midrange and high temperatures," *International Journal of Pavement Engineering*, vol. 20, no. 12, pp. 1400-1407, 2019.

[87] A. Faheem and H.U. Bahia, "Using Gyratory Compactor to Measure Mechanical Stability of Asphalt Mixtures," Wisconsin Department of Transportation, Madison, WI, 2004.

[88] ASTM, "Standard Practice for Rapid Drying of Compacted Asphalt Mixture Specimens Using Vacuum Drying Apparatus," West Conshohocken, PA, 2017.

[89] M.R. Mousa, M.A. Elseifi, Z. Zhang and K. Gaspard, "Evaluation of Moisture Damage under Crack-Sealed Asphalt Pavements in Louisiana," *Transportation Research Record*, vol. 2673, no. 3, pp. 460-471, 2019.

[90] M.A. Elseifi, M.R. Mousa and M.Z. Bashar. "Improving the Use of Crack Sealing to Asphalt Pavement in Louisiana, FHWA/LA.19/620," Louisiana Transportation Research Center, Baton Rouge, LA, 2020.

[91] G.C. Topp, J.L. Davis and A.P. Annan, "Electromagnetic Determination of Soil Water Content: Measurements in Coaxial Transmission Lines," *Water Resources Research*, vol. 16, no. 3, pp. 574-582, 1980.

[92] L.N. Mohammad, A. Herath and B. Huang, "Evaluation of Permeability of Superpave® Asphalt Mixtures," *Transportation Research Record*, Vol. 03-4464, pp. 50-58, 2003.

[93] W. Luo, "Wheel Path Wandering Based On Field Data," University of Arkansas, Fayetteville, AR, 2012.